AD-A097 564 CALIFORNIA UNIV LIVERMORE LAWRENCE LIVERMORE NATIONAL LAB F/G 4/1
ANNUAL REPORT OF LAWRENCE LIVERMORE LABORATORY TO THE FAA ON TH--ETC(U)
SEP 79 F M LUTHER DOT-FA79WAI-034
UNCLASSIFIED UCRL-50042-79 FAA/EE-80-39 NL

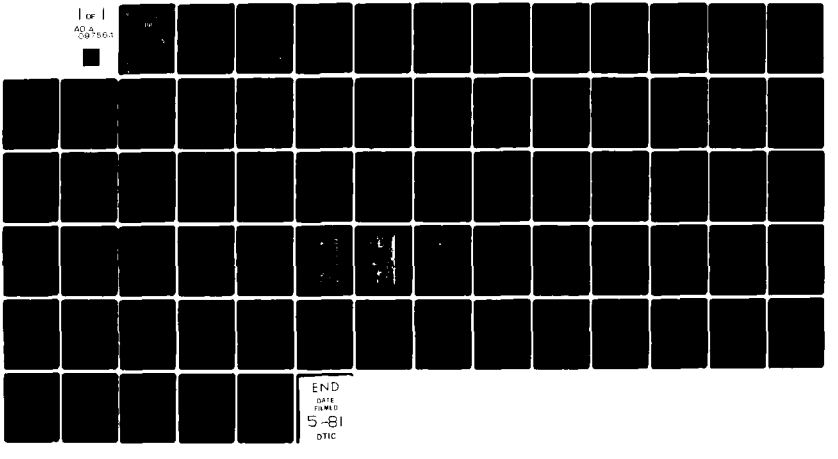

END
DATE FILMED
5-81
DTIC

FAA-EE-80-39

Annual Report of Lawrence Livermore Laboratory to the FAA on the High Altitude Pollution Program-1979

U.S. Department of Transportation
Federal Aviation Administration

Office of Environment and Energy
Washington, D.C. 20591

LEVEL II

September 1979

Frederick M. Luther
Principal Investigator

Document is available to the public through the National Technical Information Service, Springfield, Virginia 22161

Technical Report Documentation Page

1. Report No.	2. Government Accession No.	3. Recipient's Catalog No.
FAA-EE-80-39	AD-A084 760	

4. Title and Subtitle	5. Report Date
ANNUAL REPORT OF LAWRENCE LIVERMORE LABORATORY TO THE FAA ON THE HIGH ALTITUDE POLLUTION PROGRAM-1979	September 30, 1979
	6. Performing Organization Code
7. Author(s) Frederick M. Luther, Principal Investigator	8. Performing Organization Report No. UCRL-50042-79
9. Performing Organization Name and Address Lawrence Livermore Laboratory University of California Livermore, California 94550	10. Work Unit No. (TRAIS)
	11. Contract or Grant No. DOT-FA79WAI-034
	13. Type of Report and Period Covered Annual Report
12. Sponsoring Agency Name and Address U.S. Department of Transportation Federal Aviation Administration High Altitude Pollution Program Washington, D.C. 20591	14. Sponsoring Agency Code

15. Supplementary Notes

16. Abstract

This annual report documents the progress made on research in support of the High Altitude Pollution Program (HAPP) during FY-1979. The primary research emphases at LLNL are numerical modeling of the atmospheric response to stratospheric perturbations and processing and analyzing satellite data to determine stratospheric ozone concentrations. The modeling effort at LLNL covers four major research areas: photochemical kinetics, coupled kinetics and transport, radiative transfer, and meteorological analysis. Tasks completed during the past year included: comparison of model simulations of stratospheric composition with observational data, simulations of past perturbations to the stratosphere, and assessments of potential changes resulting from aircraft engine emissions and other perturbations.

The satellite data processing task has three major areas of effort: (1) radiative transfer and ozone retrieval methodology, (2) data processing, archiving, and distribution, and (3) data analysis, interpretation, and quality assurance. Progress in each of these areas is reviewed toward the goal of implementing the retrieval methodology during FY-1980.

17. Key Words	18. Distribution Statement
Ozone Perturbations, Total Ozone, NO_x Injections, Stratospheric Model, Ozone and Solar Variability, Satellite Monitoring, Ozone Data Basing.	Available to the public through the National Technical Information Service, Springfield, Virginia 22161.

19. Security Classif. (of this report)	20. Security Classif. (of this page)	21. No. of Pages	22. Price
Unclassified	Unclassified	74	

Form DOT F 1700.7 (8-72) Reproduction of completed page authorized

UCRL-50042-79
Distribution Category UC-11

Annual report of Lawrence Livermore Laboratory to the FAA on the high altitude pollution program—1979

Frederick M. Luther, Principal Investigator

Manuscript date: September 30, 1979

LAWRENCE LIVERMORE LABORATORY
University of California • Livermore, California • 94550

Available from: National Technical Information Service • U.S. Department of Commerce
5285 Port Royal Road • Springfield, VA 22161 • $7.00 per copy • (Microfiche $3.50)

PREFACE

Since July 1, 1975, Lawrence Livermore Laboratory (LLL) has been participating in the High Altitude Pollution Program sponsored by the U.S. Department of Transportation's Federal Aviation Administration. This report describes the major accomplishments and significant findings during the fiscal year ending September 30, 1979, for work performed at LLL under Reimbursable Agreement DOT-FA79WAI-034. Two major research areas are covered by this agreement: (1) numerical modeling of the atmospheric response to stratospheric perturbations, and (2) the processing, archiving, and analysis of satellite ozone data. Each of these research areas has been divided into a number of subtasks, and the successful accomplishment of these subtasks has required contributions and cooperation from many participants. The work reported here should be considered the collective effort of all those listed below.

Scientific Administration
Joseph B. Knox, Division Leader
Frederick M. Luther, Principal Investigator

Numerical Modeling
Julius S. Chang
William H. Duewer
Hugh W. Ellsaesser
Joyce E. Penner
Raymond L. Tarp
Donald J. Wuebbles

Satellite Ozone Data Analysis
James S. Ellis
Stanley L. Grotch
Stephen E. Jones
John A. Korver
Ambrosio R. Licuanan
James E. Lovill
H. Alex Magee
Linda L. Ott
Thomas J. Sullivan
Sandra S. Taylor
Roger L. Weichel
Patrick P. Weidhaas

CONTENTS

Annual report of Lawrence Livermore Laboratory to the FAA on the high altitude pollution program—1979

1. INTRODUCTION

This annual report documents the progress made on research in support of the High Altitude Pollution Program (HAPP) during FY-1979. Work performed during previous years at Lawrence Livermore Laboratory (LLL) is described in our earlier annual reports (Luther *et al.*, 1976, 1977, 1978). A review of progress made during previous years of effort on HAPP is also included in this year's report.

During the past decade, a great deal of effort has been devoted to understanding the potential environmental impact of high-altitude aircraft flights. In 1970, the Climatic Impact Assessment Program (CIAP) was created to evaluate the impact of the future operation of supersonic transport aircraft (SST's) in the stratosphere. This research program was sponsored by the U.S. Department of Transportation and was completed in 1975 with the publication of a series of monographs that assessed the potential chemical, climatic, biological, and economic effects of stratospheric aircraft emissions. Additional assessments were prepared by the Climatic Impact Committee of the National Academy of Sciences (National Research Council, 1975), by the British (COMESA, 1976), and by the French (COVOS, 1976).

The High Altitude Pollution Program was initiated in 1975 by the Federal Aviation Administration to extend the investigations carried out during CIAP so as to ensure that stratospheric aircraft emissions would not result in unacceptable environmental effects. The environmental issues that were raised relative to SST's pertain to all types of aircraft operating in the stratosphere. Consequently, the flight regimes of interest to HAPP include subsonic, supersonic, and hypersonic aircraft. The aircraft engine effluents of primary concern in terms of impact on ozone are oxides of nitrogen (NO and NO_2) and water vapor. Perturbations other than aircraft emissions have also been proposed as having a potentially significant impact on ozone (e.g., Cl and ClO from chlorofluoromethanes). The HAPP research effort also considers these other perturbations in order to address the overall problem of the combined effects of stratospheric perturbations.

Lawrence Livermore Laboratory has participated in HAPP since July 1975 under interagency agreements DOT-TSC-76-1, DOT-FA76WAI-653, and DOT-FA79WAI-034. Primary research emphasis at LLL is on numerical modeling of the atmospheric response to stratospheric perturbations. The modeling effort at LLL covers four major research areas: photochemical kinetics, coupled kinetics and transport, radiative transfer, and meteorological analysis.

Photochemical kinetics modeling spans gas-phase reaction processes and heterogeneous (i.e., gas-particle) reaction processes, constant and diurnally (and seasonally) varying photochemical reaction rates, a wide range of ambient temperatures and pressures, neutral and ionized species, processes with both accurately and poorly known rates of reaction, and species of both acknowledged and questionable importance in the stratosphere. Considerable attention has been directed toward evaluation of the sensitivity of reaction mechanisms to deficiencies in our knowledge of reaction rates, quantum yields, and reaction mechanisms.

The transport-kinetics models are intended for time-dependent calculations of the response of the atmosphere to stratospheric perturbations. These models incorporate interactive radiative and chemical processes coupled with transport, which must be parameterized in one- and two-dimensional models. These models are designed to facilitate perturbation and sensitivity studies.

Radiative transfer modeling includes: application of highly detailed models to assessment of the effect on the radiation budget of perturbations to the stratospheric composition, and development of

simplified radiative transfer models for inclusion in the transport-kinetics models. Considerable attention has been directed toward including interactive radiative processes in the transport-kinetics models in order to assess possible feedback mechanisms.

Meteorological analysis provides guidance and support for the modeling effort through in-depth studies of atmospheric processes and phenomena. A primary responsibility of this research is to develop test situations to validate various aspects of the numerical models.

In August 1976, LLL's participation in HAPP was extended to include a feasibility study to determine whether good quality total ozone data could be derived from infrared radiance measurements by a multi-channel filter radiometer (MFR) sensor carried aboard a series of satellites operated by the U.S. Air Force. These satellites are a part of the Defense Meteorological Satellite Program Block 5D series. The first four satellites in this series carry MFR sensors from which total ozone data may be derived. The MFR sensor is the first cross-track scanning sensor capable of measuring ozone, and it has a higher spatial resolution and lower noise level than previous instruments. The first satellite began transmitting MFR measurements in March 1977, and MFR data will be received from these satellites into the early 1980's. These MFR data should be useful for determining the temporal and spatial variability of ozone over this period of time.

The feasibility study was completed in May 1978, with the successful processing of 20 days of data taken during 1977. The quality of the derived total ozone data was demonstrated by comparison with corresponding ozone data obtained at selected stations in the world surface network of Dobson spectrophotometer observatories. A description of the methodology used and global maps of the total ozone data for the 20 days are contained in the report by Lovill *et al.* (1978).

Following completion of the feasibility study, LLL's effort has been directed toward archiving and processing the MFR data. Before routine data processing could begin, an automated data-basing system had to be developed. Each MFR sensor is capable of taking up to 67,500 observations (each observation consisting of 16 radiance measurements) per day, and as many as three satellites were taking data concurrently, so several million pieces of data are included in the data base for each day of coverage. Consequently, the archiving and processing of the data would be difficult without an automated data base. We have also been evaluating various aspects of the ozone retrieval methodology and making refinements. Thus, the methodology used for regular data processing will be improved over that used in the feasibility study.

The satellite data processing task has three major areas of effort: (1) radiative transfer and ozone retrieval methodology, (2) data processing, archiving, and distribution, and (3) data analysis, interpretation, and quality assurance. Work on these tasks is supported in part by the National Aeronautics and Space Administration (NASA).

The first area of effort involves detailed transmittance and simulated radiance calculations, comparisons between models and laboratory measurements, and ozone retrieval model development using regression analysis. Sensitivity studies, error analysis, and special studies with satellite radiances are also included.

The second area of effort involves MFR data calibration, optimization of data processing methodology, design and implementation of an automated data base, data processing, mapping of ozone data, and data distribution. In addition, satellite overflight times are predicted and distributed to over 36 Dobson observatories each month so that special Dobson spectrophotometer measurements can be taken for comparison with the MFR ozone data.

The third area of effort involves development of the Dobson and ozonesonde data bases, development of quality-assurance techniques and statistical analyses, comparison of the MFR ozone data with other data sources, and analyses of the data on various temporal and spatial scales. The data will be analyzed for both anthropogenic and non-anthropogenic effects.

2. ATMOSPHERIC MODELING

A fundamental tool in the LLL effort in atmospheric modeling has been the one-dimensional transport-kinetics model. This model includes as complete a set of the important chemical and photochemical reactions as is feasible and is designed for time-dependent perturbation and sensitivity studies. This model currently includes 39 chemical species and 134 chemical and photochemical reactions. Species concentrations are computed at 44 levels in the atmosphere, extending from the ground to 55 km. Vertical transport is parameterized using a one-dimensional diffusion formulation that describes hemispheric-average net vertical transport. The model can include temperature coupling between changes in composition and reaction rate coefficients and hydrostatic adjustment of pressure and density as user options, but these options are not utilized in our standard model calculations. The one-dimensional transport-kinetics model is described in more detail in Appendix A.

In addition to the one-dimensional transport-kinetics model, we have used radiative transfer codes of varying complexity for several studies. We are also in the process of developing a two-dimensional transport-kinetics model.

Since the beginning of the HAPP program, LLL has completed the following major research studies and activities:

- Sensitivity of NO_x catalytic ozone destruction to uncertainties in rate coefficients.
- Sensitivity of ozone reduction from chlorofluoromethanes to parameter uncertainties.
- Effects of changes in O_3 and NO_2 on atmospheric solar absorption.
- Effect of NO photolysis on NO_y mixing ratios.
- Analysis of chemical rate data.
- Effect of multiple scattering on species concentrations and model sensitivity.
- Effect of changes in stratospheric water vapor on ozone reduction estimates.
- Effect of atmospheric nuclear testing during the 1950's and 1960's on ozone.
- Effect of agriculture on stratospheric ozone.
- Calculation of global tropospheric OH distributions.
- Tropospheric lifetimes and potential effects on ozone of halocarbons.
- Analysis of global budgets of halocarbons.
- Effects of changes in total ozone and receiver orientation on received erythema dose.
- Effect of possible variations in solar ultraviolet flux on stratospheric ozone.
- Effects of a solar eclipse on stratospheric chemistry.
- Potential effects of space shuttle emissions.
- Potential effects of solar power satellite launch vehicles.
- Effects of a massive pulse injection of NO_x into the stratosphere.
- Effects of stratospheric perturbations on the earth's radiation budget and the climatic implications.

In addition to the listed special studies, we have continued to work on model improvements and comparisons between model calculations and observations. These comparisons are important to the verification of various aspects of the model. We have compared computed species profiles with observations for the ambient atmosphere as well as simulations of natural and man-made perturbations. Several basic types of data have proven to be useful: height and latitudinal distributions of individual species and groups of species, partitioning of related species, and local diurnal and seasonal variations of individual species. Interpretation of the results from such comparisons is not always simple because of the significant level of local variability of species concentrations. It is the overall reasonableness of the models and their predictions that provide a high level of confidence in their basic correctness. Of course, this is often a matter of judgment.

The one-dimensional transport-kinetics model has been used to assess the potential chemical effects of several man-made perturbations to the stratosphere. Whenever significant changes occur to the model chemistry or to the treatment of physical processes, the assessment studies are repeated in order to assess the effect of the changes on the model sensitivity.

The research activities that were completed during the past year are described in the following sections. One of the major accomplishments during the past year was the preparation of a detailed assessment report on the potential effects of aircraft emissions (Luther *et al.*, 1979). The reader should

refer to that report for additional material and a more detailed discussion of the topics presented here.

2.1 MODEL SIMULATIONS OF STRATOSPHERIC OBSERVATIONS

Stratospheric Composition

Comparison with observational data on trace species concentrations is an important aspect of validating the performance of numerical models of the stratosphere. Although comparisons with observations are a necessary part of model validation, these comparisons alone are not sufficient to validate the performance of the model because we know from past experience (Duewer *et al.*, 1977) that models with significantly different chemistry and sensitivity can predict very similar ambient species profiles.

Two somewhat different sets of chemical reaction rate coefficients and photolysis cross sections were used in the calculations presented in this report. Most of the calculations were performed prior to the NASA Workshop at Harpers Ferry, West Virginia (June 1979), and utilized chemical rates based primarily on JPL (1979). After the NASA Workshop, we repeated several of the perturbation calculations using chemical rates based on the recommendations of the chemistry panel at the NASA Workshop. These two chemistries are described in Appendix A as 1979a and 1979b chemistries.

In this section, we compare the results of our current one-dimensional model using 1979b chemistry with measured trace species concentrations. Much of the measurement data used in the comparisons was derived from LLL-supplied information communicated at the NASA Harpers Ferry Workshop. As such, some is preliminary in nature. The evaluation of measurements is strongly influenced by that of the NASA panels as reflected at the Workshop. Our discussion in this section closely parallels some of that in the NASA document, reflecting, in part, our participation in writing parts of that document.

$O(^3P)$. There is good agreement between model-calculated distributions and the few available measurements. However, the $O(^3P)$ concentration is in a near photoequilibrium with O_3, and the ozone column used in the calculations is calculated for equinox conditions whereas the measurements are winter measurements. Because O_3 was not measured at the same time that O was, there is some danger that the apparent good agreement is fortuitous.

O_3. Ozone profiles vary significantly with latitude and season. Total column ozone ranges from about 200 m · atm · cm in the tropics to about 400 m · atm · cm near the poles. The altitude of the peak concentration is lower near the poles than at the equator. The model-derived O_3 profile resembles observations of O_3 taken at middle latitudes.

OH, HO_2. Within the plausible error in the measurements, there appears to be reasonable agreement between theoretical calculations and the few available measurements of OH and HO_2 in the stratosphere. Data are available only between 28 and 38 km for HO_2. The point-to-point variability of the measurements for both species exceeds measurement precision. This suggests that the different air masses measured may have significantly different histories. It would be desirable if, in the future, concurrent measurements of various species (OH, HO_2, O_3, H_2O, etc.) would be made. If such concurrent measurements become available, it may be possible to explain local variability, as well as to usefully examine ratios (e.g., HO_2/HO) in relation to those expected theoretically. Comparison of the total OH column calculated by current one-dimensional models with the observations of Burnett and Burnett (1979) does not indicate significant differences in average column content.

NO. When measurements taken at middle latitudes and near noon are compared to calculated noon profiles, the calculated profiles are significantly larger than the observations above 30 km. The maximum difference occurs in the upper stratosphere where NO is the dominant NO_x species. One contribution to the difference between models and observations is the overprediction of the total NO_x content by current models. The apparent NO maximum near 40 km lends some credibility to the hypothesis that the treatment of NO photolysis may underestimate the actual upper stratospheric NO sink.

Recent measurements of NO (discussed by H. Schiff and others at the N.A.T.O. Advanced Study Institute on Atmospheric Ozone held in Portugal in October 1979) find higher concentrations in the upper stratosphere than previous measurements. These measurements agree better with model

calculations. However, the reason for disagreement with previous observations (whether it is due to natural variability or measurement errors) must be resolved.

HNO_3. Current models predict more HNO_3 than is observed above about 25 km. In part this may simply reflect the higher-than-observed NO_y concentrations currently calculated. However, this does not appear to be sufficient to explain the entire difference, nor is it likely that model overprediction of OH between 25 and 35 km is responsible for the difference, since model OH and observations are in good agreement between 28–35 km.

Total NO_y. Our theoretical model presently calculates approximately a factor of 2 more NO_y ($NO + NO_2 + HNO_3$) than has been measured. However, it should be noted that *in situ* measurements of all three species are not available with readily comparable techniques to permit an unambiguous comparison between theory and measurements.

Part of the reason for the difference between model and observation may be that the model predicts too much N_2O in the upper stratosphere, since reaction of N_2O with $O(^1D)$ is the primary source for NO_y in the stratosphere. More measurements of N_2O in the upper stratosphere would be necessary to confirm this hypothesis. The N_2O content in one-dimensional models is sensitive to the choice of vertical transport coefficient used in the calculation.

Other possible factors that might cause the models to overpredict NO_y would include: (1) A lower rate coefficient for $O(^1D) + N_2O \rightarrow 2NO$ than is currently recommended. The data for this process are not in good agreement. However, if anything, they suggest a faster rate coefficient. (2) $O(^1D)$ may be overestimated. This could happen if the quantum yield for $O(^1D)$ production from O_3 photolysis has a stronger temperature dependence than is used in the models. (3) The rate at which NO photolysis occurs may be underestimated in the models. Frederick and Hudson (1979) estimate their results to be uncertain by a factor of 3. Adoption of their treatment decreased the photolysis rate by a factor of about 3 from the previous value in the model which resulted in an increase of the model-calculated NO_y by about 40%.

HNO_3/NO_2. The ratio of HNO_3 NO_2 currently calculated by models is much higher than is observed by Evans *et al.* (1976) but is within the error bounds of other measurements. In none of these measurements were both species measured by similar techniques. Concurrent measurements taken at a given point with the same technique are needed to establish whether a discrepancy actually exists. Even then, because of the difference in chemical lifetimes, it would be difficult to determine the time history of both NO_2 and HNO_3 that led to the ratio observed. If a discrepancy does exist, one possible explanation would be that current estimates of OH in the lower stratosphere (below approximately 30 km) are too large. Another possibility would be that the sinks for HNO_3 are underestimated.

N_2O_5. We currently calculate a N_2O_5 concentration of approximately 2.5 ppb near sunrise. This can be compared to the value of 2 ppb deduced for N_2O_5 by Evans *et al.* (1978) based upon measurements of other species a few hours after sunrise. It should be noted that the measurement was not made at the latitude and season the model most nearly approximates. Until further measurements are made, the comparison is inconclusive.

Cl, ClO. The single observed Cl profile (and one additional Cl observation at a single altitude) and calculated Cl profiles agree within the measurement uncertainty of ±35%. However, the measurements suggest a larger vertical gradient in Cl mixing ratio than is predicted. More Cl measurements are needed to determine whether any seasonal or spatial variations exist and, if so, whether these are consistent with model predictions.

For ClO, at the mixing ratio maximum, with the exception of the 14 July 1977 measurement by Anderson *et al.* (1979), the resonance fluorescence measurements are within a factor of about 2 of the predicted ClO abundances. The September through December ClO measurements show a significantly sharper than predicted gradient below the mixing ratio peak. Except for the summer of 1979, summer measurements give more ClO than the September through December measurements. The 14 July 1977 measurement gives six times more ClO than is predicted near the mixing ratio peak, and exceeds by about a factor of 3 the total chlorine mixing ratio believed to be present in the stratosphere. Predicted variations of the Cl and ClO profiles with season are very small compared to the range of observed profiles. A broader data base is needed to explain the difference in these results as well as the large (factor of 10) variation in the ClO profiles observed but not predicted by one-dimensional models.

The differences between theoretical calculations and observations of the ClO gradient below

34 km also require attention. At present, speculations for explaining these differences range from the possibility of a missing chemical reaction or an incorrect rate constant in present theory to the possibility of it being an artifact of the transport parameterization used in current models, or an artifact of the measurement techniques.

Cl/ClO Ratio. The Cl/ClO ratios from the 28 July 1976 resonance fluorescence measurements (Anderson *et al.*, 1979) agree to within measurement uncertainty with most calculations. It is difficult at present to make any conclusions regarding this comparison because of the experimental uncertainties, the limited amount of data, the apparent variability of ClO, and the poor agreement between models and observations for ClO.

HCl. Although there may be significant disagreement (as large as 30–40% when compared with the IR spectra data, much larger if compared to the filter or radiometer data) above 30 km, the uncertainty in the observational data in this altitude range is such as to probably encompass the model predictions.

$ClONO_2$. The only observational data for $ClONO_2$ are from one flight by Murcray (1979). There is excellent agreement if the fast production rate for $ClONO_2$ is used in the calculations, whereas there is a factor of 3 difference if the slower production rate is used (see Section 2.4 discussion regarding the rate of production of $ClONO_2$).

Until further data are available, it is difficult to make any conclusive statements regarding this species. However, the limited amount of data available does not indicate any gross discrepancies between theory and observations.

Total ClX. There now exist a limited number of measurements for Cl, ClO, HCl, and $ClONO_2$ in the stratosphere. Except for three measurements of ClO taken in summer (Anderson, 1979; Menzies, 1979), there does not appear to be any large discrepancy between the total amount of ClX predicted and that observed. However, the summer measurements of ClO are so large as to require much more total ClX than known sources are capable of producing. This implies the possibility of an unknown source for ClX in the atmosphere, an error in the observation, or some unusual episodic event

Model Simulations of Past Perturbations

Possible Long-Term Solar Variations and Effects on Temperature and Ozone. In the study of potential anthropogenic influences on the stratospheric ozone budget it is necessary to first understand the natural variations of ozone. In order to achieve early detection of anthropogenic trends and to establish the magnitude of such effects, we must differentiate the natural stratospheric ozone variations from the man-made effects that are of comparable time scales. The suggested correlation between ozone and sunspot number is of primary interest. If this relation is real, then for the next few years the theoretically predicted effect of CFM's on ozone may not be directly detectable unless the effect of this ozone-solar cycle relation can be quantified and removed from the ozone data. At this time, the most plausible mechanism coupling the sunspot cycle and atmospheric ozone is the change in solar flux between 180 and 340 nm from solar maximum to solar minimum (Heath and Thekaekara, 1977; Callis and Nealy, 1978; Penner and Chang, 1978). Theoretically, a variation in solar flux between 180 and 340 nm of approximately 30% (maximum to minimum) can lead to local ozone changes as large as 10% near 35 km, and total ozone column changes of approximately 5% (Penner and Chang, 1978). This is comparable to the predicted CFM effect of ozone decreases of up to 5% around the year 1990. Consequently, the possible influence of periodic or aperiodic changes in solar UV flux intensities tends to obscure changes due to the present levels of CFM's, and this may continue for the next decade. The same is also true for the local ozone concentrations in the upper stratosphere.

The data that support a variation in solar UV fluxes during a solar cycle are limited (Heath and Thekaekara, 1977) and need to be confirmed with other independent measurements. Simon (1978) has pointed out the difficulty in the absolute calibration of the measuring instruments, especially those aboard a satellite.

Since the direct monitoring of solar UV fluxes and ozone are both of limited use in establishing the ozone-solar cycle relation, we are left with the monitoring of trace species other than ozone as a possible independent method for validating the effects of solar UV flux variations. We examined the possible variations of 31 trace species that result from hypothetical solar UV variations with the LLL time-dependent model of stratospheric chemistry, including self-consistently calculated stratospheric temperature and atmospheric adjustment to hydrostatic equilibrium (Penner and Chang, 1979).

From this study we identified N_2O as a most likely candidate for monitoring to study coupling between variations in solar UV and atmospheric composition. Furthermore, there remains the question of the effect of transport-related variability that can only be resolved with a set of upper stratospheric data.

The Atmospheric Nuclear Tests of the 1950's and 1960's. Past atmospheric tests of nuclear devices larger than about one megaton (TNT) yield provide a potentially significant source of NO_x to the stratosphere. During the late 1950's and early 1960's, large numbers of such tests were carried out, and the NO_x released to the stratosphere in 1961 and 1962 should have been comparable to the amount that would be released by about 2.7 years operation of a large SST fleet (i.e., one emitting approximately 10^8 molecules $cm^{-2}s^{-1}$). The paper by Chang, Duewer and Wuebbles (1979) gives an account of the predicted effects through early 1978. Figure 1 gives the computed ozone column change as a function of time. For computations made with 1979b chemistry (see Appendix A), the two curves give the ozone depletion calculated for injection altitudes based on a parameterization by Foley and Ruderman (1972) or on the lower altitude observations of Seitz *et al.* (1968). The two treatments are thought to bound the plausible range of injection altitudes.

Both treatments predict maximum ozone depletions of less than 2% for the largest annual-average change. The largest change is only about 1.25% if a 1–2–1 smoothing function is applied to annual perturbations. The computed changes are

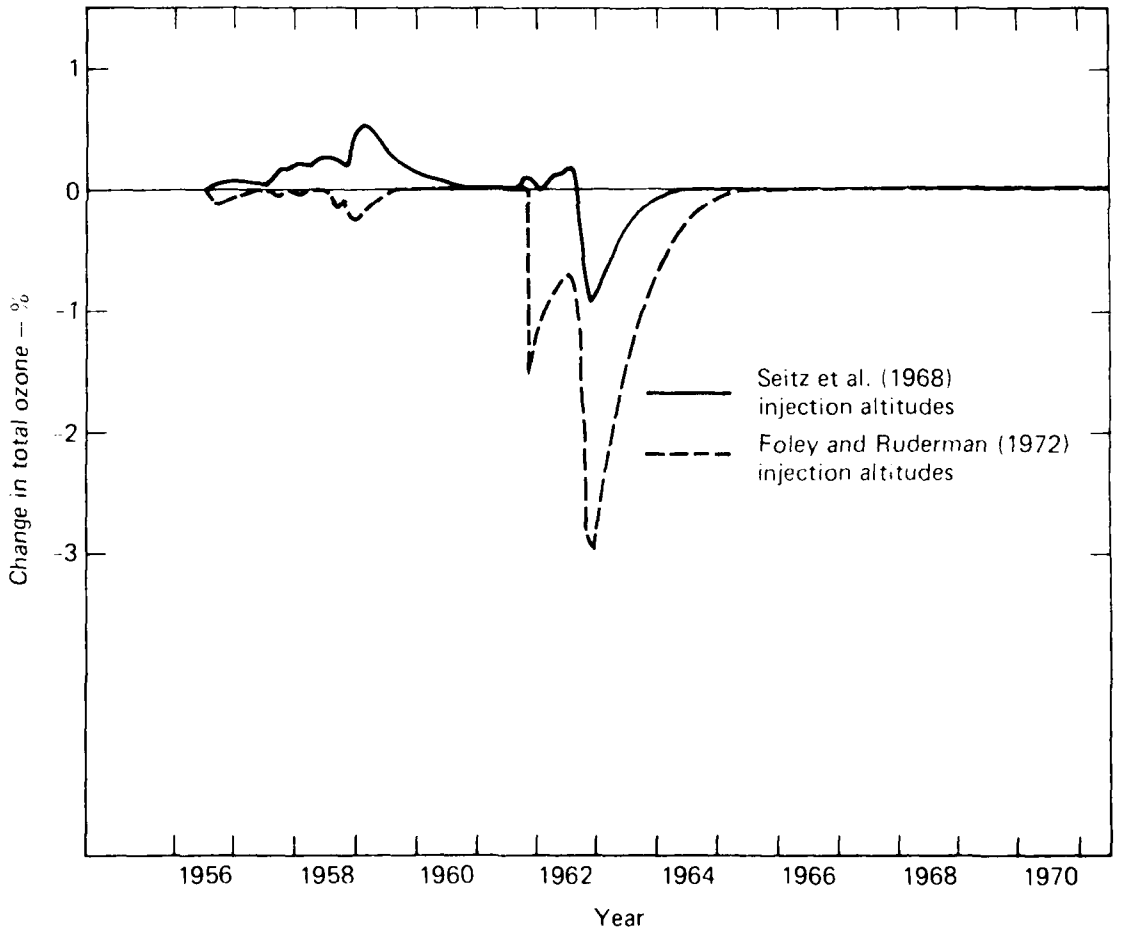

FIG. 1. Computed change in total ozone resulting from atmospheric nuclear testing during 1950's and 1960's.

clearly within the observed variability in the ozone record as analyzed by Angell and Korshover (1978).

Figure 2 gives the computed changes at selected altitudes. The ozone concentration decreases at all altitudes above 25 km. However, at lower altitudes the concentration of ozone was computed to increase significantly, which accounts for the net increase in total ozone prior to 1962 shown in Fig. 1. Some of these computed changes are much larger than the change in the ozone column. However, the predicted ozone variations at specific altitudes are still only about the same magnitude as the variations in ozone concentrations determined by the Umkehr technique.

Thus, the model-predicted response to the atmospheric nuclear tests does not lead to conflict with the ozone record, but it also does not seem to explain much of the observed ozone variation. The predicted effect on ozone of the nuclear tests should be considered in any attempt to model ozone variations during the 1960's since the predicted changes in ozone at specific altitudes are comparable to both the observed variations and to the variations calculated for such phenomena as the hypothesized variation of ultraviolet light tied to the solar cycle, or the predicted change in ozone from CFM production through 1978.

Polar Cap Absorption Events. Crutzen *et al.* (1975) noted that large polar cap absorption (PCA) events should produce significant quantities of NO_x in the middle and upper stratosphere, especially at high latitudes. Indeed the PCA events of August 1972 were estimated to have produced several times as much NO_x as the ambient content of the atmosphere in the region above 40 km. In a comparison with Nimbus 4 ozone data, Heath *et al.* (1977) found that the agreement between predicted ozone change and observation was quite good north of 75° latitude and above 4 mb (the model underpredicted the perturbation by roughly 30%). Since those calculations were made, several important changes in model chemistry have occurred. However, these changes have had only a modest effect on the sensitivity of the model to large injections of NO_x at high altitude and high latitude. There are two recent recalculations of the effect of the August 1972 PCA event in the literature. Fabian *et al.* (1979) found that their computed ozone change was in excellent agreement with observation if more recent estimates of the NO production per ion-pair are used. However, the agreement between observation and computation at lower latitudes was less satisfactory, although still qualitatively encouraging. Borucki *et al.* (1978) report similar findings, and also find that their model substantially underpredicts the ozone perturbations at altitudes near 30 km.

The August 1972 PCA events seem to provide a useful test of the short-term (several days) response of stratospheric ozone to NO_x increases above about 40 km. Unfortunately, the test is not directly applicable to lower altitude, midlatitude NO_x perturbations occurring over long (several-year) time periods. The nature of the NO_x injection and of the O_3 data do not permit resolution of questions about the adequacy of model simulations of transport phenomena or of the chemistry of the lower stratosphere. Thus, PCA events provide the only phenomenon for which models forecast an observable and observed stratospheric ozone perturbation in response to an NO_x change, but the nature of the perturbation and the response differ from the problems associated with SST operations to an extent that precludes its direct use as a calibration point for SST predictions of column ozone changes. Nonetheless, the good agreement above 40 km is encouraging since it suggests at least that models are adequately representing the short-term response of ozone to NO_x injections at higher altitudes.

The Solar Eclipse on February 26, 1979. In addition to ozone observations, measurements of other minor constituents during a solar eclipse could provide validation of the short time constant chemistry in atmospheric models. Consequently, experiments for upcoming solar eclipses, when properly supported by theoretical analysis, could contribute significantly to our understanding of atmospheric chemistry. In fact, given the proper data on trace species concentrations during an eclipse, such measurements could provide a direct demonstration that the currently proposed major reactions of NO_x, HO_x, and ClX species are indeed concurrently functioning in the stratosphere in the manner suggested by laboratory chemistry. However, the measurements yield little information about slower processes that can have large effects on model sensitivity to perturbations.

We have examined theoretically (Wuebbles and Chang, 1979) the expected effect of a solar eclipse on stratospheric minor constituents. Primary emphasis was given to the total eclipse that occurred

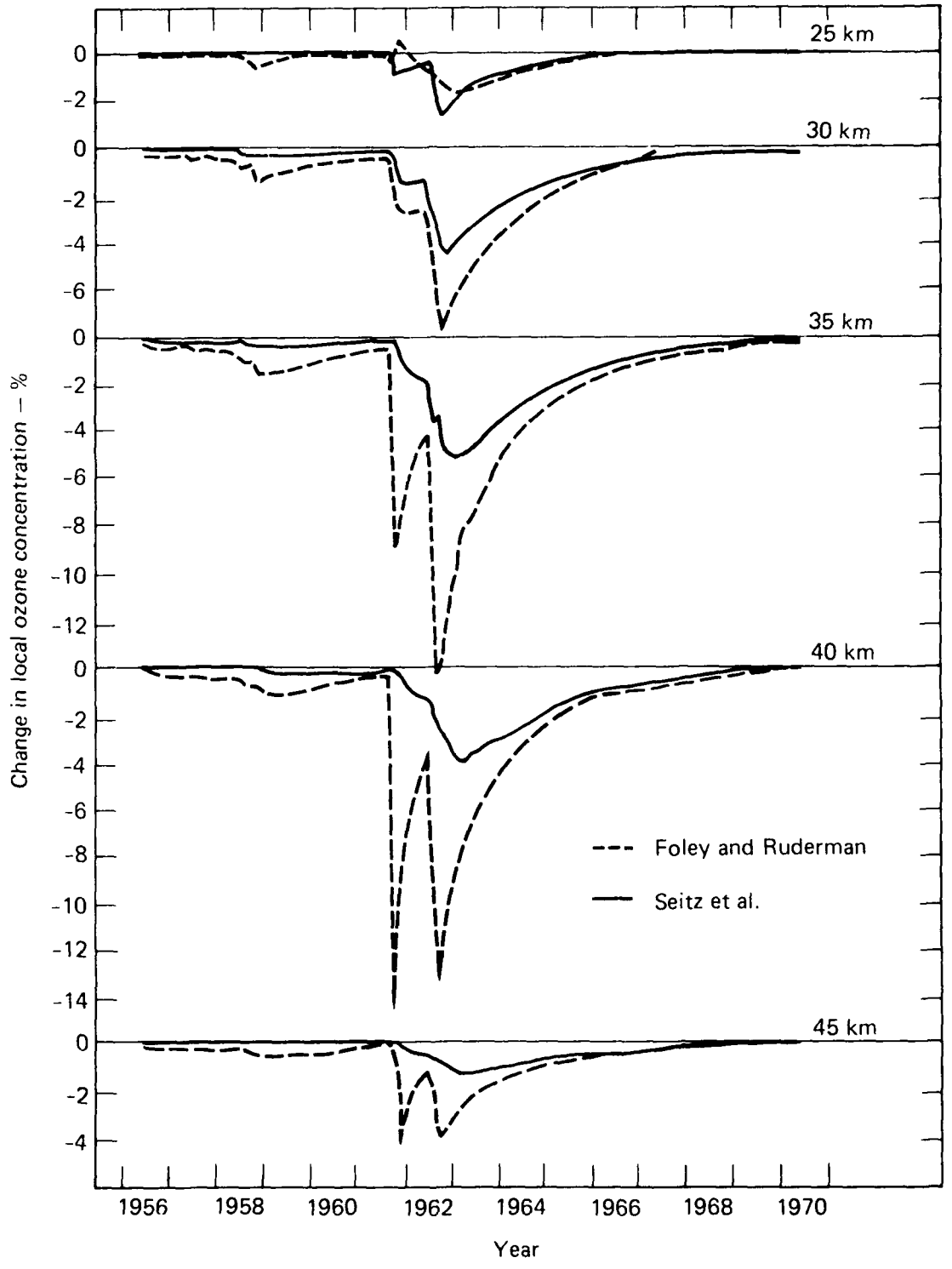

FIG. 2. Computed change in local ozone concentration at various altitudes resulting from atmospheric nuclear testing during 1950's and 1960's.

over North America on February 26, 1979. Variations similar to those computed for this particular case should be expected for other total eclipses. Totality was the longest (approximately 3 minutes) at 50°N latitude for the February 1979 eclipse.

While ozone, tropospheric water vapor, and temperature were held fixed in the model for most of our eclipse calculations, the model was also run with calculated ozone to examine the expected response of ozone to an eclipse. Our analysis has shown that fixing the ozone distribution does not significantly affect the temporal variations calculated for other species during the eclipse. Solar flux variations during the eclipse were based on Hunt (1965).

Those species having chemical lifetimes less than a few hours are expected to vary significantly from normal diurnal behavior during a solar eclipse. Local concentrations of the species could be quite variable, and therefore we should focus on relative changes rather than absolute magnitudes.

The model-calculated response of ozone during an eclipse essentially agreed with Hunt (1965). A significant increase in O_3 is to be expected in the upper stratosphere and in the mesosphere as a result of the conversion of $O(^3P)$ to ozone through the reaction $O(^3P) + O_2 + M \rightarrow O_3 + M$ accompanied by decreased photolysis of O_2 and O_3. The maximum increase in O_3, found at the end of totality, was computed to be 15% and 45% at 50 and 55 km, respectively. Larger fractional changes are expected in the mesosphere. Since most of the atmospheric ozone is at lower altitudes in the stratosphere, an insignificant change in the total ozone column is expected. Significant changes were also predicted to occur in NO, NO_2, Cl, ClO, OH, and HO_2 concentrations.

The results of this study suggest that significant and detectable variations are expected for some of the important stratospheric minor constituents during a solar eclipse. Such observations, particularly simultaneous observations of trace species, would demonstrate clearly the simultaneous functioning of the various important photochemical catalytic cycles in the stratosphere.

The model calculations were completed prior to the eclipse. Measurements during the solar eclipse of February 26, 1979, were made with NASA's aircraft. This plane carried instruments to measure NO, O_3, and temperature at 20 km (instrument of Starr, Craig, and others of NASA-Ames) and to measure the NO and NO_2 columns above 20 km (by David Murcray of University of Denver). Preliminary results by Starr and Craig show no change in O_3 at 20 km during the eclipse (as was predicted), and they show excellent agreement with the theoretically expected change in NO. A detailed comparison between this measurement and model calculations is being made. In any case, the results demonstrate that the reactions $NO + O_3$ and $NO_2 + h\nu$ occur in the stratosphere at rates similar to those computed theoretically.

2.2 POTENTIAL CHANGES IN OZONE CAUSED BY AIRCRAFT EMISSIONS

Emission Indexes and Fleet Projections

We consider the potential effects on atmospheric ozone of several different aircraft emissions scenarios. These emission scenarios were developed for three basically different applications: (1) the projected 1990 fleet, (2) a commercially viable fleet of supersonic transports, and (3) a commercially viable fleet of hypersonic transports. In all of the perturbation calculations discussed, the "ambient" or "unperturbed" atmospheric conditions refer to the model-calculated initial state rather than to atmospheric measurements.

1990 Fleets. We developed emission profiles for both high and low projected 1990 aircraft fleet sizes. In the case of the projected 1990 high fleet, we adopted the emissions factors and fleet projections used by Oliver *et al.* (1977) in their Table 2.33. The projection used by Oliver *et al.* (1977) was based on A. D. Little, Inc. (1976) with corrections to the mean flight altitude of the projected SST fleet of 142 Concordes and TU 144's and an emissions factor four times larger than used by A. D. Little, Inc. (1976) for CF6 engines (which Oliver *et al.*, 1977, treated as having the same emissions indexes as JT9D engines). The NO_x emission index for SST's was assumed to be 20 g NO_2/kg fuel.

In converting the projected emissions in Table 2.33 of Oliver *et al.* (1977) to a format compatible with the one-dimensional model, we treated the model as a Northern Hemisphere model, summed emissions over all latitudes between zero and 90°N at a given altitude, and converted kg/year at each altitude to molecules cm^{-3} s^{-1} over a 1-km-thick layer centered at even-kilometer altitudes. Table 1 gives the emission rates used in our calculation.

TABLE 1. Projected 1990 aircraft emissions of NO_x [Oliver *et al.* (1977) high estimate]; low estimate of emission rates equals 0.633 times high estimate.

Injection altitude (km)	NO_x injection rate total fleet (molecules $cm^{-3}s^{-1}$)	NO_x injection rate subsonic only (molecules $cm^{-3}s^{-1}$)
6	90	90
7	179	179
8	265	265
9	665	665
10	1167	1167
11	1161	1161
12	520	520
13	75	75
14	18[a]	12
15	18	—
16	33	—
17	43	—
18	29	—
19	8	—

[a]Emissions from the SST fleet are included at 14 km and above.

We also examined the effects of the projected subsonic fleet without the SST contribution using the emissions given in Table 1 for the subsonic fleet only. We generated a 1990 low estimate by multiplying the 1990 high estimate emissions by 0.633, the ratio of the 1990 low estimate fuel usage to the 1990 high estimate fuel usage given in Table 2.25 of Oliver *et al.* (1977).

SST Fleets of Commercially Viable Size. In treating hypothetical SST fleets of commercially viable magnitude, we have considered a fleet emitting 1000 molecules of NO_x $cm^{-3}s^{-1}$ and 1.77×10^5 molecules of H_2O $cm^{-3}s^{-1}$ over a 1-km-thick layer in the Northern Hemisphere, which is equivalent to 6.2×10^8 kg of NO_x (as NO_2) and 4.3×10^{10} kg of H_2O per year. These emission rates correspond to a fuel usage of 3.5×10^{10} kg yr^{-1} by SST's, assuming the emission indexes are 18 g NO_2/kg fuel and 1.25 kg H_2O/kg fuel. The NO_x emissions index for currently realizable SST engines has been estimated to be as high as 22 g NO_2/kg fuel or as low as 15.6 g NO_2/kg fuel. A still unresolved discrepancy exists between spectroscopic and probe sampling methods of determining NO_x in aircraft exhaust (Oliver *et al.*, 1977). If the spectroscopic analyses are correct, the above-cited emission index should be increased by a factor of 2 to 3 for SST operations.

Future technologies may be capable of reducing the NO_x emission index by several fold. A threefold reduction in the NO_x emission index is projected for some existing design concepts (Popoff *et al.*, 1978). We consider NO_x emission indexes of 18 g NO_2/kg fuel for current technology and 6 g NO_2/kg fuel for future technology.

The number of SST's corresponding to a fuel usage of 3.5×10^{10} kg yr^{-1} is difficult to determine on an absolute scale. The number of SST's corresponding to a given fuel usage is inversely proportional to the expected hours/day of flight and the fuel usage per hour. Estimates of the hours per day of flight at cruise altitude have varied from 4.4 to 7.5 hr. Estimates of fuel usage have ranged from 16,800 to 19,100 kg/hr for the Concorde; from 52,000 to 60,000 kg/hr for the B2707; and as low as 44,000 kg/hr for a hypothetical advanced design similar to the B2707 (Popoff *et al.*, 1978). Thus, more than a two-fold variation in engine emissions from a projected SST fleet is possible based on different estimates of aircraft operation and fuel consumption rate. A fuel usage of 3.5×10^{10} kg yr^{-1}, therefore, corresponds to about 750–1000 Concordes, or 180–660 advanced SST's. Thus, our standard emissions rates are compatible with a large fleet of SST's.

Hypersonic Transport Emissions. In addition to the effects of subsonic and supersonic fleets, we projected a range of emissions and environmental impacts of a possible hypersonic transport (HST) fleet. For this purpose, we adopted the emissions indexes given in CIAP Monograph 2 (1975), Chapter 6 for a fleet of research HST's of gross takeoff weight 2.27×10^5 kg operating at Mach 8 and cruise altitude of "36.68" km. According to data in CIAP Monograph 2, the hypothesized HST operations would consist of an initial acceleration to hypersonic speeds (and cruise altitude) using rocket engines, followed by about five minutes of SCRAMjet operation, followed by a cruise-mode during which most emissions would consist of liquid hydrogen boil-off for cooling. The SCRAMjet would use 670 kg/flight of liquid H_2; the rocket engines would use 2450 kg/flight of liquid H_2, and 14,650 kg/flight of liquid oxygen (CIAP Monograph 2, p. 6–7); but it would only release a total of 1650 kg/flight of water vapor and 615 kg/flight of H_2 (CIAP Monograph 2, p. 6–8). Thus, the fuel use and emissions estimates given in CIAP

Monograph 2 for rocket operations are incompatible, with not enough mass being emitted. This difficulty would be resolved by increasing the water-vapor emissions by a factor of 10. Cooling at cruise altitude would consume an additional 309 kg of liquid hydrogen per flight.

The emissions consist of H_2O, H_2, H, OH, NO, and O as given in Table 2. In analyzing the effects of HST emissions, only cooling and SCRAMjet emissions were treated, and these were based on the data presented in Table 6–9 of CIAP Monograph 2. Rocket emissions were neglected since much of the rocket emissions would occur in the troposphere. In order to approximate a commercially viable fleet, we increased the emissions to correspond to an HST fleet with 1000 flights/day. Because even these emissions are relatively small, and the CIAP-Monograph-2-based emissions estimates may not apply to commercial-scale fleet operations (they are based on research flights), we also examined the effects of a 10-fold larger emission, perhaps interpretable as longer flights or flights of heavier aircraft. The emissions of H_2O, H_2, NO, and OH were treated simply as a source of the molecules in question. Emissions of H-atoms (the code calculates H-atoms as an equilibrium species) were treated as emissions of an equivalent number of HO_2 molecules, while the small emissions of O atoms were ignored.

Because NO_x emissions are responsible for the major portion of the predicted change in total ozone, it might be attractive to use more than the stoichiometric amount of OH in the SCRAMjets in order to reduce NO_x emissions. According to CIAP Monograph 2, operating at a stoichiometric ratio of 1.5 instead of 1 would reduce NO_x emissions by more than a factor of 3 while increasing H_2O and H_2 emissions by factors of about 1.1 and 3, respectively. The net effect of these changes in emissions should be a smaller ozone perturbation.

We wish to emphasize that we performed no independent calculations of HST emissions indexes, and that the fleet projections are no more than crude parametric estimates of the approximate level of activity that might be associated with a mature, commercially successful fleet of HST's. If specific aircraft designs were to be proposed, the emissions should be independently projected.

Aircraft Assessment Results

The LLL one-dimensional transport-kinetics model has been used to assess the potential chemical effects of aircraft engine emissions in the troposphere and the stratosphere. Calculations were

TABLE 2. HST emissions on a per-flight basis. Data from CIAP Monograph 2, Ch. 6, assuming cruising speed of MACH 8, cruise altitude of 36.68 km, and H_2:O_2 ratio of 1.

	Emissions per flight		Altitude (km)	Emission rate for 1000 flights/day (molecules $cm^{-3} s^{-1}$)[a]
	(kg)	(moles)		
SCRAMJet				
H_2O	5705.0	317,000	36.68	8504
H_2	136.7	68,350	36.68	1820
H	13.1	13,100	36.68	350
OH	132.3	7,800	36.68	210
NO	137.4	4,500	36.68	123
O	34.4	2,150	36.68	58
Rocket (not included in calculation)				
H_2O[b]	16,500	917,000	0-36 mostly tropospheric	—
H_2	615	307,500	0-36	—
Cooling in flight				
H_2	308.5	154,200	36	4130

[a] Emissions in a 1-km-thick layer.

[b] H_2O emissions from rocks have been increased by a factor of 10 to permit mass balance.

made using projected fleet sizes for subsonic and supersonic aircraft as well as for a range of emission rates at particular injection altitudes. In order to determine the effect of uncertainties in various input parameters on the assessment calculations, several sensitivity studies were also performed and are reported in the following section.

Subsonic and Supersonic Aircraft Fleets. The altitude of injection has a significant effect on the computed change in ozone because of the increase in residence time with altitude and because of the variation with altitude of the dominant chemical reactions and cycles. Table 3 shows the effect on total ozone at steady state of the same NO_x injection rate at different injection altitudes. An injection rate of 1000 molecules $cm^{-3}s^{-1}$ over a 1-km-thick layer was used for NO_x, and there was no injection of H_2O.

Injections of NO_x over the altitude range of 7 to 20 km resulted in a net increase in total ozone in each case. The change in total ozone increased with increasing injection altitude for the troposphere and lower stratosphere. Throughout this region HO_x chemistry is the dominant chemical destruction process for ozone. When HO_x chemistry is more efficient than NO_x catalytic destruction of ozone, injections of NO_x lead to a net increase in odd oxygen production through the reaction sequences:

$$\begin{aligned} &NO + NO_2 \rightarrow NO_2 + OH \\ &NO_2 \xrightarrow{h\nu} NO + O \\ &\text{net} \quad HO_2 \rightarrow OH + O \end{aligned} \qquad (1)$$

and

$$\begin{aligned} &NO_2 + OH \xrightarrow{M} HNO_3 \\ &OH + HNO_3 \rightarrow H_2O + NO_3 \\ &NO_3 \xrightarrow{h\nu} NO_2 + O \\ &\text{net} \quad 2OH \rightarrow H_2O + O \end{aligned} \qquad (2)$$

The reaction sequence in Eq. (1) acts to shift HO_x more toward OH, thereby increasing the conversion of OH and HO_2 to H_2O by the reaction $HO_2 + OH \rightarrow H_2O + O_2$. Reaction sequence in Eq. (2) acts to reduce HO_x as OH and HO_2 are converted to H_2O and HNO_3. Conversion to H_2O, and to a lesser extent HNO_3, acts as a sink for HO_x, since the chemical lifetimes of these reservoir species can be long compared to the time for transport into the troposphere. Injections of NO_x act to increase the rates of the above reactions. The net effect of reaction sequences (1) and (2) is a reduction of HO_x and an increase in odd oxygen production, both of which contribute to an increase in ozone. Of course, the odd-hydrogen species may have been generated through reaction of $O(^1D)$ with H_2O. If this is the case, the odd oxygen produced via (1) or (2) only regenerates that used in the initiation of a catalytic cycle. It is important, nonetheless, because these sequences compete for HO_x with odd-oxygen destroying sequences.

Increases in NO_x concentration in the upper stratosphere lead to a reduction in ozone concentration in this region due to the greater importance of the NO_x catalyzed ozone destruction at these altitudes. The 20-km injection of NO_x resulted in a smaller net increase in total ozone than did the 17-km injection case, since more NO_x reached the upper stratosphere causing a greater reduction in ozone concentration at high altitudes relative to the increase at lower altitudes. This effect was found to be sensitive to the shape of the K_z profile used, however.

The standard model uses fixed-value boundary conditions for all species (except CCl_4) at the ground. Using flux boundary conditions for the species N_2O, CH_4, CH_3Cl, and HCl, resulted in slightly larger increases in total ozone (approximately 0.1% in absolute change) when compared to the fixed boundary condition case. Consequently, the choice of boundary condition has only a very small effect on the assessment results. Fixed-value

TABLE 3. Change in total ozone resulting from NO_x injection of 1000 molecules $cm^{-3}s^{-1}$ distributed over a 1-km-thick layer centered at injection altitude. Calculations were made using 1979a chemistry (Appendix A).

Injection altitude (km)	Change in total ozone (%)
7	0.25
9	0.40
11	0.64
13	0.84
17	1.34
20	1.31

boundary conditions are used in the model calculations unless otherwise noted.

The model was tested for interference effects by comparing the effect of simultaneous injections at the various injection altitudes given in Table 3 with the sum of the changes in ozone for individual injection altitudes. Table 4 shows that there is a destructive interference. That is, the simultaneous injections resulted in less change in total ozone than the sum of the changes caused by individual injections. This implies that summing the results of separate calculations for subsonic and supersonic fleets will not give the same answer as considering the effect of the two fleets simultaneously.

The effect of NO_x emissions by subsonic and supersonic fleets projected for 1990 are given in Table 5. Using the high estimate of the fleet sizes, the effect of subsonic and supersonic aircraft combined is estimated to be an increase in total ozone of 2.01%. This number represents the steady state change in ozone due to constant NO_x emission rates at the rates estimated for 1990. The subsonic fleet alone (injection altitudes up to 14 km) is estimated to cause an increase in total ozone of 1.86%. The small effect of the supersonic fleet is due primarily to the small fleet size projected for 1990. Using the lower estimate for fleet emissions, the corresponding numbers for ΔO_3 are 1.39% for the combined fleets and 1.29% for the subsonic fleet alone.

It should be noted that the effects of the existing 1979 subsonic fleet are of the order of a 0.5% increase in total ozone. This effect is not negligible when compared to the estimated present-day effects of CFM's. Thus, an accurate assessment of the effects of subsonic aircraft will be important in interpreting ozone data for trends due to other anthropogenic influences.

The changes in ozone concentration for the high and low estimates of subsonic and supersonic fleet emissions are shown in absolute concentration in Fig. 3. The largest absolute increase in ozone concentration occurs near 12 km, and the region of increasing ozone extends up to about 26 km. Between 26 and 39 km there is a small decrease in ozone concentration.

TABLE 4. Synergism test using fixed boundary conditions and 1979a chemistry.

Case	ΔO_3 (%)
Simultaneous injections	3.68
Sum of individual injections	4.78

TABLE 5. Computed change in total ozone at steady state using NO_x emission estimates for 1990 subsonic and supersonic fleets (1979b chemistry).

Case	Change in total ozone (%)	
	Subsonic and supersonic	Subsonic only
Oliver *et al.* (1977) high 1990 fleet estimate	2.01	1.86
Low 1990 fleet estimate	1.39	1.29

It should be recognized that the bulk of the ozone change calculated for the subsonic fleet occurs in the upper troposphere. As a result, it is sensitive to the treatment of such poorly understood phenomena as wet and dry removal processes and surface boundary conditions for rarely measured species. The tropospheric pressures differ from the pressure conditions used in most direct measurements of chemical rate coefficients (to a greater degree than stratosphere pressures). Heterogeneous reactions, which might have a significant effect on the calculations, are not included, and the one-dimensional treatment is not as good an approximation for the troposphere as it is for the stratosphere because of the strong latitudinal and longitudinal gradients in many trace species. Thus, the results for the 1990 fleet estimates are suggestive but are not definitive.

Assessments of potential changes in ozone due to future large fleets of supersonic transports have focused on injection altitudes of 17 and 20 km. In updating these assessments, we have assumed an emission index of 18 g/kg fuel for NO_x and 1250 g/kg fuel for H_2O. These emission indexes are based on current engine technology. It may be possible through future advances in technology that the NO_x emission index could be reduced to 6 kg (one-third of present value). Calculations of ΔO_3 given a constant fuel consumption rate at cruise altitude (3.5×10^{10} kg/yr in a hemispheric shell) are shown in Table 6 for different emission indexes. The NO_x emission rate of 1000 molecules $cm^{-3}s^{-1}$, which roughly estimates the emissions from a commercially viable fleet, was chosen as a reference case. The equivalent annual hemispheric injection rates of NO_x and H_2O are given in Table 7.

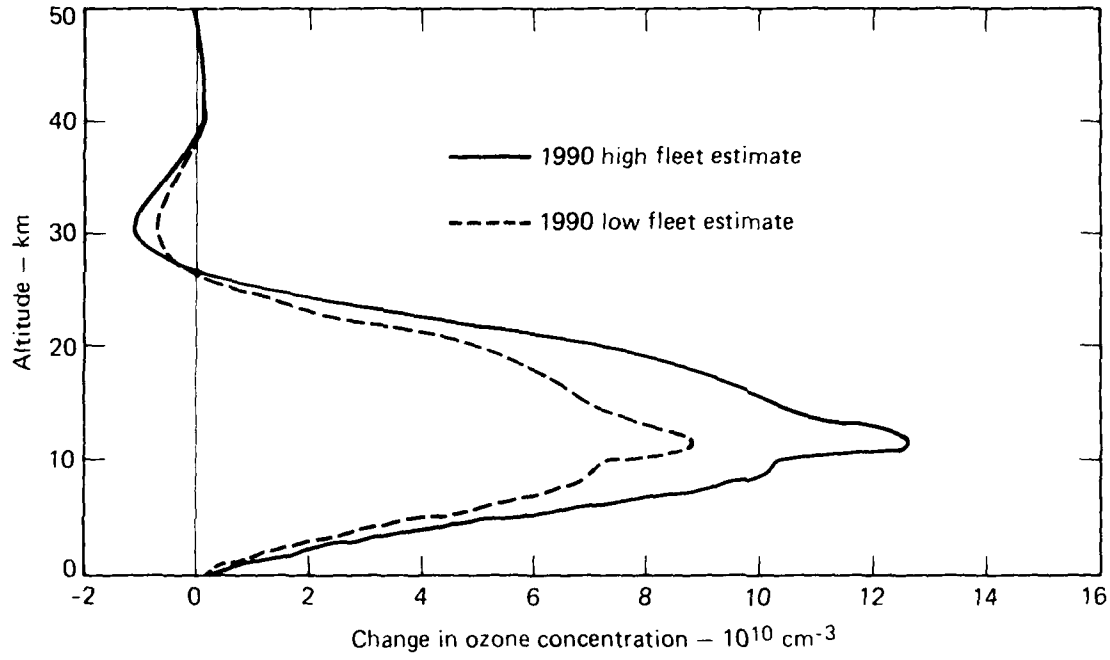

FIG. 3. Change in ozone concentration expressed as molecules cm^{-3} (1979b chemistry) computed for 1990 high and low fleet estimates.

TABLE 6. Change in total ozone due to NO_x and H_2O emissions distributed over a 1-km-thick layer centered at injection altitude.

Injection altitude (km)	Injection rate (molecules cm^{-3}s^{-1})		Change in total ozone (%)	
	NO_x	H_2O	1979a Chemistry	1979b Chemistry
17	1000	0	1.34	1.25
17	1000	177,000	1.18	—
17	333	177,000	0.32	—
20	1000	0	1.31	1.14
20	1000	177,000	0.91	—
20	333	177,000	0.07	—

For each of the perturbations considered, there was an increase in total ozone. When the water vapor injection is included with the NO_x injection, there is less of an increase in total ozone because of the additional ozone destruction caused by HO_x which is produced from dissociation of H_2O. Even for the advanced technology case (reduced NO_x emission), the increase in total ozone due to the NO_x injection is greater than the reduction due to the H_2O injection, the net effect being a very small increase in total ozone.

TABLE 7. Equivalent annual hemispheric injection rates for various NO_x and H_2O emissions.

Species	Injection rate (molecules cm^{-3}s^{-1})	Injection rate (kg/yr)[a]
NO_x	333	2.1×10^8
NO_x	1,000	6.2×10^8
H_2O	177,000	4.3×10^{10}

[a]Hemispheric injection assuming uniform injection over a 1-km-thick layer.

Hypersonic Transport Fleet. The hypothesized hypersonic transport fleet making 1000 flights per day was calculated to cause a -0.218% change in the ozone column. Emissions from a fleet ten times larger were calculated to cause a -2.06% change in the ozone column. The NO_x emissions from the latter fleet by themselves caused an ozone change of -2.13%.

Figure 4 shows the local percentage changes in ozone vs altitude for the 10,000 flight per day HST emissions and the NO_x emissions alone from 10,000 flights per day of HST's. (Because ΔO_3 is roughly linear in emissions rate over the range considered, large fleets were chosen to avoid comparing very small local changes that might contain significant numerical noise.) As is evident, the NO_x emissions dominate the ozone changes below approximately 40 km, while H_2O and H_2 emissions are responsible for most of the ozone change at higher altitudes. Because most of the ozone column is below 40 km, the integral column change is largely a result of the NO_x emissions.

Effect of Variations in Background ClX. The effect of aircraft engine emissions on stratospheric

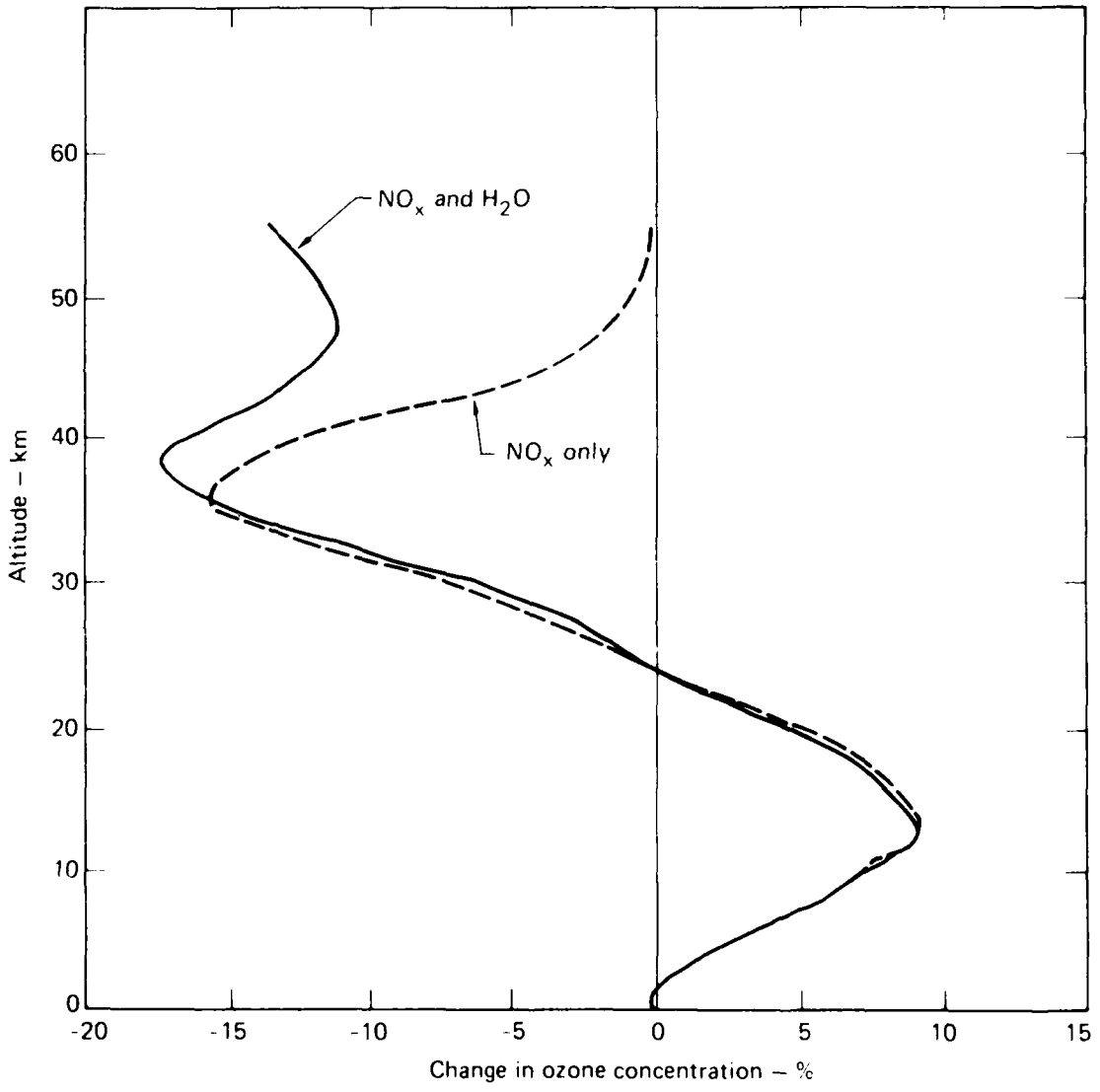

FIG. 4. Change in ozone concentration caused by HST emissions for a fleet with 10,000 flights per day (1979b chemistry).

composition is coupled with other stratospheric perturbations. As chlorofluoromethanes (CFM's) continue to be released to the atmosphere, there will be a gradual increase in the background concentration of ClX (Cl + ClO + HCl). Model calculations indicate a present day stratospheric ClX concentration of more than 1 ppbv. Assuming CFM releases at the 1976 release rate indefinitely into the future, the background ClX concentration is projected to increase to 2 ppbv around 1990 and to 4 ppbv around 2020. To assess the effect of changes in background ClX concentration on the model sensitivity, several NO_x perturbation calculations were repeated using a range of ClX concentrations. The results are shown in Table 8. In each case the ClX concentration was held constant. So the change in total ozone is the steady state value for a constant injection rate (i.e., the ΔO_3 value does not pertain to any particular year) relative to a natural atmosphere with the same ClX concentration.

Table 8 shows that the change (increase) in total ozone resulting from an NO_x injection increases as the ClX concentration increases. The reason for the increase in ΔO_3 is related to the mechanism by which an NO_x injection leads to an increase in total ozone. The increase in total ozone comes about because for these magnitudes of NO_x injections, NO_x interferes with the more efficient ozone destruction by HO_x and ClX. Increasing the background ClX concentration means that there is more ozone destruction by ClX in the ambient case, so there is more that can be interfered with by the injected NO_x.

Effects of Uncertainties in Chemical Rate Coefficients. Probably the best method for assessing the sensitivity of model predictions to errors in the inputs that describe fairly well understood quantities (e.g., rate constants for which experimental precision is the dominant source of error) is a Monte Carlo calculation (e.g., Stolarski *et al.*, 1978). As yet, no such calculation has been carried out for a perturbation resulting from aircraft operations. In part this reflects the hypothesis that prediction error is dominated by systematic error in poorly understood reactions.

Even a full sensitivity analysis (like that of Butler, 1979) has not yet been performed. The most recent sensitivity study on the NO_x system was a partial sensitivity analysis carried out in 1975 by Duewer *et al.* (1976, 1977). The major conclusions of that study were that large prediction errors were possible, and that a few reactions dominated the error. Subsequent events have shown these conclusions to be valid. The large changes in model sensitivity to NO_x injection that have occurred have been dominated by changes in the rate coefficients for the five reactions that were identified as plausible sources of error in the 1975 and 1977 reports. In the intervening years, many rate coefficients have been determined or redetermined with substantially improved accuracy. For the majority of the reactions in the model, experimental precision is probably a reasonably good estimate (as well as a lower bound) to the actual error in the measured rate, and model predictions are only weakly sensitive to modest errors in most rate coefficients. Nonetheless, the composite error in prediction caused by such errors could be significant, although, since it is unlikely that random errors will reinforce each other, this is not too likely to be realized.

Table 9 gives the change in O_3 calculated for several perturbations using the structure of our current model but using the rate coefficients recommended in NBS 866 (1975) and NBS 513 (1978) as well as the current results. In calculating the response for 1975 and 1977 chemistries, we excluded species (such as HOCl or HNO_4) that the LLL

TABLE 8. Effect of variations in background ClX on computed change in total ozone (1979a chemistry).

Injection altitude (km)	NO_x injection rate (molecules $cm^{-3}s^{-1}$)	Change in total ozone (%)		
		1.14 ppb ClX	1.83 ppb ClX	3.76 ppb ClX
17	500	0.65	0.72	0.89
17	1000	1.22	1.34	1.69
17	2000	2.14	2.37	3.03
20	500	0.61	0.75	1.12
20	1000	1.04	1.31	2.03
20	2000	1.42	1.91	3.28

TABLE 9. Effect of choice of rate coefficients on model sensitivity using structure of current LLL model.

Chemistry	1950 ambient O_3 (DU)	Change in total ozone (%)				
		1990 high subsonic	17-km SST[a]	20-km SST[a]	CFM 1978	CFM steady-state[b]
1975 (NBS 866)	288	-0.31	-3.94	-9.12	-0.76	-7.5
1977 (NBS 513)	366	1.43	1.20	-0.52	-0.98	-12.7
1979a (JPL, 1979[c])	324	2.01	2.57	2.18	-1.92	-19.4
1979b (NASA, 1979)	327	1.86	2.00	1.06	-1.30	-14.2

[a] NO_X injection rate of 2000 molecules $cm^{-3}s^{-1}$ over a 1-km-thick layer. Contribution to ClX due to CFM's is not included in calculations.

[b] CFM's released at 1976 rate.

[c] Rate of $OH + ClO \rightarrow HCl + O_2$ is set to zero.

model contemporary with the rate compendium in question did not include. In addition, we include the results of calculations made using the 1979a chemistry with the rate coefficient for the reaction $OH + ClO \rightarrow HCl + O_2$ set to zero.

The conclusion to be drawn from Table 9 is that over the last five years, changes in evaluated recommendations for chemical rate coefficients have resulted in substantial changes in the model predicted response to perturbation, and that even recent recommendations appearing a few months apart carry a significant amount of uncertainty. (However, the differences between model predictions are not such as to change any qualitative conclusions if one restricts one's self to post-1976 models with consistent physics.)

A comparison of the results in Table 9 with the results of LLL calculations in earlier years given in Fig. 5 for some of the perturbations demonstrates that other changes in model structure have had quantitatively significant effects, but would have had little effect on the qualitative conclusions drawn from model predictions of aircraft effects. The results in Fig. 5 demonstrate the combined effects of the evolution of our understanding of stratospheric chemistry and evolution of the treatment of physical phenomena such as multiple scattering of light, the averaging of reaction rates over diurnal cycles, the treatment of boundary conditions, and the transport parameterization. Although many different factors have contributed to the variation described in Fig. 5, the evolution of model chemistry has been the most important single factor.

The uncertainty limits for reactions in the various evaluations [NBS 513 (1978), NBS 866 (1975), NASA 1010 (1977), JPL (1979), NASA 1049 (1979)] have generally become smaller when individual reactions are considered. However, over the same period, new and often highly uncertain reactions have been recognized, and it is far from obvious that the error that might be associated with rate coefficients actually included in models has gotten smaller over the last decade. Moreover, "new" reactions have been introduced to the modeling community at a fluctuating but not obviously decreasing rate.

Effect of Temperature Feedback and Hydrostatic Adjustment. In the calculations up to this point, the *U.S. Standard Atmosphere* (1976) temperature profile was used, and temperature was not allowed to change. Changes in the concentrations of species that are radiatively important (either solar or longwave) will affect the temperature profile by changing radiative fluxes and heating or cooling rates. At a given pressure level, as the temperature changes, the air density will also change as defined by the equation of state. Since chemical reaction rates are affected by changes in temperature and air density, it is important to assess the magnitude of these effects on the assessment calculation.

Air density can be computed in a one-dimensional model by assuming hydrostatic equilibrium (i.e., the pressure at any height is determined by the weight of the column of air above that point, and the air density is determined by the equation of state given the temperature). Expressed mathematically,

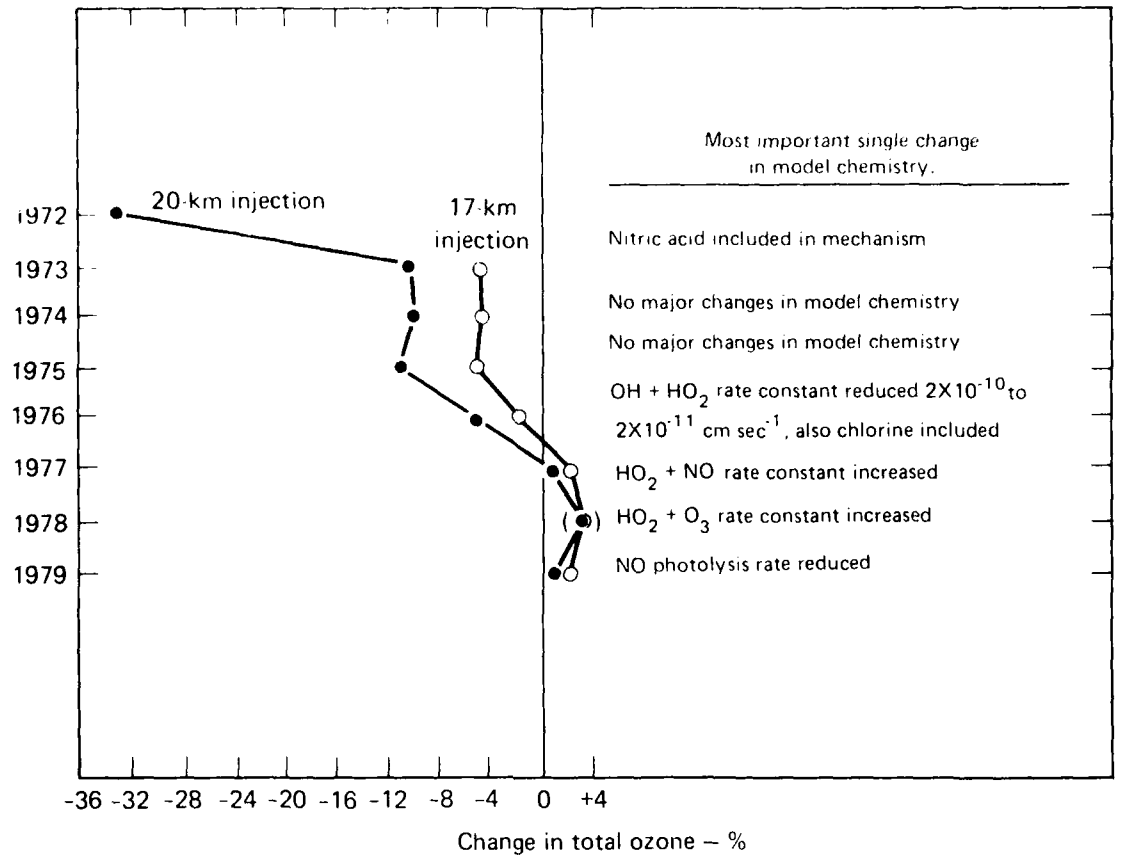

FIG. 5. Historical evolution of LLL model calculations of change in total ozone due to an NO_x injection of 2000 molecules $cm^{-3}s^{-1}$ over a 1-km-thick layer centered at either 17 km (open circles) or 20 km (solid circles). This injection rate was a standard for assessment and comparison purposes and did not pertain to any particular fleet estimate. Values for 1978 are approximate.

$$dP = -\rho g\, dz \tag{3}$$

and

$$P = \rho RT \tag{4}$$

where P is pressure, ρ is density, g is the acceleration of gravity, z is altitude, R is the gas constant and T is temperature. The temperature is computed using a radiative transfer model assuming radiative equilibrium in the stratosphere (see Appendix A). In our calculations, the temperature profile is computed above 13 km, and is specified below this altitude. Changes in surface temperature may be imposed, but they are not calculated in this version of the model. The model includes solar absorption and longwave exchange by O_3, H_2O and CO_2 along with solar absorption by NO_2 (Luther *et al.*, 1977).

We assume that the change in surface temperature is negligible. Ozone reductions of up to 30% due to NO_x injections were computed to cause less than a 0.1 K change in surface temperature by Ramanathan *et al.* (1976). An increase in the stratospheric water vapor mixing ratio of 2 ppmv is estimated to cause an increase in surface temperature of <0.2 K (Grobecker *et al.*, 1974, p. F125). Increasing the surface temperature in our model by 0.2 K causes a change in total ozone of –0.06%. Neglecting changes in surface temperature of this magnitude has no significant effect on the results.

In studying the effect of temperature feedback and hydrostatic adjustment on model sensitivity, we

considered four calculation alternatives: (1) temperature feedback with hydrostatic adjustment, (2) temperature feedback without hydrostatic adjustment, (3) constant temperature using the ambient computed temperature and pressure profiles, and (4) constant temperature using the *U.S. Standard Atmosphere* (1976) temperature and pressure profiles. The results are presented in Table 10.

The constant temperature calculation using the ambient computed temperature profile (consistent with hydrostatic adjustment) is the reference case with which to compare the effects of temperature feedback and hydrostatic adjustment. Table 10 shows that inclusion of temperature feedback leads to a larger increase in total ozone compared to the constant temperature calculation (ambient profile). When hydrostatic adjustment is included, the increase in total ozone is even larger. To understand these effects, we need to look at the change in temperature versus height.

For analysis purposes, we consider the results for an NO_x injection rate of 1000 molecules $cm^{-3}s^{-1}$ and an H_2O injection rate of 177,000 molecules $cm^{-3}s^{-1}$ at 20 km. The change in local ozone concentration is shown in Fig. 6 and the change in the temperature profile is shown in Fig. 7. The temperature increases below 20 km causing an increase in the chemical destruction rate of ozone. Thus, there is less of an increase in ozone concentration in this region when temperature feedback is included. Conversely, above 20 km the temperature decreases, thereby slowing the rates of reaction and leading to less ozone reduction in this region.

In the case with hydrostatic adjustment, the air in the 14–20 km region expands due to the rise in temperature. As the air expands it lifts the atmosphere above so that a given pressure level is raised in altitude relative to the ambient profile. Conversely, where the temperature decreases, there is contraction.

The results with temperature feedback and hydrostatic adjustment represent the most complete model calculations in terms of physical processes and feedback mechanisms. The changes in ozone concentration computed with these processes included are shown in Fig. 8 for various injection rates of NO_x and H_2O at an injection altitude of 17 km. The results for an NO_x injection rate of 1000 molecules $cm^{-3}s^{-1}$ with and without a simultaneous H_2O injection are nearly identical below 26 km. The injection of H_2O only leads to noticeable differences in the computed change in ozone concentration above 26 km.

Given the same H_2O injection rate, the results for NO_x injection rates of 1000 or 333 molecules $cm^{-3}s^{-1}$ are quite different. The lower NO_x injection rate causes much less change in ozone concentration in the middle and lower stratosphere; the relative magnitudes of the change in ozone concentration being roughly proportional to the NO_x injection rate. *This result indicates that the NO_x injection rate* is a much more important (and sensitive) parameter than the H_2O injection rate in estimating the effects of projected aircraft fleets.

Another important conclusion from Table 10 is that the choice of temperature profile in a constant temperature calculation can have a significant effect on model sensitivity. The difference between the ΔO_3 values using the ambient or the *U.S. Standard Atmosphere* (1976) temperature profile is the same

TABLE 10. Effect of temperature feedback and hydrostatic adjustment on model sensitivity (1979a chemistry).

Injection altitude (km)	Injection rate (molecules cm^{-3} s^{-1})		Change in total ozone (%)			
	NO_x	H_2O	Temperature feedback with hydrostatic adjustment	Temperature feedback without hydrostatic adjustment	Constant ambient temperature[a]	U.S. standard atmosphere temperature
17	1000	0	1.45	1.30	1.20	1.34
17	1000	177,000	1.37	1.24	1.04	1.18
17	333	177,000	0.43	0.40	0.26	0.32
20	1000	0	1.36	1.17	1.10	1.31
20	1000	177,000	1.29	1.03	0.70	0.91
20	333	177,000	0.33	0.27	-0.02	0.07

[a]The temperatures and pressures were computed at equilibrium using temperature feedback and hydrostatic adjustment; they then were kept fixed for the perturbation calculation.

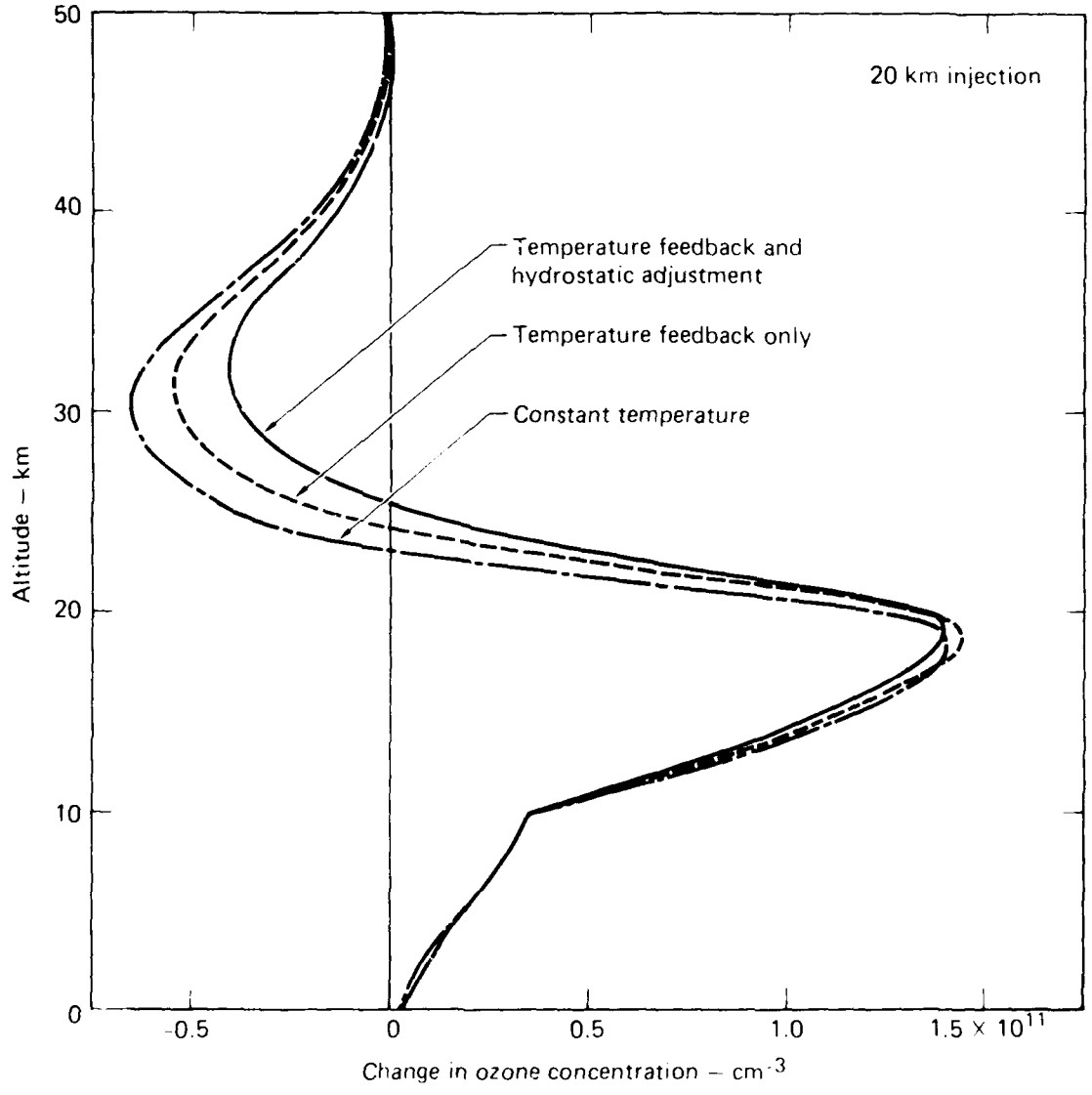

FIG. 6. Change in ozone concentration due to NO_x injection of 1000 molecules $cm^{-3}s^{-1}$ and H_2O injection of 177,000 molecules $cm^{-3}s^{-1}$ at 20 km.

magnitude as the difference between including and not including temperature feedback.

2.3 POTENTIAL CHANGES IN OZONE RESULTING FROM OTHER PERTURBATIONS

Many potentially significant perturbations to stratospheric ozone have been proposed. In order to put the effects of aircraft engine emissions presented in Section 2.2 in perspective, we present assessments for other anthropogenic perturbations. Just as the effects of aircraft emissions were shown to depend on the effects of other perturbing influences, such as the concentration of ClX and the atmospheric temperature structure, the changes in O_3 resulting from the other perturbations considered here also depend on the interference effects of multiple perturbations.

Our effort has been primarily directed toward the assessment of predicted changes for individual perturbations since future perturbation scenarios are often quite uncertain. Of the perturbation scenarios considered here, only the increases in the

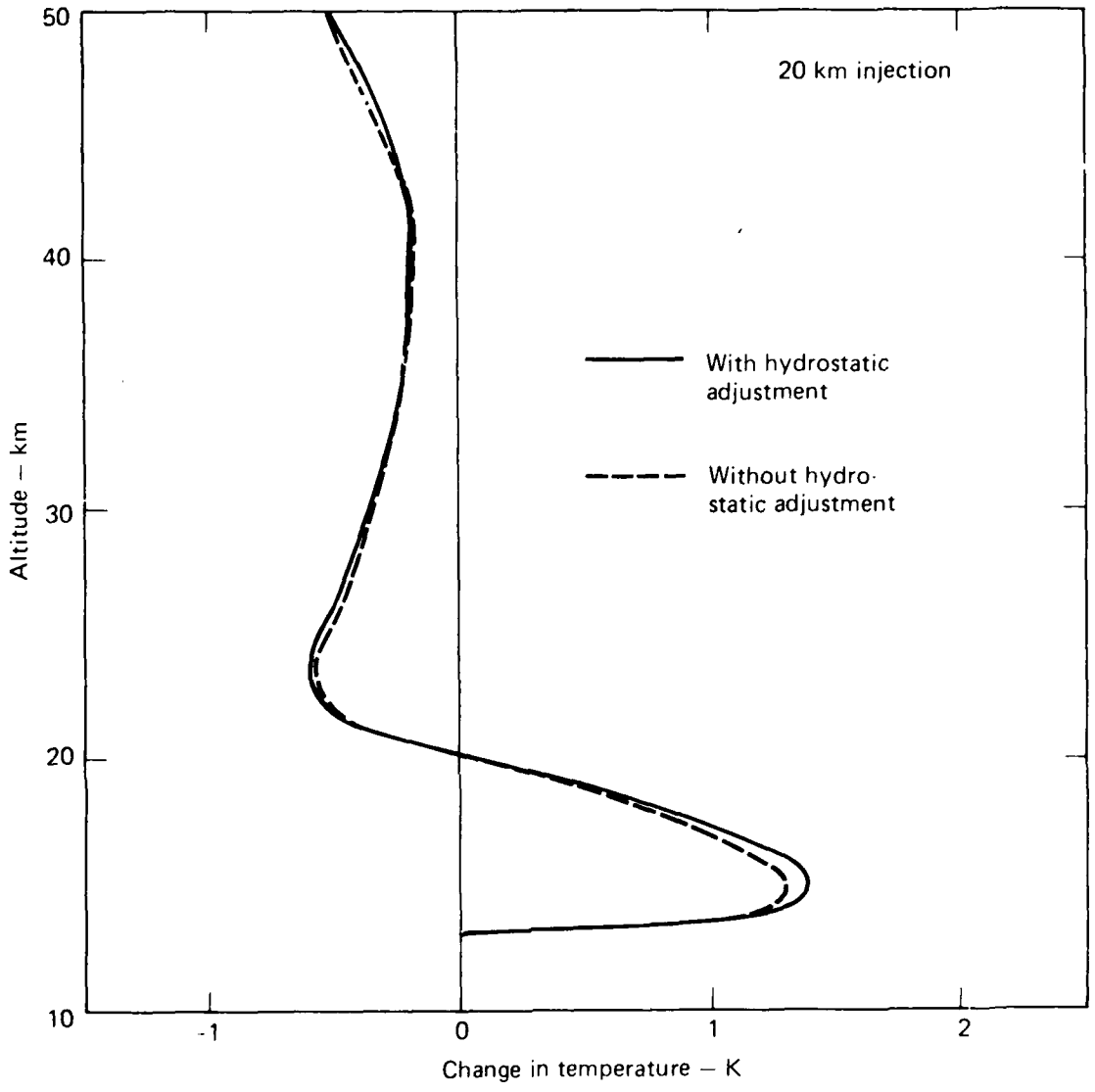

FIG. 7. Change in temperature vs altitude for 20-km injection perturbation described in Fig. 6 (1979a chemistry).

concentrations of chlorofluoromethanes and CO_2 are well established. Increases in N_2O and increases in stratospheric HC_3CCl_3 are predicted on uncertain knowledge of budgets and, in the case of CH_3CCl_3, uncertain tropospheric chemistry.

Chlorofluoromethanes

It has been firmly established that the chlorofluoromethanes, $CFCl_3$ and CF_2Cl_2, have been increasing in the troposphere and stratosphere, and the observed increase is consistent with model estimates based on the historical production rates. The CFM's are photolyzed in the stratosphere to yield free chlorine which may catalytically destroy ozone.

Quantitative estimates of the depletion of ozone have changed as models, physics, and chemistry have improved. In 1976 the predicted change in total O_3 due to steady-state production of CFM's at 1973 rates was estimated to be -7.5% (National Research Council, 1976b). In 1977 a major change in the model chemistry occurred when the rate for

$$HO_2 + NO \rightarrow OH + NO_2 \qquad (5)$$

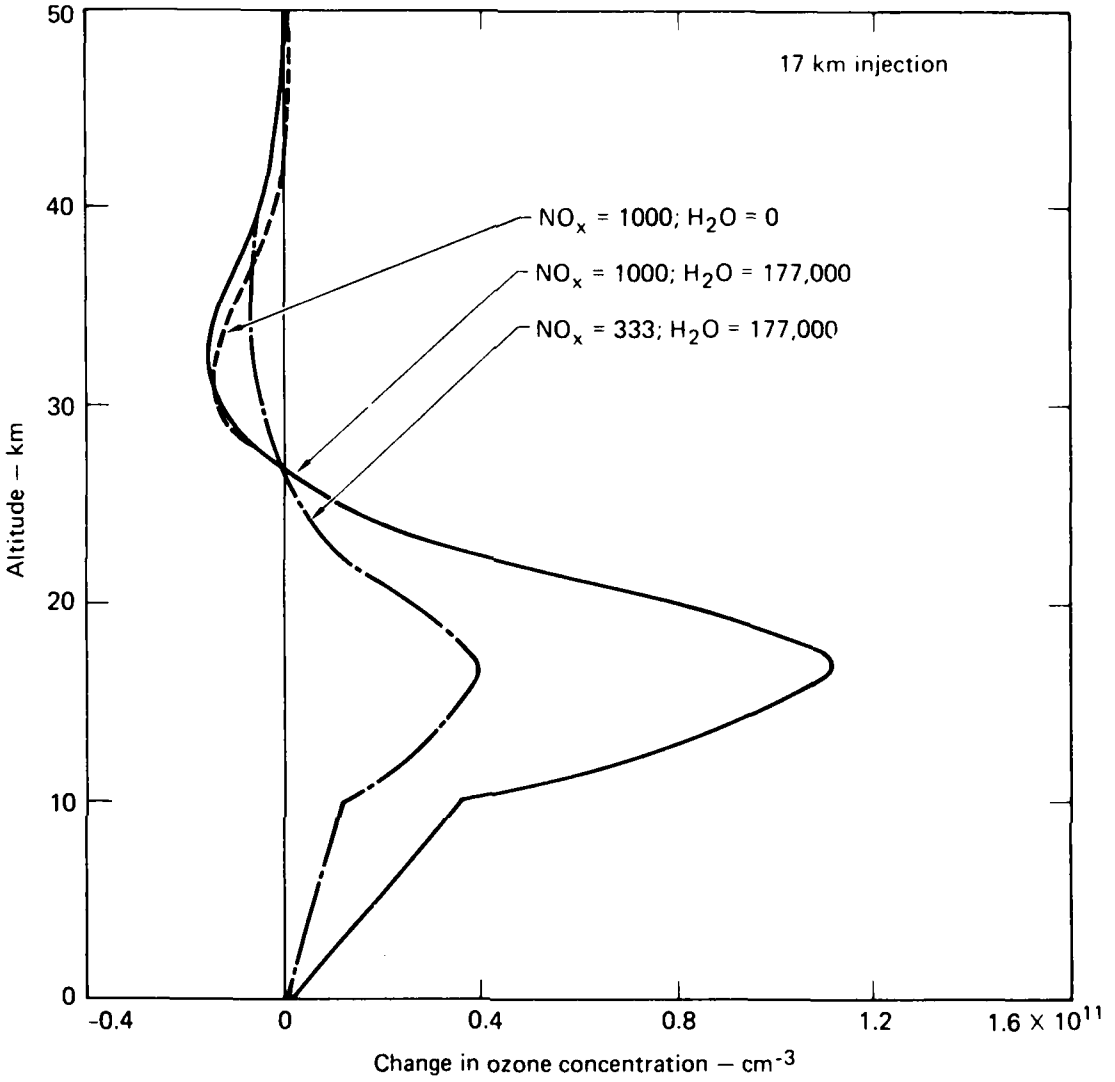

FIG. 8. Change in ozone concentration, due to various NO_x and H_2O injection rate at 17 km. Injection rates have units of molecules $cm^{-3}s^{-1}$ over a 1-km-thick layer. Calculations include temperature feedback and hydrostatic adjustment (1979a chemistry).

was measured to be almost 40 times faster than previously thought (Howard and Evenson, 1977). In addition, some models at that time adopted diurnally-averaged reaction rates and multiple scattering effects. The depletion estimates in 1977 ranged from -10.8 to -16.5% for the various modeling groups (NASA, 1977); the LLL estimate was -15.0%. With 1979b chemistry, we predict a change of -14.2% in total O_3 at steady-state assuming constant CFM production at the 1976 rates. (The 1976 production rates are 3.2% smaller for $CFCl_3$ and 2.9% larger for CF_2Cl_2 than those for 1973.)

Many changes to chemical rate constants on the order of 30% or more occurred between our 1977 chemistry and our 1979b chemistry. One major change affecting the CFM perturbation calculation was the inclusion of HOCl. HOCl is formed by the reaction,

$$ClO + HO_2 \rightarrow HOCl + O_2 , \qquad (6)$$

and is destroyed by photolysis,

$$HOCl \xrightarrow{h\nu} OH + Cl \quad . \qquad (7)$$

Destruction of O_3 is more efficient at lower altitudes if HOCl is included in the model. When HOCl is included, ClX shifts to more Cl and less ClO. Also, a new catalytic ozone destruction cycle is created that does not depend on the limited amount of O atom,

$$\begin{aligned} OH + O_3 &\rightarrow HO_2 + O_2 \\ Cl + O_3 &\rightarrow ClO + O_2 \\ ClO + HO_2 &\rightarrow HOCl + O_2 \\ HOCl &\xrightarrow{h\nu} Cl + OH \end{aligned} \qquad (8)$$

$$\text{net} \qquad 2O_3 \rightarrow 3O_3$$

Figure 9 shows a number of calculated time histories for ozone under various assumptions regarding the future release rates for CFM's. For curve A it was assumed that CFM production continued at the 1976 rate until 1982, then it was lowered by 25%. In 1987, it was lowered again by 25%. The eventual steady-state ozone depletion for this case was 7.5%. For curve B, the 1976 production rate continued until 1982 and was then cut by 25%. The ozone depletion at steady state was 10.8% for this case. For curve C the 1976 production rate was used for the entire time, and the steady-state ozone depletion was 14.0%. For curve D the 1976 production rate was assumed to continue through 1980, then the CFM production was increased by 7%/year up to the year 2000. The steady-state depletion for this case is 37.9%. Case E is almost the same as case D except that the increased CFM production begins in 1978. The rate of increase is such that the production rate doubles by 1990 and doubles again by 2000. The steady-state ozone depletion is 38.6%. The 1979a chemical rates were used in all of these model calculations.

Increase in N_2O

Concern that human perturbations to the nitrogen cycle might lead to enhanced concentrations for atmospheric N_2O has stimulated interest in

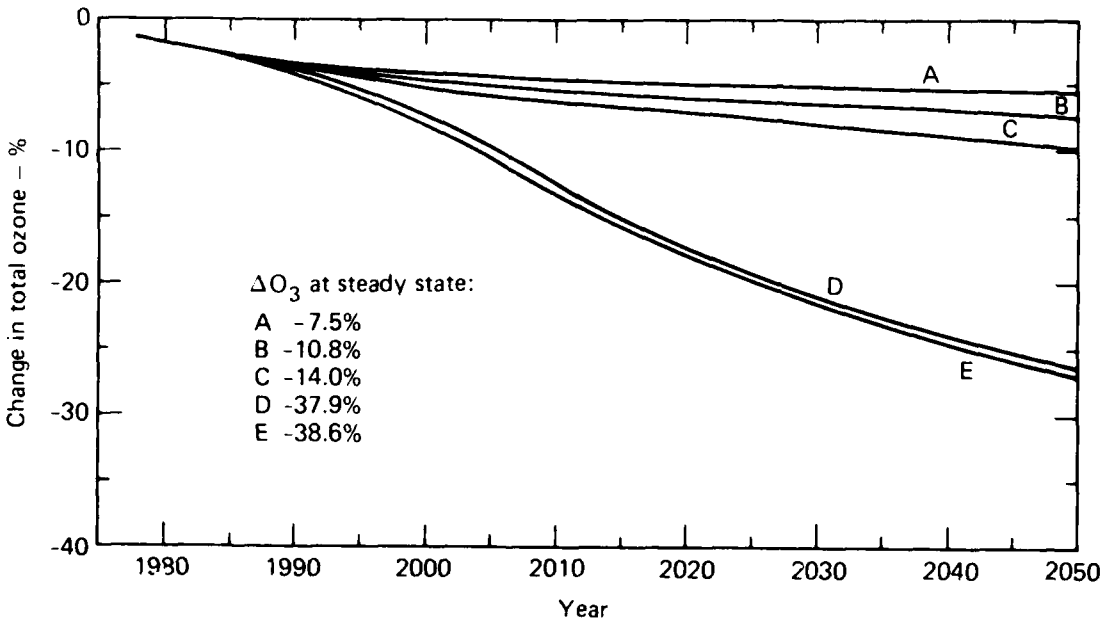

FIG. 9. Change in total ozone as a function of time for various CFM release rate scenerios. Curve A: 1976 CFM release rate until 1982, reduced by 25%, and further reduced by 25% after 1987. Curve B: 1976 release rate until 1982 and reduced by 25% thereafter. Curve C: 1976 release rate constant throughout period. Curve D: 1976 release rate through 1980 followed by release rate increase of 7% per year up to year 2000 followed by being constant thereafter. Curve E: Same as D except the increase in release rate begins in 1978. All calculations were based upon 1979a chemical rates.

the budget for this gas. Tropospheric N_2O is the major source for stratospheric NO_x so perturbations in N_2O are expected to alter stratospheric chemistry.

The fertilizer source of fixed nitrogen is currently estimated to be about 4.2×10^7 tN/yr, which converts to a source of 1.5×10^6 tN/yr as N_2O (estimate of Logan *et al.*, 1978). Combustion provides about 1.5×10^6 tN/yr as N_2O directly (Weiss and Craig, 1976; Pierotti and Rasmussen, 1976). These anthropogenic sources are thus currently significant relative to the natural sources and could grow in the future and lead to a doubling of N_2O perhaps by the early part of the next century (Logan *et al.*, 1978). This doubling time is very uncertain due to the lack of detailed understanding of the cycle for N_2O.

The level of atmospheric N_2O determines the atmospheric response to chlorine changes, and vice versa, mainly because of the coupling of chemistry by $ClONO_2$. Figure 10 illustrates how the percentage change in total O_3 with increased N_2O depends on the level of background ClX and on the chemical rate constants in the model. The dashed curves were produced using chemical rate constants that were used in 1978 (see Luther, 1978). The solid line refers to results using the 1979a rate coefficients. The major differences between the 1978 and 1979 chemistries as they affect this perturbation are: (1) the NO photolysis rate is slower in the 1979 chemistries so that the background level of NO_x is approximately 40% higher, and (2) the $ClONO_2$ formation rate via $ClO + NO_2 \xrightarrow{M} ClONO_2$ is almost four times slower in the 1979a chemistry. Both

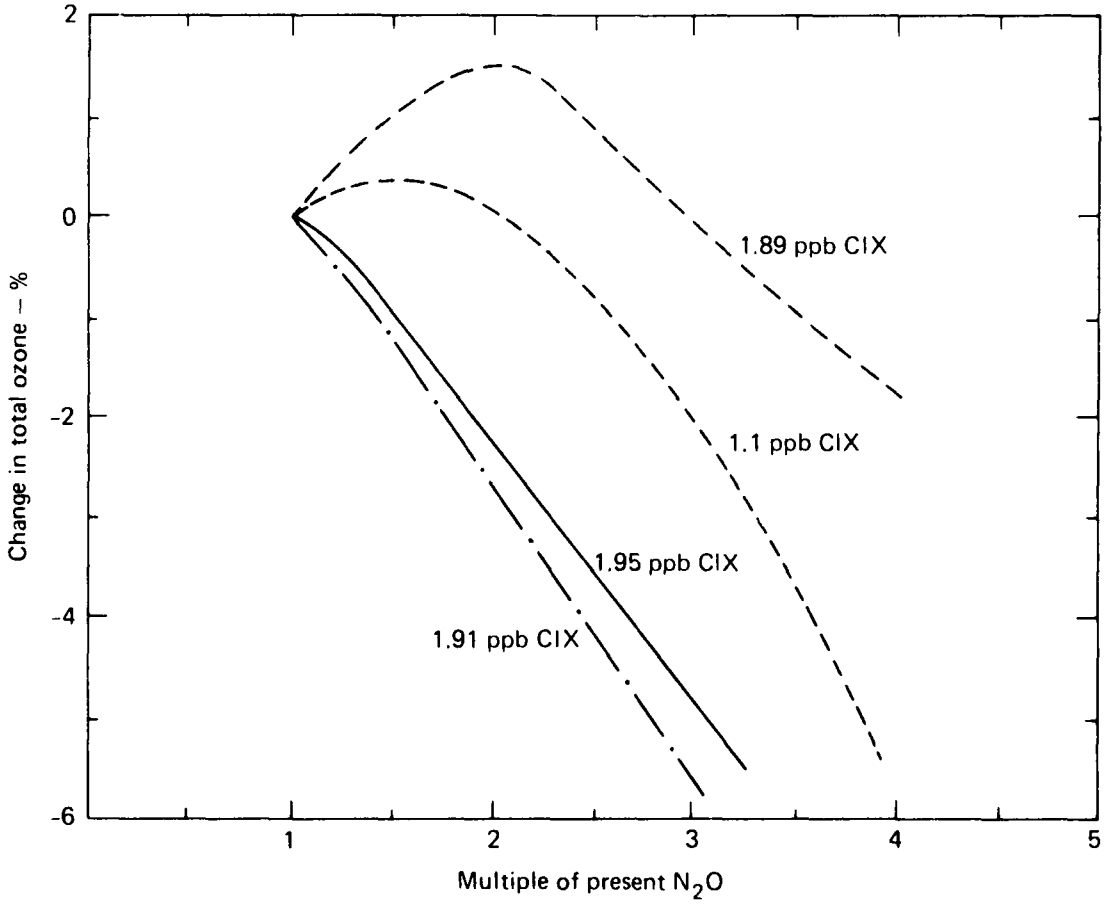

FIG. 10. Change in total ozone due to an increase in N_2O expressed in multiples of present ground level concentration which is 325 ppbv. Results produced using 1979a rate coefficients are indicated by the solid line. Results using chemical rate data that were used in 1978 (Luther, 1978) are shown by dashed curves. Dash-dot line refers to results using fast $ClONO_2$ formation rate (see text).

changes tend to diminish the predicted O_3 increase as N_2O is increased. Even for 1.95 ppbv ClX, ozone decreases for all N_2O perturbations with the 1979a chemistry. This remains true even for the fast rate of $ClONO_2$ formation as indicated by the dot-dash line in Fig. 10, so most of the qualitative change in results is due to the change in NO photolysis.

Doubling of CO_2

Systematic measurements of CO_2 since 1958 (Keeling *et al.*, 1976a and b) have shown a rise in atmospheric CO_2 concentrations that has been attributed primarily to the use of fossil fuels. The CO_2 levels were 315 ppm in 1958, 320 ppm in 1965, and 334 ppm in 1978. By the year 2000 atmospheric CO_2 is expected to be between 365 and 400 ppm. Detailed prediction of the doubling time depends on uncertain knowledge of the budget for CO_2. Assuming that fossil fuel usage continues to increase at 4.3%/yr and that about half of the CO_2 released resides in the atmosphere, the atmospheric CO_2 concentration would double by about 2030, but estimates using other assumptions vary from 2015 to 2070. It is possible that the concentration could be limited to less than 500 ppm by shifting away from fossil fuels and relying more on solar and nuclear energy.

An increase in CO_2 is expected to lead to changes in the thermal structure of the atmosphere. In particular, a doubling of CO_2 has been estimated to increase the global mean surface temperature by 1.5 to 3 K due to the greenhouse effect (Schneider, 1975; Augustsson and Ramanathan, 1977). The temperature should decrease in the stratosphere, where the infrared opacity is smaller than in the troposphere.

We tested the effect of tropospheric temperature changes by increasing the specified temperature below 14 km by 2 K when CO_2 was doubled from 320 to 640 ppm. The calculated change in the ozone profile (Fig. 11) for this case was nearly the same as for the case where the tropospheric temperature remained unchanged (local ozone concentrations were within 2.6% at all altitudes). The calculated temperature changes above 14 km were also similar, differing by less than 0.7 K. In this test the background atmosphere remained fixed (no hydrostatic adjustment). When hydrostatic adjustment was included, the local ozone increase near 40 km was about 15%, which was larger than the perturbation for no tropospheric temperature change but smaller than the calculated change when hydrostatic adjustment was neglected entirely. Without hydrostatic adjustment, the stratospheric temperature decrease leads to an increase in O_3 at all altitudes. The O_3 increase tends to offset the calculated temperature decrease due to CO_2 above 40 km by increasing solar absorption by O_3. The calculated temperature decrease is a maximum near 42 km.

With hydrostatic adjustment, however, ozone *decreased* above 45 km even though the temperature decreased. This is due to the decrease in background air density. As a result of the ozone decrease, the temperature decreased further above 45 km.

The increase in total O_3 for a doubling of CO_2 was 5.06% with hydrostatic adjustment and 4.74% without. The larger change for the hydrostatic case reflects the behavior of O_3 near 25 km, as shown in Fig. 11. At this level, the photolysis rates for O_2 and O_3 both decreased for doubled CO_2 as a result of the larger optical depth (more O_3 above 25 km). The change in optical depth is larger for the case without hydrostatic adjustment, so the photolysis rate for O_2 decreases more for this case, causing a smaller increase in O_3. When the surface temperature was increased 2 K, the change in total ozone was 4.17% without hydrostatic adjustment.

Increase in CH_3CCl_3

The use and release of methylchloroform, CH_3CCl_3, which is used as a cleaning agent, has been increasing at a steady rate. Its presence in the atmosphere has been observed since 1974 (Cox *et al.*, 1976), and it has been suggested that its continued use will lead to a reduction of ozone (McConnell and Schiff, 1978). The sinks for CH_3CCl_3 are photolysis and reaction with OH in the stratosphere,

$$CH_3CCl_3 + h\nu \rightarrow \text{products} \qquad (9)$$

$$CH_3CCl_3 + OH \rightarrow CH_2CCl_3 + H_2O \ . \qquad (10)$$

Stratospheric destruction of CH_3CCl_3 leads to release of Cl atoms which are able to destroy ozone. Reaction (10) is also effective in the troposphere, so the growth of stratospheric CH_3CCl_3 is limited. The effectiveness of reaction (10) for removing tropospheric CH_3CCl_3, however, is fairly uncertain.

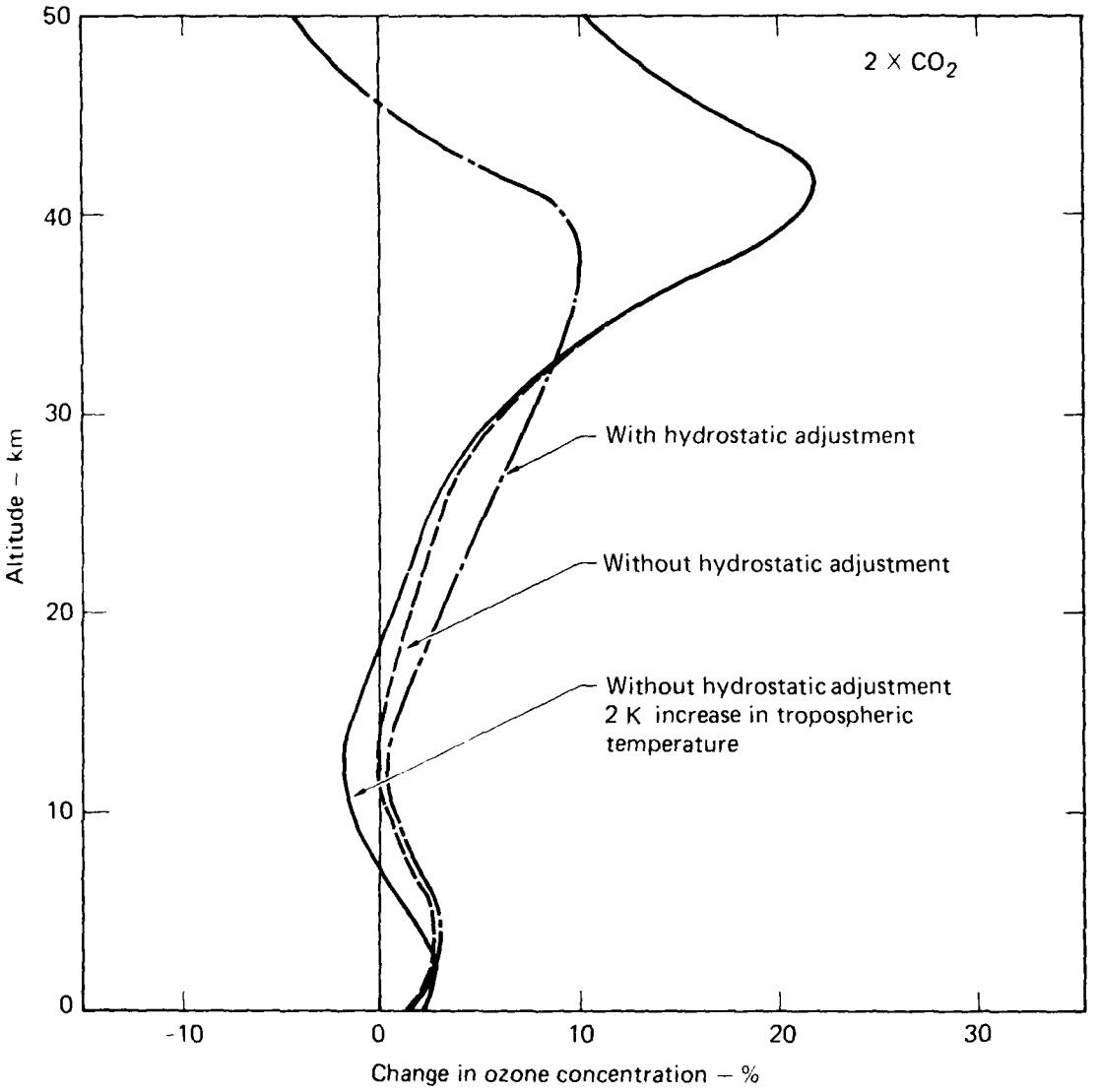

FIG. 11. Change in ozone concentration due to a doubling of CO_2 concentration (1979a chemistry).

The major uncertainties result from inadequate knowledge of the tropospheric OH distribution and the rate of reaction. The rate for reaction (10) is uncertain since there are several conflicting measurements of its rate at room temperature and of its temperature dependence (JPL, 1979). Comparison of the budget for CH_3CCl_3 with available measurements leads to an estimate for the tropospheric lifetime of between 8 and 11 years (Penner and Chang, 1978). Model calculated lifetimes are considerably shorter, implying larger tropospheric destruction rates, on average, than conform to the measurements. For example, using the historical release rate data from Neely and Plonka (1978) in our one-dimensional model, we calculate an average abundance near the surface for January 1978 of 47.3 pptv using the 1979a chemistry. The rate coefficient for reaction (10) was 2.5×10^{-12} exp(-1450/T) (see JPL, 1979). We calculate 66.1 pptv using the 1979b chemistry and a rate coefficient of 5.4×10^{-12} exp(-1820/T) for (10). These rates differ by about a factor of 2 at temperatures characteristic of the upper troposphere and by about 50% near the surface. Measurements taken by R. Rasmussen (private communication, 1979) give an average concentration of 101 pptv for CH_3CCl_3.

With CH_3CCl_3, $CFCl_3$, and CF_2Cl_2 releases included in our model, the calculated reduction in total ozone in 1978 was 1.7% (relative to 1950) using 1979b chemistry, whereas without CH_3CCl_3, O_3 decreased by 1.3%. The total stratospheric chlorine burden increased by 7%. Figure 12 shows the time history for O_3 depletion at constant 1976 production rates for $CFCl_3$ and CF_2Cl_2. The CH_3CCl_3 release rate at the earth's surface is constant at 1.23×10^7 molecules cm^{-2} s^{-1} beyond 1978. At steady state ozone decreased 15.2%, whereas without CH_3CCl_3 it decreased 14.2%. Of course, the

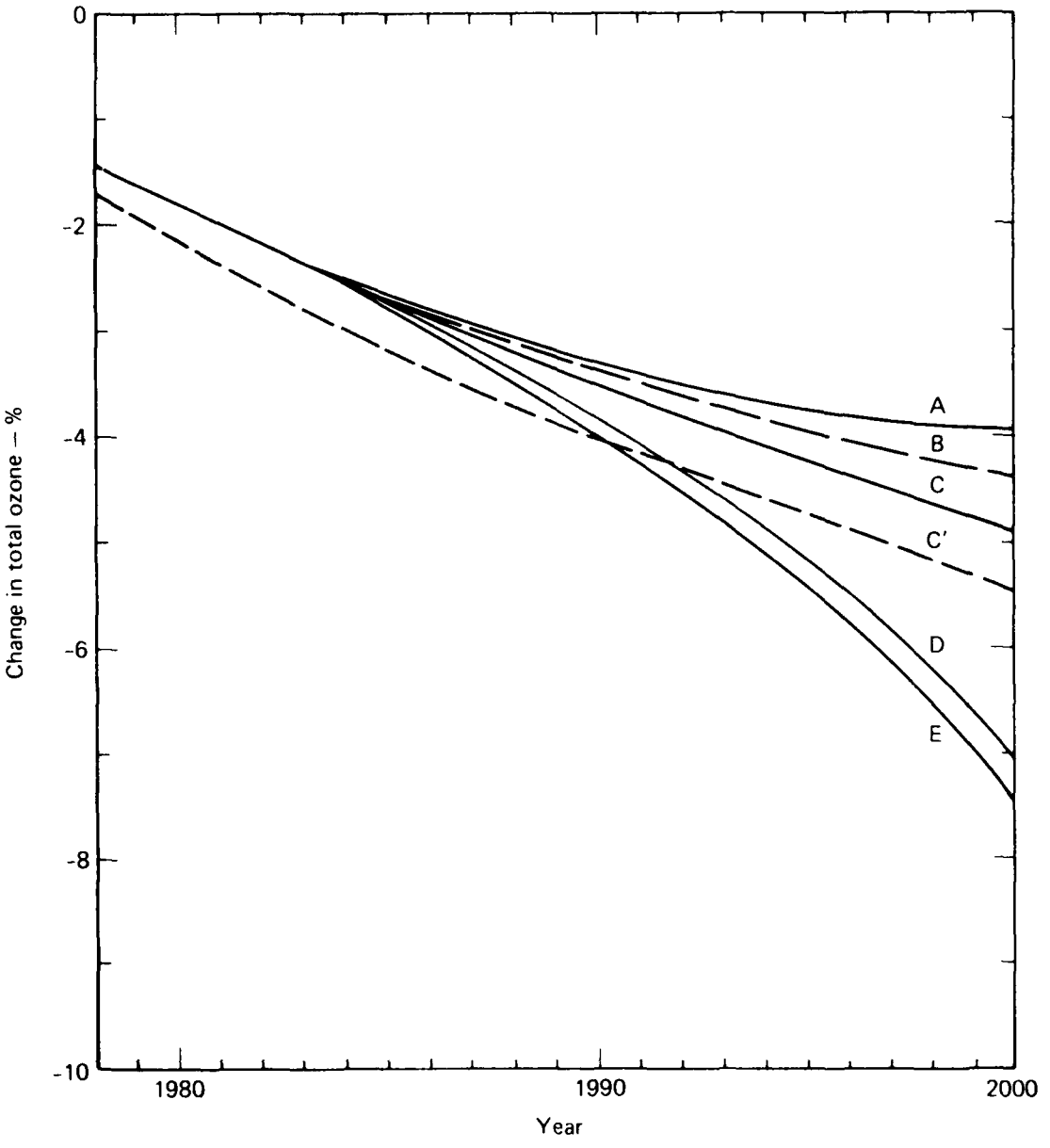

FIG. 12. Enlargement of period from 1980 to 2000 for calculations presented in Fig. 9. Curve C' is same scenario as Curve C except 1979b model chemistry is used with exception that CH_3CCl_3 is added.

effects of CH_3CCl_3 could be much greater if its use were to continue to increase. Because of significant uncertainties in the model treatment of photochemistry in the lower troposphere, these results must be considered preliminary.

2.4. EFFECTS OF SPECULATIVE REACTIONS AND MECHANISMS

There are several reactions that have been suggested to be of possible importance in the stratosphere but have not been measured yet. Also, there are a few reactions for which anomalous pressure/temperature dependencies have been suggested but not demonstrated. We have examined the sensitivity of model predictions to a subset of such hypothetical reactions. The subset selected was based on the following criteria: (1) the hypothesized reaction or mechanism has at least some support from laboratory work, and (2) the hypothesized reaction appears to have the potential for causing a major change* in predicted effects of SST's or CFM's. The reasons for selecting these two criteria were to reduce the number of possible cases to be considered and to focus attention on mechanisms that appear to have a maximum potential for altering model predictions. It must be stressed that most of the mechanisms considered here have no more than a weak basis in actual measurement. The purpose of this section is to suggest experiments that might deserve some priority. It is not to suggest that the hypothesized mechanisms or their computed effects are particularly likely to be true.

In this section we will discuss the major effects on the computed ambient atmosphere and model sensitivity of the various mechanisms considered. Although the changes to the ambient species concentration profiles may tend to either improve or worsen the agreement with observations for various species, we have not established a criterion for agreement (or disagreement) upon which to evaluate the likelihood that the mechanism actually occurs or to eliminate it from consideration. By combining the description of the effects on the ambient profiles discussed in this section with the comparison with observations discussed in Section 2.1, the reader can form his own opinion on this matter.

*In this context a major change would consist of a change in the computed steady-state effect of chlorofluoromethanes at 1975 levels by at least 50% or a change in sign or two-fold increase in computed SST effects. Not all of the cases studied actually have such large effects and some mechanisms not studied might have larger effects.

Chlorine Nitrate Formation

In terms of published evaluations of mechanistic data, perhaps the most plausible speculation is that roughly 75% of the reaction between ClO and NO_2 forms a relatively short-lived species isomeric with chlorine nitrate, and the effective rate of chlorine nitrate formation is only about one-fourth of the observed rate of reaction between ClO and NO_2. In JPL (1979) (and NASA, 1979) no firm choice is made between the assumption that all of the reactions between ClO and NO_2 lead to chlorine nitrate and the assumption that only about 25% do, although most modelers have adopted the first assumption. The choice of treatment for this reaction is one of the major differences between the 1979a and 1979b chemistries. As can be seen from Table 11, if the slower rate of chlorine nitrate formation is assumed, the calculated effects of an SST fleet become more positive than in the base case, while the computed effects of CFM's become more negative. In each case, the fractional change is of the order of a factor of 1.3. Clearly, the correct treatment of chlorine nitrate formation is of substantial importance. It is also worth noting that if the isomeric products have greater photolytic stability than $ClONO_2$, or if, as impurities, they account for some of the observed absorption spectrum of $ClONO_2$, the effect of chlorine nitrate isomers on predictions might actually be reversed. This could happen if the mean rate of loss of some $ClNO_3$ products were to be slower than that presently assumed for $ClONO_2$ so that larger concentrations of $ClNO_3$ species would be generated.

When the low rate is assumed for chlorine nitrate formation, a significant (>10%)* change in the ambient state is computed for Cl, ClO, HCl, HOCl, and $ClNO_2$, all of which increase by nearly a factor of 2 at 25–30 km, while $ClNO_3$ is reduced by a factor of 3 to 4 at almost all altitudes. Thus, this hypothesis exacerbates the apparent disagreement between observation and calculation for the shape of the ClO vertical profile and destroys the apparent

*All percent changes reported in this section refer to *fractional* changes in the quantity relative to the standard (1979b model) ambient conditions or model sensitivity.

TABLE 11. Results of sensitivity calculations for speculative chemical reactions and mechanisms.

Model content	Ambient ozone column (Dobson units)	Change in total ozone (%)		
		17-km NO_x injection[a]	20-km NO_x injection[a]	CFM production[b]
Baseline Model (1979b)–NASA 1049 (1979) 2 ppb ClX	322	1.25	1.14	-14.6
Slower rate of $ClONO_2$ formation	312	1.42	1.54	-19.3
Photolysis of $XONO_2$ to XO + NO_2 products	324	1.35	1.20	-12.2
Pressure- and temperature-dependent HO_x disproportionation reactions	339	0.47	-0.40	-8.9
HCl production from ClO + OH, ClO + HO_2	334	0.74	0.02	-4.4
ClO_3 production, $K_{equilibrium}$ as for ClO_2 from NASA 1010; no other reaction of ClO_3	322	1.24	1.11	-14.0
$OClO_2$ production $K_{equilibrium}$ as for ClO_2 from NASA 1010; subsequent chemistry described in text	337	1.51	1.40	-6.91
$OClO_2$ production $K_{equilibrium}$ as for ClO_2 from JPL (1979); subsequent chemistry described in text	323	1.27	1.16	-14.0
$OClO_2$ production $K_{equilibrium}$ as for ClO_2 from NASA 1010; subsequent chemistry described in text and P,T-dependent HO_x disproportionation reactions	353	0.49	-0.51	0.73

[a]Rate of emission is 1000 molecules (NO) $cm^{-3}s^{-1}$ over a 1-km-thick layer.

[b]Constant release rate at 1976 levels.

agreement between calculation and the preliminary chlorine nitrate measurement reported by Murcray (1979).

Photolysis of $XONO_2$ Species

Almost equally uncertain are the products of the photolysis of species of the form $XONO_2$, where X = OH, Cl, NO_2. In the base case, it has been assumed that all of these reactions lead to X + NO_3. This assumption is largely based on the experimental results of Chang *et al.* (1979) for chlorine nitrate.

Other products are possible, perhaps the most distinct (in terms of model predictions) would be XO + NO_2 (or for N_2O_5, $2NO_2$ + O). In a computation in which all of these photolyses were assumed to yield XO + HO_2 products (except N_2O_5 which was assumed to yield $2NO_2$ + O), the computed effects of SST emissions became more positive by 5–10% (of the change computed for the base case) while the effects of CFM's became less negative by about 17%. Thus, resolving the question of photolysis products of XOClO species is of modest importance to perturbation calculations.

In terms of species concentrations, only NO_3 and N_2O_5 displayed large changes (both were reduced by a factor of two to three at the region of their largest mixing ratios, and by up to 90% at some (lower) altitudes). Several other species displayed changes on the order of 10–15% at some altitudes.

Pressure-Dependent Rates for HO_x Disproportionation Reactions

A significant pressure, inverse temperature and water vapor dependence has been reported for the reaction $HO_2 + HO_2 \xrightarrow{M,H_2O} H_2O_2 + O_2$ (Cox, 1978; Hamilton and Lii, 1977; Cox and Burrows, 1979). Furthermore, while the measurements of the reaction HO_2 + OH at low pressures seem only mildly inconsistent with each other, the indirect values inferred at higher pressures (Hochanadel *et al.*, 1972; DeMore and Tschuikov-Roux, 1974; DeMore,

1979) are substantially (two to four fold) faster than the values measured at low pressures. In this context, the poorly understood pressure, temperature, and water vapor dependence of $HO_2 + HO_2$ suggests the possibility that $HO_2 + OH$ may also be affected by similar phenomena. As can be seen in Table 11, when we assumed that the expression given by Cox (1978) for $k_{HO_2+HO_2}$,

$$k_{HO_2 + HO_2} = \frac{3.25\times10^{8}+4\times10^{-10}(M)/[1+3.5\times10^{-16}(M)e^{-2060/T}]}{8(M)+4.08\times10^{20}} \quad (11)$$

and an expression for k_{OH+HO_2} designed to yield a low-pressure value compatible with Chang and Kaufman (1978), and a high pressure value compatible with the larger rate constants reported at high pressure, i.e.,

$$k_{HO_2 + OH} = (5\times10^{-30}\times M + 3\times10^{-11})(300/T)^{3} \quad , \quad (12)$$

there were major changes in model predictions for both SST's and CFM's. Here it should be emphasized that the expression used for the rate constant for reaction of HO_2 with OH is completely arbitrary. It was designed to approximately fit high- and low-pressure data. Had a Lindeman-Hinshelwood expression been fitted to the same data, or had a constant ratio to the $HO_2 + HO_2$ rate been assumed, the effects would have been different (probably larger) but equally plausible. The form chosen reflects the postulation of a pressure independent abstraction mechanism coupled with a pressure dependent enhancement reflecting complex formation (with a limiting value well above 1×10^{-10} at room temperature).

Elucidation of the pressure and temperature dependencies of the HO_x radical disproportionation reactions should be of high priority to those concerned with SST effects and of considerable importance to those concerned with CFM production effects. The assumed change in the $HO_2 + OH$ reaction is substantially more important than the change in the $HO_2 + HO_2$ reaction within the stratosphere. However, the $HO_2 + HO_2$ reaction is of significant importance in the troposphere, and the effects of subsonic aircraft operations are expected to be sensitive to it, as would be the effects of CH_3CCl_3 emissions.

When the above assumptions were made about the HO_x disproportionation reactions, many species changed by roughly a factor of 2 between approximately 10 and 20 km. Roughly two-fold reductions (between approximately 10 and 20 km) occurred for OH, HO_2, Cl, ClO, and CH_2O, while H_2O_2 was reduced by roughly the square of the fractional reduction in HO_2. Computed NO and NO_2 displayed two-fold increases over the same altitude range. Species that were only slightly changed included HNO_3 (<10% changes) and CH_4 (approximately 10% increase at high altitudes).

Thus, changes in the HO_x disproportionation rates akin to those considered here would cause substantial changes in computed profiles of short lived species in the region from 10 to 20 km. Some of these changes tend to improve agreement with observation, others tend to reduce it. Although CH_4 increases at higher altitudes, the increase is not large enough to demand a major revision in K_z even if future experiments should suggest the pressure-dependent disproportionation rates used here to be fair approximations of reality. For CH_4 to increase substantially at higher altitudes, it would be necessary for an increase in k_{OH+HO_2} to extend to substantially lower air densities.

All of the above speculations have at least some direct basis in laboratory measurements. The speculations that follow are even more tenuous than the above.

HCl Formation from HO_x + ClO

The reaction between OH and ClO could yield $HO_2 + Cl$ or $HCl + O_2$ at low pressures, or a three-body process might yield a moderately stable species of the form HOOCl (a peroxide) or HOClO (an acid). Either of these last species might be expected to be unstable with respect to disproportionation in a condensed phase, but gas phase stability seems possible. In any case, the production of $HCl + O_2$ from HO + ClO would seem likely to have the most drastic effect on model predictions. The overall reaction has a rate constant of 9.2×10^{-11} at room temperature, and the products $HO_2 + Cl$ account for at least 65% of the products (Leu and Lin, 1979). These products have little effect on model sensitivity.

An investigation of the effect of this reaction producing HCl assuming a rate constant of 2×10^{-12} cm^3/s suggested that model sensitivity to

a CFM perturbation could be reduced by approximately 40%; at 1×10^{-12} cm^3/s the sensitivity would be reduced by roughly 20%.

A similar argument could be applied to the reaction:

$$HO_2 + ClO \rightarrow HOCl + O_2 \quad (13)$$

$$HO_2 + ClO \rightarrow HCl + O_3 \quad (14)$$

The only evidence suggesting a plausible role for reaction (14) is that at temperatures below room temperature, the rate of the overall reaction increases substantially as the temperature is reduced (C. Howard *et al.*, NOAA Aeronomy Laboratory, Boulder, private communication, 1979). This suggests the possibility that a five-centered complex might be formed and HCl + O_3 eliminated. If the rate of HCl formation via this reaction were to be as large as 1×10^{-12} cm^3/s, then the effect of CFM's would be reduced by approximately 50%, and, if the rate were to be even larger, increases might be computed from CFM releases.

Table 11 gives the sensitivities obtained when both $HO + ClO \rightarrow HCl + O_2$ and $HO_2 + ClO \rightarrow HCl + O_3$ were assumed to have rate constants of 1×10^{-12} cm^3/s. As is evident, these reactions might have a major impact on both CFM and SST effects, and they might have a smaller but significant effect on computed CFM effects at rates as low as approximately 1×10^{-13} cm^3/s.

The effect on the model sensitivity to an NO_x perturbation is largely a result of there being a lessened rate of ClX and HO_x catalytic destruction of ozone with which NO_x can interfere. Also, null cycle sequences involving ClX and HO_x are not as effective in competing with ozone-destroying sequences for NO. The reduced sensitivity to CFM perturbations results from both an increase in the rate at which HCl is formed and a transfer of ClO and HO_x radicals out of odd-oxygen destroying sequences and into null sequences.

There is the possibility that the reaction $HO_2 + HO_2 \rightarrow H_2O + O_3$ might occur to some extent. An analysis of available data (H. Johnston, University of California at Berkeley, private communication, 1979) suggests an upper limit of about 5% of the total rate for this reaction. If the similar reaction $HO_2 + ClO \rightarrow HCl + O_3$ had a branching ratio of less than 0.05, it would have no more than a modest effect on model sensitivity (based on calculations made in 1978, the reaction $HO_2 + HO_2 \rightarrow H_2O + O_3$ would need to have a branching ratio of nearly 0.1 to be of even marginal significance in stratospheric perturbation studies).

The model-calculated ambient atmosphere with rates for both $OH + ClO \rightarrow HCl + O_2$ and $HO_2 + ClO \rightarrow HCl + O_3$ set to 10^{-12} cm^3/s contained about half as much Cl, ClO, $ClONO_2$, $ClNO_2$ and HOCl as did the normal ambient, whereas HCl increases of about a factor of 2 were calculated near 30 km. No other measured species were significantly (>10%) affected, although H_2O_2 and CH_3OOH were reduced by about 30% between 25 and 35 km.

Although model predictions are indeed sensitive to these reactions, the likelihood that they occur is probably not very great. Thus, while an effort should be made to measure them, an upper limit less than approximately 10^{-13} cm^3/s would resolve most of the issues they raise.

ClO_3 Chemistry

A final mechanism that was studied was the possibility that O_2 and ClO add to form a molecule with a binding strength comparable to that of ClOO, the complex formed from Cl and O_2. There is evidence for some such phenomenon from the effect of added O_2 on the quantum yield for ozone loss in systems containing Cl_2, O_3 and O_2 (Wongdontri-Stuper *et al.*, 1978; J. Birks, University of Colorado, private communication, 1979).

If it is assumed that the formation and decomposition rate constants for the process $ClO + O_2 \rightarrow ClO_3$ are those given in NASA 1010 (1977) for $Cl + O_2 \rightarrow ClO_2$ and no subsequent chemistry occurs (only the formation and thermal decomposition of the complex occur), then model sensitivities are virtually unaffected. Approximately 2 to 5% of the inorganic chlorine in the lower stratosphere is in the form of ClO_3, and all computed changes in ambient concentrations are small. Even though the coupling between ClO and ClO_3 is very rapid, and ClO_3 is computed to be larger than ClO between approximately 6 and 22 km, most of the ClO_3 apparently comes from the much more abundant HCl and $ClONO_2$. However, if the structure of the ClO_3 complex were $OClO_2$, then it is possible that the following reactions would occur:

$$OClO_2 \xrightarrow{h\nu} O + OClO \quad (15)$$

and

$$OClO_2 + NO \rightarrow OClO + NO_2 \cdot \qquad (16)$$

Because ClO and OClO have comparable heats of formation, the endoergicity of the photolysis would approximate 60 kcal plus the binding energy of the complex. This suggests an endoergicity for reaction (15) comparable to that for NO_2 photolysis. Thus, at least in principle, reaction (15) might have an effective J value as large as about $10^{-3}s^{-1}$. The reaction $OClO + NO \rightarrow NO_2 + ClO$ has a rate constant of about 3×10^{-13} cm^3/s at room temperature (JPL, 1979). Given the similarities in the reactions, a similar sort of rate constant might be estimated for $OClO_2 + NO$. If one assumes that the J value for $OClO_2$ photolysis is $10^{-4}s^{-1}$, that the rate of reaction with NO is 1×10^{-12} cm^3/s, and that the formation and decomposition rates are those given for ClO_2 in NASA 1010 (1977), then one estimates a moderate (20%) increase in the (small) ozone increase computed from SST operations and more than a 50% reduction in the effect of CFMs. If on the other hand one assumes the same subsequent chemistry but a lower stability for the complex, say that given for ClO_2 in JPL (1979), then no significant effect on model sensitivity is predicted.

Thus, for the formation of a complex between O_2 and ClO to significantly affect model sensitivity, the complex must have a binding energy approaching 6 kcal, and either photolysis or reaction with NO must be reasonably fast. However, if the complex were to be stable (bound by more than 8 kcal) and the subsequent chemistry were reasonably fast, one might even compute a decrease in ozone for NO_x injections and an increase in column ozone from CFM increases. Similarly, if the HO_x reactions were pressure-dependent *and* $OClO_2$ were to have the chemistry discussed above, one would calculate a decrease in column ozone for the 20-km NO_x injection and an increase in column ozone from the CFM scenario (see Table 11). There is, of course, a lengthy chain of speculative assumptions required to achieve such results.

Even though the $OClO_2$ chemistry discussed above is completely speculative, its potential for large effects may justify the attempt to study it by those chiefly interested in CFM effects.

Finally, it should be noted that the simplest (but probably not the most likely) route back to computed effects of SST operations (like those obtained in CIAP Monograph 3 (1975) and National Research Council (1975a) would be for the HO_x disproportionation reactions to have fast rates (either via the pressure/temperature effects hypothesized above, or through an error in the post 1976 measurements) and for the reaction of $HO_2 + NO$ to be slower than is now thought to be the case. Although it seems unlikely that the growing body of experimental results involving HO_2 chemistry would all be wrong (at least at low pressures where many of the measurements have been direct and the data analysis reasonably straightforward), it cannot be denied that the new measurements have produced a startling number of unexpected negative temperature dependencies for apparently bimolecular reactions involving HO_2 (and ClO as well). While theories of reaction rates can no doubt be created to fit such data, the pre-existing theories do not easily lead to the observed rate constants. Although it seems very likely that the resolution of such problems will indeed come via a modification of theory, additional confirmatory measurements of some of the anomalous temperature dependences using independent, if perhaps less direct, techniques would still be welcomed.

2.5 STRATOSPHERIC WATER VAPOR

The review of our knowledge and observational data on stratospheric H_2O revealed several apparent paradoxes which remain to be resolved. These are illustrated by the data summarized in Figs. 13 and 14. These data indicate upward and poleward directed gradients of H_2O immediately downstream (in the Hadley flow) from the tropical tropopause source for air (and contained tracers including H_2O) entering the stratosphere. As pointed out previously (Ellsaesser, 1974), these appear to require a sink for H_2O in the stratosphere. However, possible sinks proposed, such as the Antarctic winter freeze-out and the "cold finger" of overshooting cumulonimbi, do not appear adequate. An alternative possibility is that observational data have been accumulated mostly from the downwind edges of continents where cumulonimbi penetrations are most likely to be concentrated; thus the gradients indicated in Figs. 13 and 14 may exist only in such areas and not be representative of zonal averages as

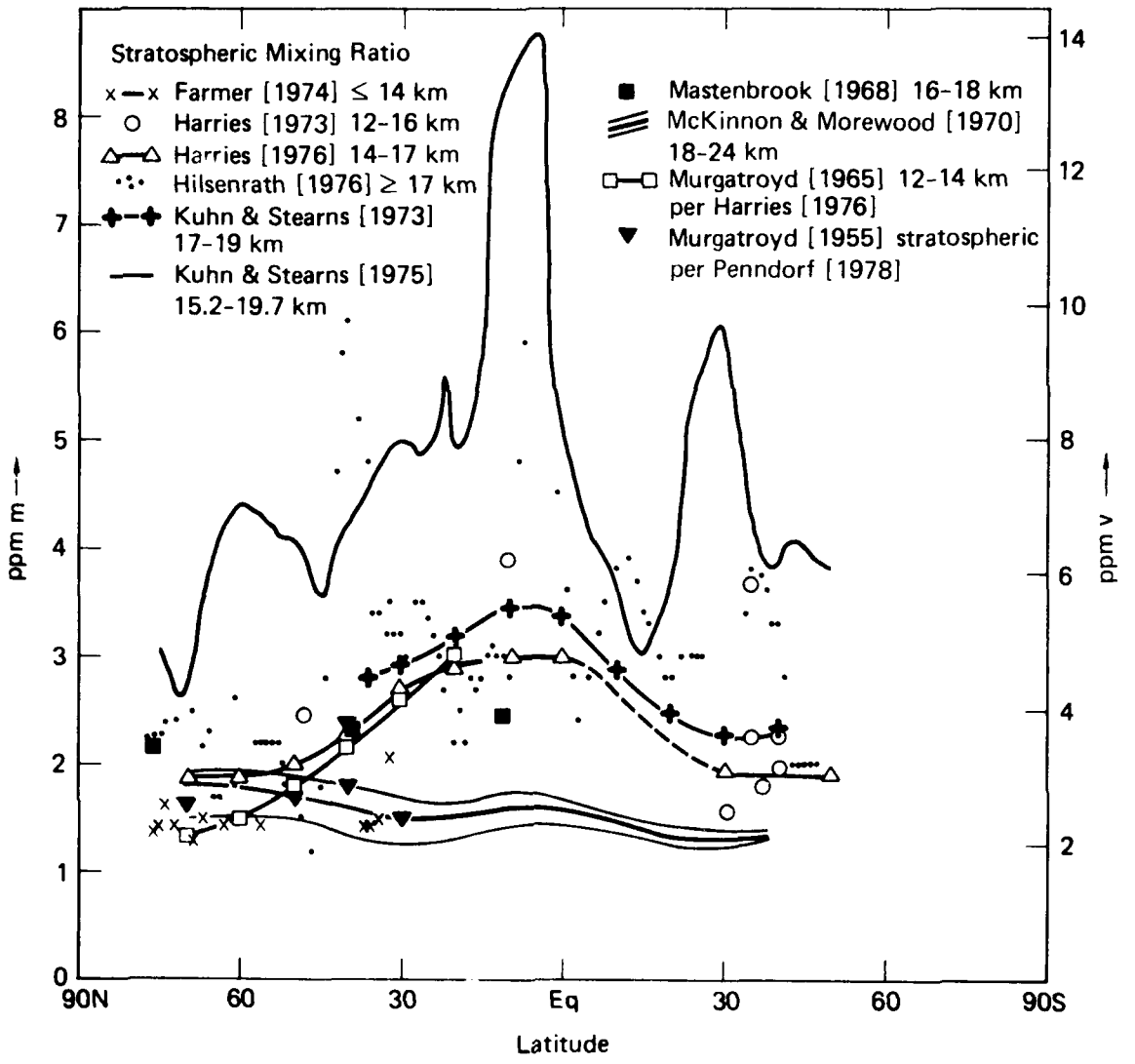

FIG. 13. Summary of observations of the latitudinal gradient in stratospheric H_2O. Data sources identified by references.

they have been interpreted to be. If valid, disappearance of these gradients would obviate the need for an H_2O sink in the stratosphere.

An even greater paradox is indicated by two other observational phenomena: (1) the frequent occurrence of dry air with mixing ratios $\leqslant 3$ ppmm (i.e., typical of the lower stratosphere) as much as 100 mb beneath the tropical tropopause in clearly tropospheric air (such mixing ratios are not only untypical of what has until now been our concept of tropospheric air, but they are actually lower than would be produced by passage through the overlying ambient tropical tropopause) and (2) on those so-called "wet" days when soundings do conform to the Brewer-Dobson theory by showing saturated air at and below the tropical tropopause and/or when cumulonimbus penetrations of the tropopause are sighted, the mixings ratios at and just about the tropical tropopause are generally $\geqslant 6$ ppmm.

These observations appear to imply that the aridity of the stratosphere is *not* controlled by freeze-drying at the tropical tropopause and that there exists in the troposphere a mechanism for drying the tropical tropospheric air above 200 mb to mixing ratios $\leqslant 3$ ppmm typical of the lower stratosphere. As of now the only mechanism which

suggests itself is cirrus clouds. If there exist seeding agents, possibly including the cirrus ice crystals themselves, which at temperatures of −50 to −80°C and pressures below 200 mb, can condense vapor out of what is now regarded as unsaturated air and cause the resulting hydrometeors to fall to higher pressures and temperatures before re-evaporating, we could explain many currently puzzling observations. An additional strong argument for a tropospheric mechanism for drying the air to stratospheric mixing ratios is that it would open a new pathway for significant transfers of air from the troposphere to the stratosphere—and that is through the tropopause-gap. Many have suggested this pathway before based on tracers such as O_3, but most have considered it as insignificant since it appeared to offer no way of maintaining the aridity of the stratosphere. However, if the air is dried by a mechanism operating in the troposphere, this objection goes away.

A third paradox is due to the H_2O believed to be added to the stratosphere by the oxidation there of CH_4 entering with the Hadley circulation from the troposphere. This should impose a downward directed gradient of H_2O in the middle and upper stratosphere with a total difference in H_2O mixing ratio somewhat less than 2 ppmm and an equatorward directed gradient in the lower stratosphere since the return Hadley flow through the polar tropopauses presumably must carry more H_2O than is carried by the entering Hadley flux through the tropical tropopause. A downward directed gradient is shown by many soundings, but most of these show a total difference in mixing ratio of more than 2 ppmm. Also, an equatorward directed gradient of approximately the right magnitude is shown by what are considered to be the two most reliable sets of observations of stratospheric H_2O, the MRF* and the Mastenbrook series. Such a gradient is also shown by the observations of McKinnon and Morewood (1970)

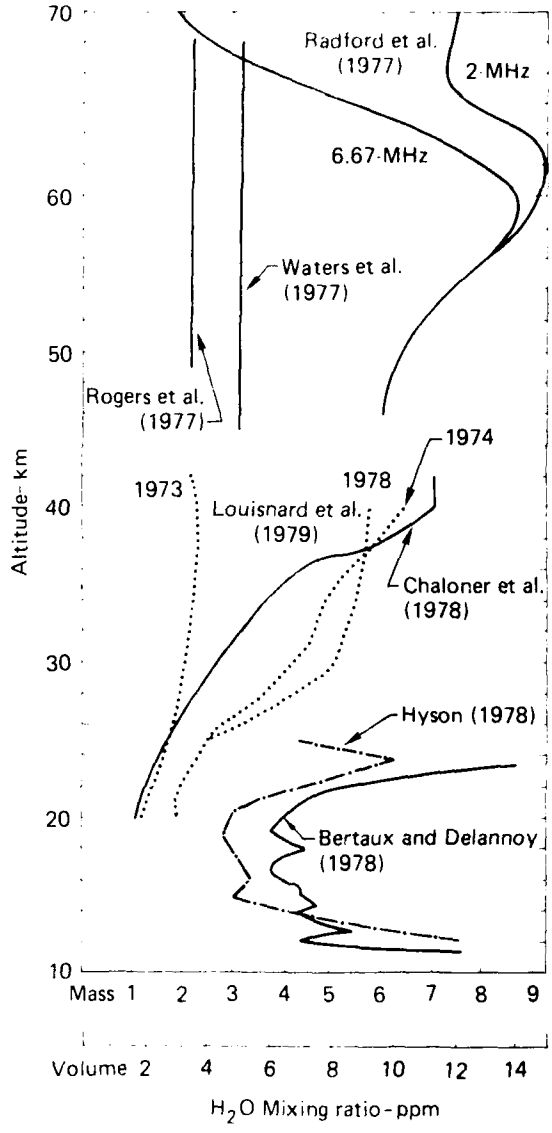

FIG. 14. Summary of recent soundings of stratospheric and mesopheric H_2O.

(see Fig. 13). However, for the inferences drawn above to be correct requires that the data of most investigators of stratospheric H_2O are incorrect or unrepresentative.

*MRF is the acronym for the series of British meteorological research flights

3. SATELLITE OZONE DATA PROCESSING, ARCHIVING, AND ANALYSIS

3.1 OVERVIEW

Measurements of ozone have been made on a regular basis for several decades. The Dobson spectrophotometer instrument is the most widely used ground-based instrument. This instrument measures the differential attenuation of sunlight in adjacent spectral bands in the UV Huggins band of ozone from which the total column of ozone is determined. The Dobson instrument has been in use since 1929, and approximately 100 ozone observatories have used this instrument. Since 1960 the data from many of the Dobson sites have been compiled and published by the Atmospheric Environment Service of Canada. Presently, data from 61 Dobson sites are being published routinely. These sites are located principally on continents in the Northern Hemisphere. The largest data voids are over the oceans and in the Southern Hemisphere.

Global satellite measurements of total ozone were first made in 1969 using the infrared interferometer spectrometer (IRIS). Later, the backscatter ultraviolet spectrometer (BUV) and the IRIS sensors were both flown on the Nimbus 3 (launched in 1970) and Nimbus 4 (launched in 1972) satellites. The longest continuous satellite ozone data record is that of the Nimbus 4 BUV instrument that operated from April 1972 to July 1977. The multichannel filter radiometer (MFR) infrared sensor was first flown in 1977 on a Defense Meteorological Satellite Program (DMSP) Block 5D series satellite, which is operated by the U.S. Air Force. Four satellites in this series have been launched, and the data from these satellites are expected to extend into 1980. The period covered by each of the four DMSP satellites is shown in Table 12.

In addition to the DMSP satellite, ozone data are being obtained by sensors aboard the NASA Nimbus 7 and NOAA TIROS N satellites that were launched in November 1978. The TIROS N satellite carries a high resolution infrared sensor and the Nimbus 7 satellite carries a solar BUV sensor and a TOMS* instrument. The series of NASA and NOAA satellites is expected to provide global ozone data into the late 1980's. The DMSP MFR sensors were the only satellite ozone monitoring systems operating between mid-1977 and November 1978.

All of the DMSP satellites are in polar, sun-synchronous orbits with basically the same orbital parameters. F4 is somewhat different in that it is in a nighttime ascending orbit (i.e., F4 ascends from southeast to northwest on the night side), whereas the others are in daytime ascending orbits. Consequently, although F2 and F4 are only about an hour apart in their overpass times, their flight-track (and site-scan) geometries are different, thereby better enabling F4 to fill data-void areas of F2 and F3. We receive the MFR radiance data on magnetic tape from the U.S. Air Force Global Weather Central, and the raw data are forwarded to the Environmental Data Service of NOAA where they are archived.

*Total Ozone Mapping Spectrometer.

TABLE 12. Data periods covered by MFR sensors[a] on DMSP satellites.

DMSP satellite	Data period	Local overpass time
F1	March 1977 - July 1977	11-12 a.m. and p.m.
F2	July 1977 - Spring 1980 (estimated)[b]	9-10 a.m. and p.m.
F3	August 1978 - January 1980	6-7 a.m. and p.m.
F4	June 1979 - January 1980	10-11 a.m. and p.m.

[a]The F4 MFR sensor may be turned back on at a later time if satellite battery problems are solved or if there is a change in the power management plan.

[b]F2 has already exceeded its designed lifetime.

The MFR sensor measures infrared radiances for 16 channels. The channel characteristics are given in Table 13. Total ozone amounts are determined from sets of radiance measurements using an empirical relationship that is developed using linear regression analysis. Total ozone is currently modeled as a linear combination of terms involving functions of the MFR radiances for four channels (1, 2, 7, and 16) and the secant of the zenith angle. The coefficients used in the retrieval model are determined by regression analysis using sets of simulated radiances derived from detailed radiative transfer calculations. Historical vertical temperature and ozone concentration profiles are used as input to the calculations, and calculations are made for various cloud amounts, surface temperatures, and instrument scan angles. Different sets of regression coefficients are derived for each latitude band (currently, we are using 11 bands) and for different times of the year.

Temperature-dependent molecular absorption coefficients for the 9.6-μm ozone band and the 15-μm carbon dioxide band are determined from high-resolution, line-by-line calculations. These coefficients are used to compute transmittance profiles for the various channels, given the temperature and optically active gas concentration profiles. Transmittances due to the water vapor continuum absorption in the atmospheric window are calculated with an "e-type" model. A regression model based on data from line-by-line calculations plus continuum effects is used for the tropospheric water vapor transmittance calculations in the 15-μm spectral region. A Goody random band model is employed to calculate the transmittances due to the 14-μm ozone band. See Lovill *et al.* (1978) for more detail regarding the retrieval methodology as it was employed during the feasibility study.

The total column ozone data derived from the MFR measurements are compared with an independent set of ground-based measurements of total ozone in order to evaluate the MFR-retrieval methodology. This set of data consists of Dobson ozone measurements that are taken close in time to DMSP satellite overpasses. Currently, 36 Dobson observatories are providing special sets of ozone measurements for comparison purposes. We provide each observatory predictions of the daily overpass times for each DMSP satellite.* The North American Air Defense Command (Colorado Springs) satellite tracking facility provides us with the orbital parameters for each of the DMSP satellites, which are input to the computer code that predicts the satellite overpass times.

In addition to the comparison with Dobson measurements, comparisons will also be made between the MFR-derived ozone measurements and total ozone data from TIROS N and Nimbus 7.

*Special Dobson measurements are not being taken at F3 overpass times because its overpasses are near sunrise and sunset.

TABLE 13. Nominal MFR channel characteristics.[a]

Channel number	Center (μm)	Center (cm^{-1})	Half width (cm^{-1})	Species	NESR[b]
1	15.0	668.5	3.5	CO_2	0.30
2	14.8	676.0	10.0	CO_2	0.09
3	14.4	695.0	10.0	CO_2	0.10
4	14.1	708.0	10.0	CO_2	0.11
5	13.8	725.0	10.0	CO_2	0.11
6	13.4	747.0	10.0	CO_2	0.12
7	12.0	835.0	8.0	Window	0.11
8[c]	18.7[d]	535.0	16.0	H_2O	0.15
9	24.5[d]	408.5	12.0	H_2O	0.14
10	22.7[d]	441.5	18.0	H_2O	0.09
11	23.9[d]	420.0	20.0	H_2O	0.12
12	26.7[d]	374.0	12.0	H_2O	0.18
13	25.2[d]	397.5	10.0	H_2O	0.16
14	28.2[d]	355.4	15.0	H_2O	0.25
15	28.3[d]	353.5	11.0	H_2O	0.33
16	9.8	1022.0	12.5	O_3	0.05

[a]After Nichols (1975).

[b]NESR = Noise Equivalent Spectral Radiance in $mW/(m^2\ sr\ cm^{-1})$.

[c]Not on Flight Model 1.

[d]Not used in this investigation.

3.2 RADIATIVE TRANSFER AND RETRIEVAL METHODOLOGY

Several of the many investigations required to validate and document the physics, mathematics, and software as applied in the development of the total ozone retrieval model implemented in early 1978 have been completed or are in progress. The

assumptions made and shortcuts taken in developing the initial methodology and several items pointed out by various reviewers are also being evaluated.

Techniques and software were developed to compare line-by-line calculated absorption spectra against laboratory spectroscopic measurements. The laboratory data of Dr. Gryvnak and Dr. Burch at Ford Aerospace and Communications Corp. for the 15-μm carbon dioxide bands were obtained, and software to read and display the data were developed. A version of the line-by-line software was modified to produce calculations for the homogeneous paths used in the laboratory investigation for direct high-resolution comparisons. Initial results indicated considerable disagreement. A spectral shift was obvious and the magnitude of the absorption was somewhat lower for the theoretical calculations. Discussions with Dr. McClatchey (Air Force Geophysics Laboratory) and Dr. Burch revealed that similar disagreements had also been found in their studies. Dr. McClatchey felt that the position of lines and bands in the spectrum were quite good in his theoretical line parameter data that are used as input to our line-by-line calculations. Our analysis indicated that the spectral shift was probably due to some instrument error in the spectroscopic data. Further discussions with Dr. Burch lead to the conclusion that the laboratory spectrum was observed through a "skewed" instrument slit function.

Software was developed to degrade our line-by-line calculations with a skewed slit function. Subsequent displays of the data using slit function widths appropriate for the laboratory data indicated that this was probably the cause for the apparent shift, since good agreement was obtained for the positions of lines and bands.

The disagreement in absorption magnitude has been investigated by adjusting two different input parameters which might be the source of error. One possible source of error in the laboratory data is in establishing the amount of carbon dioxide in the optical path of the spectrometer. An adjustment of approximately +8.6% in the reported concentrations produces results that are greatly improved. Dr. Burch felt that an error that large was highly unlikely. He suggested that a similar effect would result from a theoretical half-width error for the absorption lines, and that these parameters were not well known.

Calculations using a +8% adjustment in the half-widths produces results that give good agreement with the laboratory data. This was true for the data that were observed through a skewed slit function and for later higher-resolution data that were properly taken.

The results of our efforts were made available to Drs. Burch and McClatchey, and further discussions will be held in order to reach an agreement on the most probable cause for the discrepancies. If these questions can be resolved within the next few months, new line-by-line carbon dioxide calculations will be carried out including the necessary adjustments before regular data processing begins.

Comparisons similar to those for the carbon dioxide bands are also being made for the ozone bands in the near future. The laboratory data available for the ozone bands are not of high resolution, and the fine details of the spectra cannot be compared. However, the low-resolution absorption magnitudes will still be useful for evaluating the accuracy of our calculations. The comparison is accomplished by degrading the high-resolution line-by-line calculations by numerically applying an appropriate spectrally-weighted instrument slit function. Initial comparisons for ozone also indicate discrepancies in results for the 9.6-μm bands.

The homogeneous path line-by-line calculations and laboratory measurement comparisons are critical evaluations, since measurements for inhomogeneous paths are very limited and of little use (because exact temperature, pressure, and concentration specifications are not well known). Transmittances for atmospheric paths, therefore, must be determined from accurate homogeneous calculations appropriately applied for atmospheric conditions specified during the simulation process.

The final step in the verification of the spectral calculations is to compare simulated space measurements against actual satellite radiometer measurements. Some data have already been collected for this purpose. Also, software is under development to perform the necessary calculations and to analyze the results.

We are preparing to process 45 days of MFR data to compare our ozone data with similar data for the same period using the TIROS N and Nimbus 7 sensors. The data period for comparison covers January 1 to mid-February 1979. In preparation for this comparison, several codes required for generating the simulated radiances and total ozone

retrieval models are being modified to implement changes to improve their accuracy and computational efficiency. For example, the running time of the codes used to generate simulated radiances has been reduced more than 50%. Additionally, recent ozonesonde data have been obtained from the World Ozone Data Center (Downsview, Canada) in order to bring our ozonesonde data base up to date. The ozonesonde data are used as input to the simulated radiance calculations. The ozonesonde data base includes nearly 6000 soundings from which representative sets of data are selected for the season for which the radiances are simulated.

Software has been developed to perform various analyses on retrieval results. Extraction of various parameters and data for specific regions and times from existing archives is now possible. These extractions can now be printed and displayed, and various manipulation options are being developed for performing analyses of various retrieval problems.

3.3 DATA BASING AND DATA PROCESSING

The major task for the past year has been the development of an automated data basing, archiving, and processing system. The computing capability at the Atmospheric Release Advisory Capability (ARAC) center at LLL will be used for data basing and data processing. We have purchased some additional hardware to supplement the capabilities of the DEC VAX 11/780 computer system which became operational in June 1979 at the ARAC center. A seven-track tape drive was added to enable the input data tapes from AFGWC to be handled, and a floating point accelerator was added to enhance the computation speed for MFR data processing. A 176 megabyte disc system was added to increase the online data storage capacity. One disc can hold one month of satellite and processed data, which is a convenient size for building the long-term archival data base and for data analysis purposes.

High density tape (6250 bpi) has been selected as the long-term storage medium for the data base. Disc packs had initially been considered as the storage medium, but they were rejected when investigation showed that there is a serious risk of catastrophic disc failure and head crashes when the disc packs are handled frequently. The tape medium provides considerably less vulnerability, can be inexpensively duplicated, is cost effective over the data collection period even with the necessary additional hardware, and provides only slightly inferior accessibility to the data.

The presently available 1600 bpi tape technology will be used through the software development phase of this effort since the 6250 bpi tape technology has only recently become available for use on the VAX 11/780 computer system. The high density tape drive has been ordered and will arrive before regular data processing is scheduled to begin.

An LLL-developed scientific data management system called FRAMIS has been chosen for use with the SOAC/DMSP data base. This is a "relational algebra" approach at the forefront of current data base technology. LLL's Computation Department has already invested in a multi-man-year effort to develop this capability and plans considerable expansion and enhancement in the coming year. The system is currently available on the CDC 7600 computers, and we have completed most of the modifications necessary to transfer FRAMIS to the VAX 11/780 computer system. Testing of the initial capability is scheduled to begin in December 1979. Nearly 300 computer routines are being rewritten to run on the new system.

The codes that process and calibrate the raw DMSP radiometer data are being converted to the VAX 11/780 system. Part of the conversion involves the word size dependency problem (AFGWC = 36 bits, LLL 7600 = 60 bits, and VAX 11/780 = 32 bits), and part involves the development of a new quality control package to evaluate the sensor data stream continuously while processing the radiometer data and to provide a record of that performance for the data base archive quality assurance.

Significant progress has been made in how total ozone data are mapped and contoured. We completed the development of a computer code that generates an "intelligent fill" in data-void areas of the daily global ozone analysis. The code generates the fill-field by first mapping and averaging the satellite ozone retrievals in 2-deg latitude-longitude bins. The bins remaining empty after 24 hours of satellite data mapping require filling. Filling is accomplished by one of the following methods, which depends on the data available. The preference for

each method decreases in the order listed: (1) interpolate between the binned data of the day preceding and the day following, (2) use the binned data from the day preceding or the following, (3) use the zonal average values that are computed from the binned data for that day, or (4) use zonal average values that are taken from known climatology.

The resulting global fill-field is not combined with the binned data until it is smoothed. It is smoothed by applying an elementary filter that approximates a bivariate normal function three successive times. After each pass of the filter, the filtered fill-field is overlayed with the 2-deg binned data for that day. The overlaying and filtering process blends the fill-field in the data-void areas with the binned data outside the data-void areas for that day. Also, the filtering process removes small-scale features (e.g., 5-deg horizontal wavelength and smaller) but retains large-scale features (e.g., a wavelength of 60 deg is retained at 96% of its original amplitude) in the data-void areas. Thus only the large-scale features that change little in amplitude and position from day to day are used as an "intelligent fill."

The generated fill-field may be used with either the spline analysis code or the newly developed filter analysis code, which are used to generate ozone contour maps. In either code, the fill-field is used only to fill the data void regions of the global dataset.

The methodology of the filter analysis code is essentially to compute an average grid point value in each 2-deg latitude-longitude bin, fill the data-void bins using the fill-field, and filter the gridded data using a Lanczos filter (Duchon, 1979) having a preselected cutoff frequency. The methodology of the spline analysis is to divide the globe into 10-deg latitude-longitude regions, fit the data within a region in a least-squares sense with B-splines assuring continuity across region boundaries, and treating filled portions of the region as data points.

A study of the two methods has shown that the filter method requires 85% less computer time and fits the input data better than the spline method for all filter cutoff wavelengths (or cutoff frequency) smaller than 20-deg latitude-longitude. The smoothness of the analysis, generated using the filter method, can be varied by varying the cutoff wavelength; increasing the cutoff wavelength increases the smoothness. Two examples of analyses with cutoff wavelengths (λ_c) of 10 and 16 deg are shown in Figs. 15 and 16, respectively. The shaded areas of each map indicate data-void regions. The analysis in Fig. 16 is aesthetically more pleasing than Fig. 15, but has less information content than the analysis in Fig. 15. We experimented with a number of values of λ_c ranging from 6 to 20 deg and selected 10 deg as a balance between aesthetics and information content.

We have also developed codes that generate analyses at 2.5-deg latitude-longitude grid intervals matching the National Meteorological Center (NMC) global temperature/pressure-height grid. This analysis requires 35% less computer time than the 2-deg analysis using the filter method. The 2.5-deg analysis is essentially the same as the 2-deg analysis except for a modulation of the minimum and maximum (L and H) values on the order of 1%. Figure 17 is an example of the 2.5-deg analysis using λ_c = 10 deg.

Our plan is to process the 45 days of data (January 1–February 15, 1979) for comparison with data from TIROS N and Nimbus 7 using the filter method at 2-deg latitude-longitude grid point intervals. When regular data processing begins, we will process the data at 2.5-deg grid intervals using the filter method.

3.4 DATA ANALYSIS

During the past year the number of Dobson observatories that have agreed to take special ozone measurements increased from 33 to 37. Also, measurements from the second Dobson instrument (which is automated) at Arosa are being sent to us. The locations of the participating Dobson observatories are shown in Fig. 18. Special observations are made daily at the time of DMSP satellite overpasses. The data that we receive are entered into a Dobson ozone data base for comparison with the MFR-derived ozone data. The Dobson data base extends from Spring 1977 to the present. All of the Dobson data that we receive are also forwarded to the NOAA Satellite Physics Branch, Silver Spring, Maryland, where they are in turn sent to other NOAA and NASA users. Quality assurance codes were developed to check the Dobson data for any obvious or suspected errors. Software was also written to provide information in a graphical format on the availability of ozone data in the Dobson data base for each individual station.

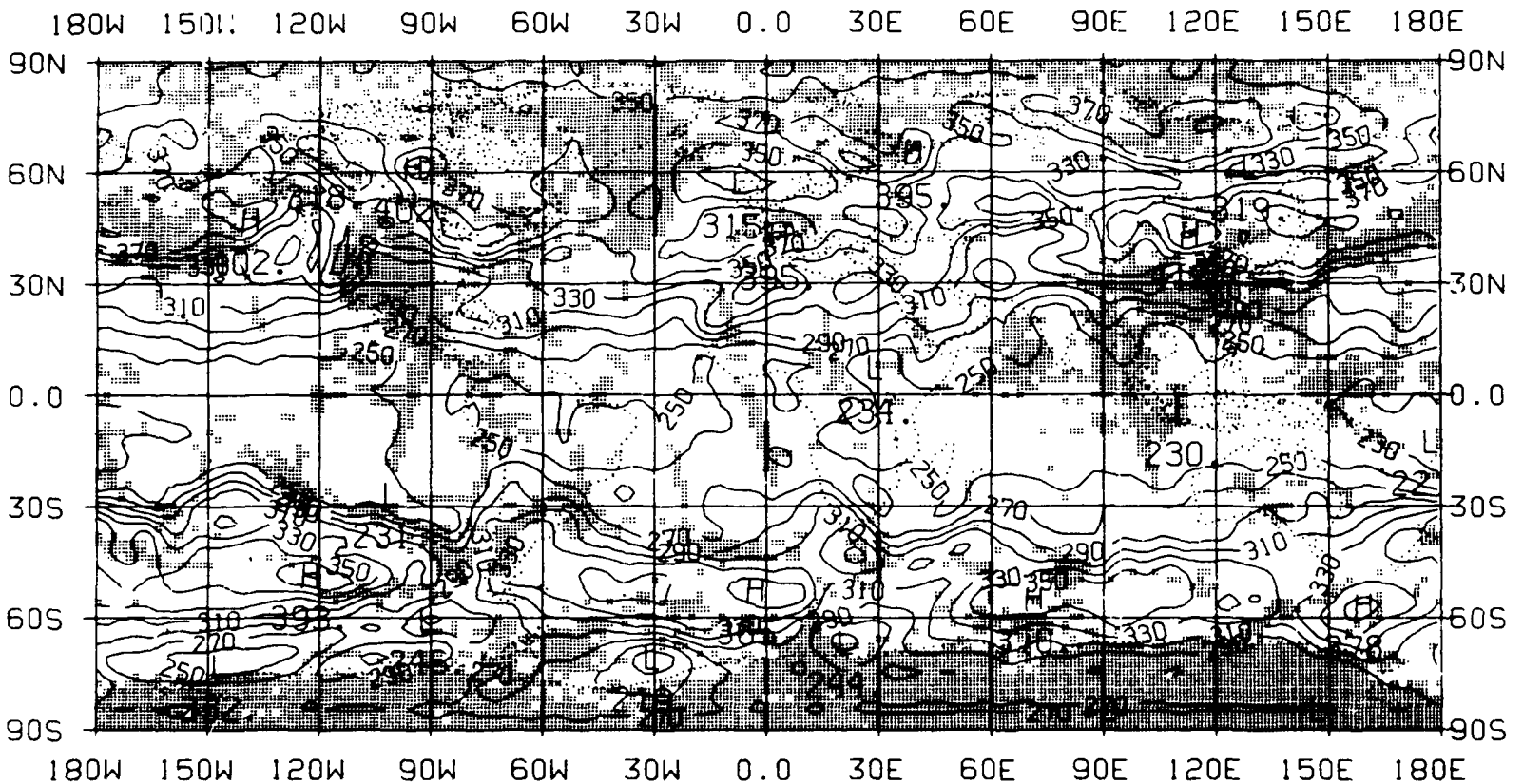

FIG. 15. Analysis for June 21, 1977 at 2-deg grid interval ($\lambda_c = 10°$).

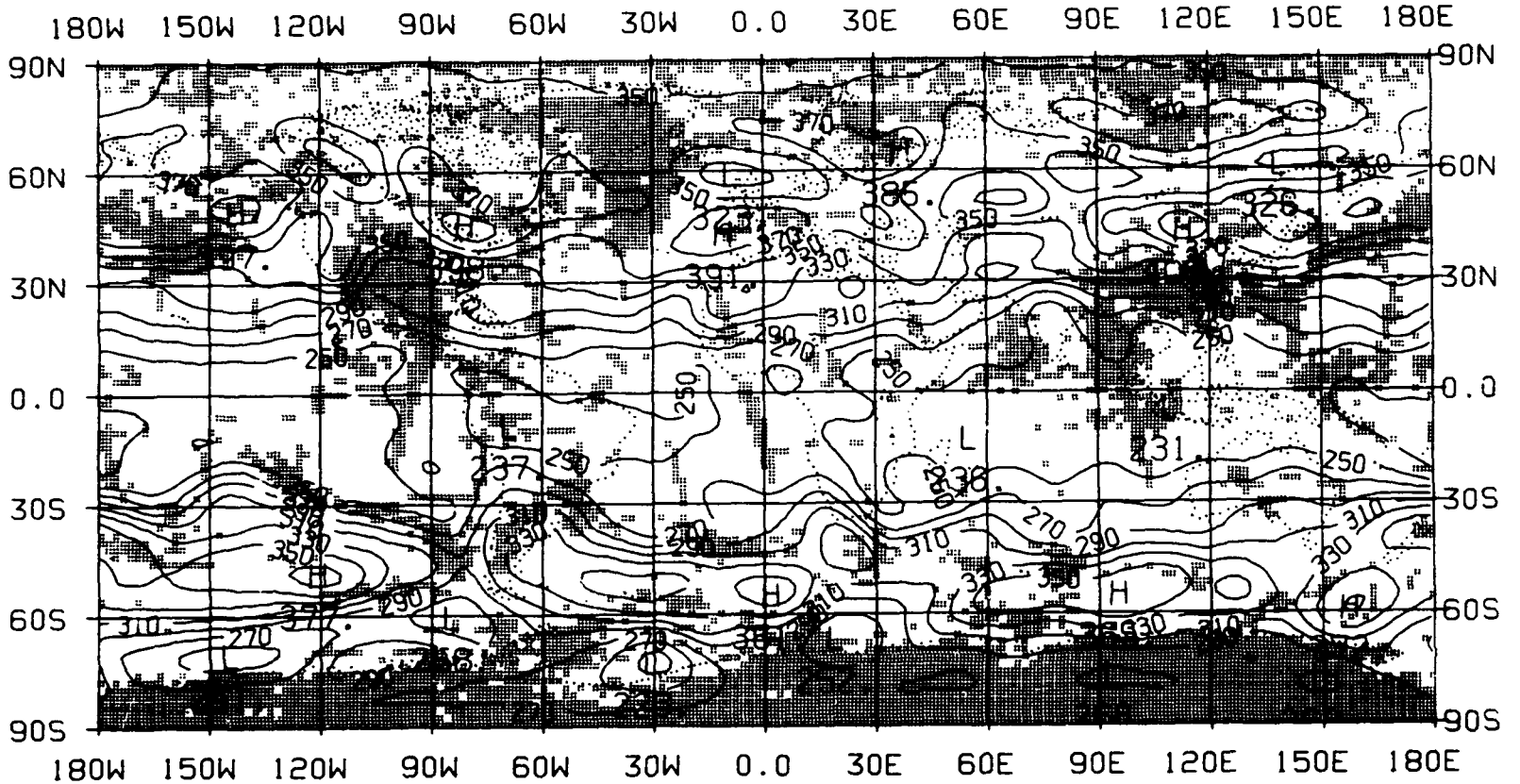

FIG. 16. Analysis for June 21, 1977 at 2-deg grid interval ($\lambda_c = 16°$).

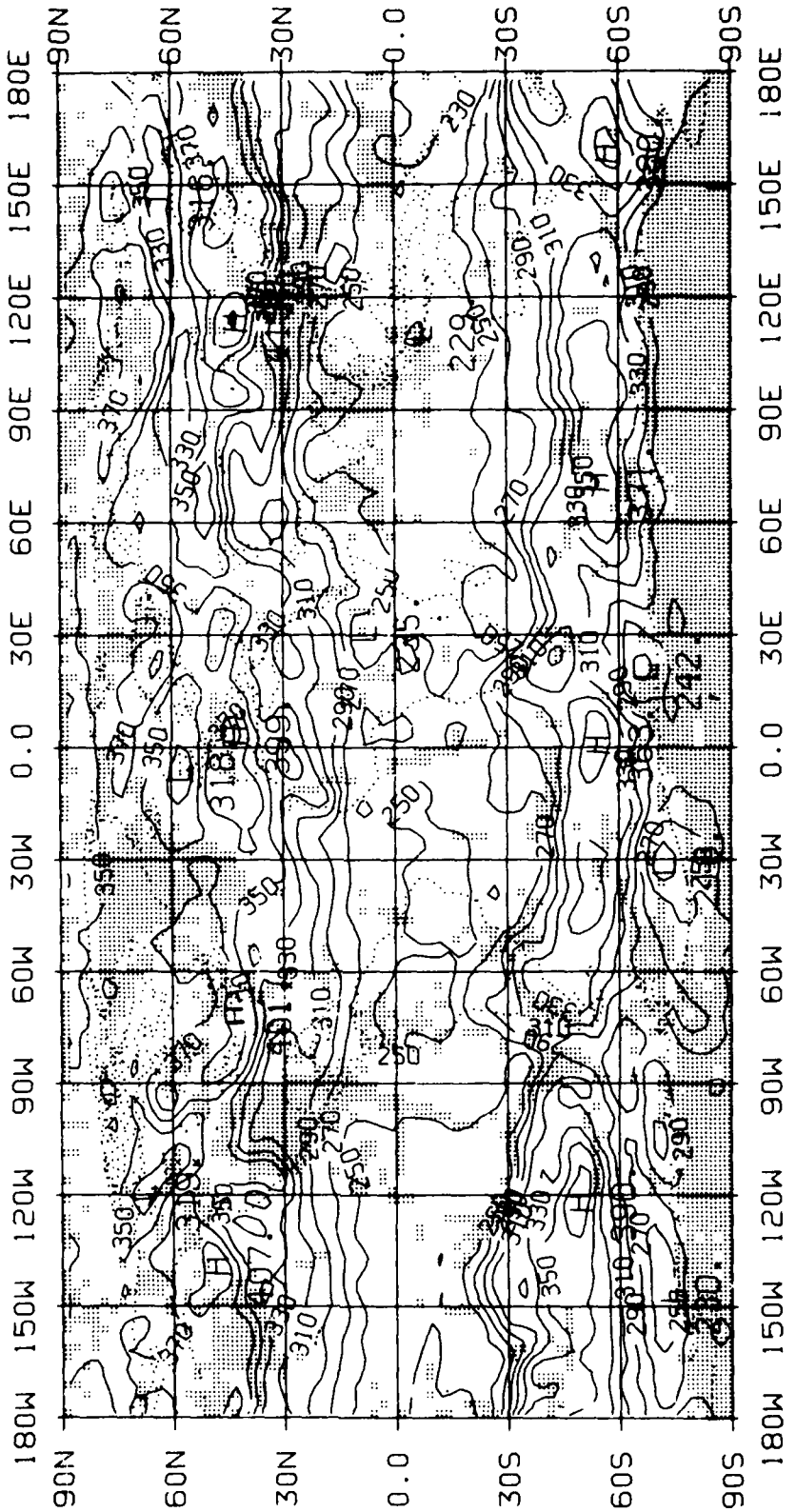

FIG. 17. Analysis for June 21, 1977 at 2.5-deg grid interval ($\lambda_c = 10°$).

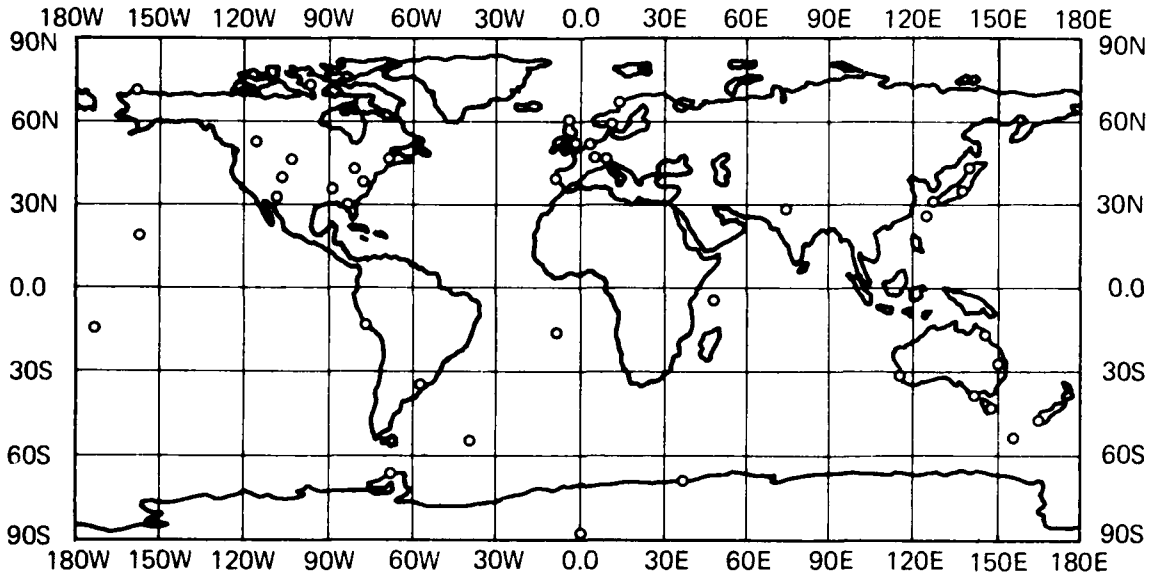

FIG. 18. Location of Dobson spectrophotometer observatories where special measurements of total ozone are taken for comparison with MFC-derived total ozone data.

Preliminary analyses have been made between the MFR ozone data that we processed during the feasibility study and conventional meteorological data fields. Upper-atmospheric data of temperature, pressure-height, wind velocity and humidity were obtained from the National Meteorological Center, Boulder, Colorado. Computer codes were built to access the upper-tropospheric and stratospheric data. Black and white and color graphics routines were used to display multi-parameter variability. A polar map projection is currently being used for displaying the data.

A comparison between the spatial variabilities of total ozone and 100-mb temperatures is shown in Fig. 19 for the Southern Hemisphere. The polar projection extends from the South Pole to 20°S latitude. The ozone data are the average of the 13 days of MFR data that have been processed from June 1977. The Southern Hemisphere was chosen for comparison because it is dynamically more active than the Northern Hemisphere at this time of year.

The total ozone isolines in middle latitudes indicate a dominance of wave number five. The 100-mb temperature data indicate a dominance of wave number five or six. At several locations the total ozone and temperature waves are out of phase with each other. Examples of this may be seen over South America and near Africa. At these locations, relatively higher (lower) amounts of total ozone are associated with warmer (colder) lower-stratospheric temperatures. Total ozone maxima occurring near longitudes of 10°E, 170°E and 80°W at 50°S latitude are located near cores of warm stratospheric air. The relationships between temperature and total ozone just described are not apparent at all locations in the map. The region of high total ozone south of Australia corresponds well with the location of high ozone values for June indicated by London *et al.* (1976) for data from 1957–1967. The MFR total ozone data show more structure in this feature than is indicated by London *et al.* (1976).

Software is being developed that will be used to perform a power spectral analysis of the ozone field from MFR data. Also, work has begun on code development for spherical harmonic analyses of the MFR total ozone data. This line of research is one of several to be followed in later months. A number of methods of discerning relationships among various atmospheric variables are being tested and analyzed. Thus far the methods have been applied to a three-day period (in June 1977) in the Southern

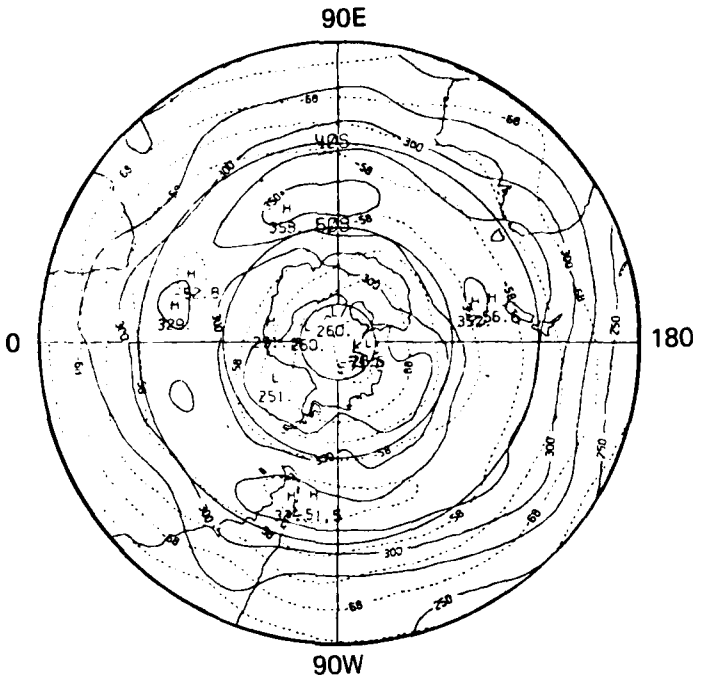

FIG. 19. Southern Hemisphere June 1977 total ozone (units: M.atm.cm; solid line) from satellite MFR and 100-mb temperature (°C; dashed line) from radiosonde.

Hemisphere. Several promising graphical display and data analysis tools have been developed which should prove to be very useful when we begin regular data processing.

4. WORK IN PROGRESS

We are in the process of developing a two-dimensional transport-kinetics model which will be in the programming and initial validation stage during most of Fiscal Year 1980. This model will be used to study latitudinal and seasonal effects of various atmospheric perturbations.

A steady state version of the one-dimensional transport-kinetics code is under development which will significantly reduce the computation time needed for steady-state calculations. Most of our sensitivity studies involve computing the change in total ozone at steady state, so this code will be used extensively in the future.

Routine processing of the DMSP MFR data will begin in the spring of 1980 and will extend through Fiscal Year 1981. In all, data from four satellites with overlapping coverage over a three-year period will be processed. Daily maps of total ozone and monthly statistics and comparisons with Dobson data will be published for distribution to the scientific community. We will also be conducting studies of the spatial and temporal variability of ozone related to natural and man-made influences.

REFERENCES

Anderson, J., "In Situ Measurements of Cl, ClO, HO, HO_2, O_3, and O," paper presented at the Workshop on Upper Atmospheric Measurements, Seattle, Washington, September 5-7, 1979.

Anderson, J. G., H. J. Grassl, R. E. Shetter, and J. J. Margitan, "Stratospheric Free Chlorine Measured by Balloon Borne in situ Resonance Fluorescence," manuscript dated February, 1979.

Angell, J. K. and J. Korshover, "Global Ozone Variations: An Update into 1976," *Mon. Wea. Rev.*, **106**, 725, 1978.

Arthur D. Little, Inc., "Stratospheric Emissions Due to Current and Projected Aircraft Operations," C77327-10, 1976.

Augustsson, T. and V. Ramanathan, "A Radiative-Convective Model Study of the CO_2 Climate Problem," *J. Atmos. Sci.*, **34**, 448-451, 1977.

Bertaux, J. L. and A. Delannoy, "Vertical Distribution of H_2O in the Stratosphere as Determined by UV Fluorescence In-Situ Measurements," *Geophys. Res. Lett.* **5**, 1017, 1978.

Borucki, W. J., D. S. Colburn, R. C. Whitten, L. A. Capone, M. Covert, "Model Analysis of the Ozone Depletion Due to the August 1972 Solar Proton Event," *EOS* **59**, 284, 1978.

Burnett, C. R. and E. B. Burnett, "Spectroscopic Measurements of the Vertical Abundance of Hydroxyl (OH) in the Earth's Atmosphere," *EOS*, **60**, 336, 1979.

Butler, D., NASA Goddard Space Flight Center, private communication, 1979.

Callis, L. B., Jr. and J. E. Nealy, "Solar UV Variability and Its Effect on Stratospheric Thermal Structure and Trace Constituents," *Geophys. Res. Lett.*, **5**, 249, 1978.

Chaloner, C. P., J. R. Drummond, J. T. Houghton, R. F. Jarnot, and H. K. Roscoe, "Infra-Red Measurements of Stratospheric Composition: I. The Balloon Instrument and Water Vapour Measurements," *Proc. Roy. Soc. Lond.*, **A364**, 145, 1978.

Chang, J. S., J. R. Barker, J. E. Davenport, and D. M. Golden, "Chlorine Nitrate Photolysis by a New Technique: Very Low Pressure Photolysis," *Chem. Phys. Lett.*, **60**, 385-390, 1979.

Chang, J. S., W. H. Duewer and D. J. Wuebbles, "The Atmospheric Nuclear Test of the 50's and 60's: A Possible Test of Ozone Depletion Theories," *J. Geophys. Res.*, **84**, 1755-1765, 1979.

Chang, J. S. and F. Kaufman, "Upper Bound and Probable Value of the Rate Constant of the Reaction OH + $HO_2 \rightarrow H_2O + O_2$," *J. Phys. Chem.*, **82**, 1683-1687, 1978.

CIAP Monograph 2, "Propulsion Effluents in the Stratosphere," U.S. Department of Transportation, Washington, D.C., 1975.

CIAP Monograph 3, "The Stratosphere Perturbed by Propulsion Effluents," DOT-TST-75-53, U.S. Department of Transportation, Washington, D.C., 1975.

Cox, R. A., "Kinetics of HO_2 Radical Reactions of Atmospheric Interest," papers presented at WMO Symposium on Geophysical Aspects and Consequences of Change in the Composition of the Stratosphere, Toronto, 26-30 June, 1978, WMO No. 511, 1978.

Cox, R. A. and J. P. Burrows, "Kinetics and Mechanism of the Disproportionation of HO_2 in the Gas Phase," *J. Phys. Chem.*, **83**, 2560-2568, 1979.

Cox, R. A., R. G. Derwent and A. E. J. Eggleton, "Photochemical Oxidation of Halocarbons in the Troposphere," *Atmos. Env.*, **10**, 305-308, 1976.

Crutzen, P. J., I. S. Isaksen, and G. C. Reid, "Solar Proton Events: Stratospheric Sources of Nitric Oxide," *Science*, **189**, 457-459, 1975.

DeMore, W. B., "Reaction of HO_2 with O_3 and the Effect of Water Vapor on HO_2 Kinetics," *J. Phys. Chem.*, **83**, 1113-1118, 1979.

DeMore, W. B. and E. Tschuikow-Roux, "Temperature Dependence of the Reaction of OH and HO_2 with O_3," *J. Phys. Chem.*, **78**, 1447-1451, 1974.

Duchon, C. E., "Lanczos Filtering in One and Two Dimensions," *J. Appl. Meteor.*, **18**(8), 1016–1022, 1979.

Duewer, W. H., D. J. Wuebbles, H. W. Ellsaesser, and J. S. Chang, *NO_x Catalytic Ozone Destruction: Sensitivity to Rate Coefficients*, Lawrence Livermore Laboratory, Livermore, CA, UCRL-77917, 1976; *J. Geophys. Res.*, **82**, 935–942, 1977.

Ellsaesser, H. W., "Water Budget of the Stratosphere," *Proceedings of the Third CIAP Conference*, pp. 273–283, DOT-TSC-OST-74-15, NTIS, Springfield, VA, 1974.

Evans, W. F. J., J. B. Kerr, D. I. Wardle, J. C. McConnell, B. A. Ridley, and H. I. Schiff, "Intercomparison of NO, NO_2, and HNO_3 Measurements With Photochemical Theory," *Atmosphere*, **14**, 189, 1976.

Evans, W. F. J., H. Fast, J. B. Kerr, C. T. McElroy, R. S. O'Brien, D. I. Wardle, J. S. McConnell and B. A. Ridley, "Stratospheric Constituent Measurements from Project Stratoprobe," papers presented at WMO Symposium on the Geophysical Aspects and Consequences of Changes in the Composition of the Stratosphere, Toronto, 26–30 June 1978, WMO No. 511, 1978.

Fabian, P., J. A. Pyle, and R. J. Wells, "The August 1972 Solar Proton Event and the Atmospheric Ozone Layer," *Nature*, **277**, 458–460, 1979.

Farmer, C. B. "Infrared Measurements of Stratospheric Composition," *Can. J. Chem*, **52**, 1544, 1974.

Foley, H. M. and M. A. Ruderman, "Stratospheric Nitric Oxide Production from Past Nuclear Explosions and Its Relevance to Projected SST Pollution," Paper P-894, Institute for Defense Analysis, Jason, Arlington, VA, 1972.

Frederick, J. D. and R. D. Hudson, "Predissociation of Nitric Oxide in the Mesosphere and Stratosphere," *J. Atmos. Sci.*, **36**, 737–745, 1979.

Grobecker, A. J., S. C. Coroniti, and R. H. Cannon, Jr., "CIAP Report of Findings, The Effects of Stratospheric Pollution by Aircraft," Report DOT-TST-75-50, U.S. Department of Transportation, Washington, D.C., 1974.

Hamilton, E. J., Jr. and R. R. Lii, "The Dependence of H_2O and on NH_3 of the Kinetics of the Self Reaction of HO_2 in the Gas Phase Formation of $HO_2 \cdot H_2O$ and $HO_2 \cdot NH_3$ Complexes," *Int. J. Chem. Kinet.*, **9**, 875–885, 1977.

Harries, J. E., "Measurements of Stratospheric Water Vapor Using Infrared Techniques," *J. Atmos. Sci.*, **30**, 1691, 1973.

Harries, J. E., "The Distribution of Water Vapor in the Stratosphere," *Rev. Geophys. Space Phys.*, **14**, 565, 1976.

Heath, D. F., A. J. Krueger, and P. J. Crutzen, "Influence of a Solar Proton Event on Stratospheric Ozone," *Science*, **197**, 886–889, 1977.

Heath, D. F. and M. P. Thekaekara, "The Solar Spectrum Between 1200 and 3000 *Å*," in *The Solar Output and Its Variation*, O. R. White (ed.), Colorado Assoc. Univ. Press, Boulder, CO, p. 193, 1977.

Hilsenrath, E., B. Guenther, and P. Dunn, "Water Vapor in the Lower Stratosphere Measured from Aircraft Flight," NASA Preprint X-912-76-239, GSFC, Greenbelt, MD, 1976.

Hochanadel, C. J., J. A. Ghormley, and P. J. Ogren, "Absorption Spectrum and Reaction Kinetics of HO_2 Radical in the Gas Phase," *J. Chem. Phys.*, **56**, 4426–4432, 1972.

Howard, C. J. and D. M. Evenson, "Kinetics of the Reaction HO_2 with NO," *Geophys. Res. Lett.*, **4**, 437, 1977.

Hunt, B. G., "A Theoretical Study of the Changes Occurring in the Ozonosphere During a Total Eclipse of the Sun," *Tellus*, **18**, 516–523, 1965.

Hyson, P., "Stratospheric Water Vapour Measurements Over Australia 1973–1976," *Quart. J. Roy. Met. Soc.*, **104**, 225–228, 1978.

JPL Publication 79-27, "Chemical Kinetic and Photochemical Data for Use in Stratospheric Modeling," NASA Panel for Data Evaluation, 1979.

Keeling, C. D., J. A. Adams, Jr., C. A. Ekdahl, Jr., and P. R. Guenther, "Atmospheric CO_2Variations at the South Pole," *Tellus*, **28**, 552–564, 1976a.

Keeling, C. D., R. B. Bacastow, A. E. Bainbridge, C. A. Ekdahl, Jr., P. R. Guenther, L. S. Waterman, and J. F. S. Chin, "Atmospheric CO_2 Variations at Mauna Loa Observatory, Hawaii," *Tellus*, **28**, 538–551, 1976b.

Kuhn, P.M., L. P. Stearns, and M. S. Lojko, "Latitudinal Profiles and Stratospheric Water Vapor," *Geophys. Res Letts.*, **2**, 227–230, 1975.

Kuhn, P. M. and L. P. Stearns, "Interim Letter Report No. 10 for Period 1 Feb–1 May 1973," for the Climatic Impact Assessment Program, U.S. Department of Transportation, NOAA, Boulder, CO, 1973.

Leu, M. T. and C. L. Lin, "Rate Constants for the Reactions of OH with ClO, Cl_2, and Cl_2O at 298 K," *Geophys. Res. Lett.*, **6**, 425–428, 1979.

Logan, J. A., M. J. Prather, S. C. Wofsy, and M. B. McElroy, "Atmospheric Chemistry: Response to Human Influence," *Phil. Trans. Roy. Soc. London*, **290**, 187–234, 1978.

London, J., R. D. Bojkov, S. Oltmans, and J. I. Kelley, *Atlas of Global Distribution of Total Ozone, July 1957–June 1967*, National Center for Atmospheric Research, Boulder, CO, Technical Note NCAR/TN/113-STR, 276 pp., 1976.

Louisnard, N., A. Girard, and G. Eichen, "Measures du profil vertical de concentration de la vapeur d'eau stratospherique," *C. R. Acad. des Sciences, Paris*, Oct. 1979, and private communication.

Lovill, J. E., T. J. Sullivan, R. L. Weichel, J. S. Ellis, J. G. Huebell, J. A. Korver, P. P. Weidhaas, and F. A. Phelps, *Total Ozone Retrieval from Satellite Multichannel Filter Radiometer Measurements*, Lawrence Livermore Laboratory, Livermore, CA, UCRL-52473, 1978.

Luther, F. M., *et al.*, *First Annual Report of Lawrence Livermore Laboratory on the High Altitude Pollution Program*, Lawrence Livermore Laboratory, Livermore, CA, UCRL-50042-76, 1976.

Luther, F. M., *et al.*, *Annual Report of Lawrence Livermore Laboratory to the High Altitude Pollution Program—1977*, Lawrence Livermore Laboratory, Livermore, CA, UCRL-50042-77, 1977.

Luther, F. M., *et al.*, *Annual Report of Lawrence Livermore Laboratory to the FAA on the High Altitude Pollution Program—1978*, Lawrence Livermore Laboratory, Livermore, CA, UCRL-50042-78, September 30, 1978.

Luther, F. M., D. J. Wuebbles, and J. S. Chang, "Temperature Feedback in a Stratospheric Model," *J. Geophys. Res.*, **82**, 4935–4942, 1977.

Luther, F. M., J. S. Chang, W. H. Duewer, J. E. Penner, R. L. Tarp, and D. J. Wuebbles, "Potential Environmental Effects of Aircraft Emissions," Lawrence Livermore Laboratory, Livermore, CA, UCRL-52861, 1979.

Mastenbrook, H. J., "Water Vapor Distribution in the Stratosphere and High Troposphere," *J. Atmos. Sci.*, **25**, 299, 1968.

McConnell, J. C. and H. I. Schiff, "Methyl Chloroform: Impact on Stratospheric Ozone," *Science*, **199**, 174–177, 1978.

McKinnon, D. and H. W. Moorewood, "Water Vapor Distribution in the Lower Stratosphere Over North and South America," *J. Atmos. Sci.*, **27**, 483–493, 1970.

Menzies, R. T., "Remote Measurement of ClO in the Stratosphere," *Geophys. Res. Lett.*, **6**, 151, 1979.

Murcray, D., "Infrared Techniques for Remote Sensing," paper presented at Workshop on Upper Atmospheric Measurements, Seattle, Washington, September 5–7, 1979.

Murgatroyd, R. J., P. Goldsmith, and W. E. H. Hollings, "Some recent measurements of humidity from aircraft up to heights of about 50,000 feet over southern England," *Quart. J. Roy. Met. Soc.*, **81**, 533, 1955.

Murgatroyd, R. J., "Ozone and Water Vapour in the Upper Troposphere and Lower Stratosphere, Meteorological Aspects of Atmospheric Radioactivity," *Tech. Note 68*, W. Bleaker (ed.), pp. 68–94, WMO, Geneva, 1965.

NASA Reference Publication 1010, "Chlorofluoromethanes and the Stratosphere," R. D. Hudson (ed.), 1977.

NASA Reference Publication 1049, "The Stratosphere: Present and Future," R. D. Hudson and E. I. Reed (eds.), 1979.

National Research Council, Climatic Impact Committee, *Environmental Impact of Stratospheric Flight: Biological and Climatic Effects of Aircraft Emissions in the Stratosphere*, National Academy of Sciences, Washington, D.C., 1975a.

National Research Council, *Halocarbons: Effects on Stratospheric Ozone*, see Appendix D, National Academy of Sciences, 1976.

NBS Special Publication 513, *Reaction Rate and Photochemical Data for Atmospheric Chemistry—1977*, R. F. Hampson, Jr., and D. Garvin (eds.), National Bureau of Standards, Washington, D.C., 1978.

NBS Technical Note 866, "Chemical Kinetics and Photochemical Data for Modeling Atmospheric Chemistry," R. F. Hampson, Jr. and D. Garvin (eds.), National Bureau of Standards, Washington, D.C., 1975.

Neely, W. B. and J. H. Plonka, "Estimation of Time Averaged Hydroxyl Radical Concentrations in the Troposphere," *Environ. Sci. and Tech.*, **12**, 317, 1978.

Nichols, D. A., "DMSP Block 5D Special Meteorological Sensor H, Optical Subsystem," *Opt. Engr.*, **14**, 284–288, 1975.

Oliver, R. C., E. Bauer, H. Hidalgo, K. A. Gardner, and W. Wasylkiwskyj, *Aircraft Emissions: Potential Effects on Ozone and Climate: A Review and Progress Report*, Federal Aviation Administration Report FAA-EQ-77-3, 1977.

Oliver, R. C., E. Bauer, and W. Wasylkiwskyj, *Recent Developments in the Estimation of Potential Effects of High Altitude Aircraft Emissions on Ozone and Climate*, Report No. FAA-AEE-78-24, U.S. Department of Transportation, Federal Aviation Administration, Washington, D.C., 1978.

Penndorf, R., *Analysis of Ozone and Water Vapor Field Measurement Data*, Report No. FAA-EE-78-29, NTIS, Springfield, VA, 1978.

Penner, J. E. and J. S. Chang, "Possible Variations in Atmospheric Ozone Related to the Eleven Year Solar Cycle," *Geophys. Res. Lett.*, **5**, 817–820, 1978.

Penner, J. E. and J. S. Chang, *The Relation Between Atmospheric Trace Species Variabilities and Solar UV Variability*, Lawrence Livermore Laboratory, Livermore, CA, UCRL-83029, submitted for publication, 1979

Pierotti, D. and R. A. Rasmussen, "Combustion as a Source of Nitrous Oxide in the Atmosphere," *Geophys. Res. Lett.*, **3**, 265, 1976.

Poppoff, I. G., R. C. Whitten, R. P. Turco, and L. A. Capone, "An Assessment of the Effect of Supersonic Aircraft Operations on the Stratospheric Ozone Content," NASA RP-1026, 1978.

Radford, H. E., M. M. Litvak, C. A. Gottlieb, E. W. Gottlieb, S. K. Rosenthal, and A. E. Lilley, "Mesopheric Water Vapor Measured from Ground-Based Microwave Observations," *J. Geophys. Res.*, **82**, 472, 1977.

Ramanathan, V., L. B. Callis, and R. E. Boughner, "Sensitivity of Surface Temperature and Atmospheric Temperature to Perturbations in the Stratospheric Concentration of Ozone and Nitrogen Dioxide," *J. Atmos. Sci.*, **33**, 1092–1112, 1976.

Rogers, J. W., A. T. Stair, T. C. Degges, C. L. Wyatt, and D. J. Baker, "Rocketborne Measurements of Mesospheric H_2O in the Auroral Zone," *Geophys. Res. Lett.*, **4**, 366, 1977.

Schneider, S. H., "On the Carbon Dioxide Climate Confusion," *J. Atmos. Sci.*, **32**, 2060, 1975.

Seitz, H., B. Davidson, J. P. Friend, and H. W. Feely, *Numerical Models of Transport Diffusion and Fallout of Stratospheric Radioactive Material (Final Report on Project STREAK)*, USAEC Report NYO-3654-4, 1968.

Simon, P. C., "Irradiation Solar Flux Measurements Between 120 and 400 nm. Current Position and Future Needs," *Planet. Space Sci.*, **26**, 355–365, 1978.

Stolarski, R. S., D. M. Butler, and R. D. Rundel, "Uncertainty Propagation in a Stratospheric Model: II. Monte Carlo Analysis of Imprecisions Due to Reaction Rates," *J. Geophys. Res.*, **83**, 3074, 1978.

U.S. Standard Atmosphere, 1976, NOAA-S/T 76-1562, U.S. Government Printing Office, Washington, D.C., 1976.

Waters, J. W., J. J. Gustincic, R. V. Kakar, A. R. Kerr, H. K. Roscoe, and P. N. Swanson, NASA Report TMX-73630, NTIS, Springfield, VA, 1977.

Weiss, R. F. and H. Craig, "Production of Atmospheric Nitrous Oxide by Combustion," *Geophys. Res. Lett.*, **3**, 751, 1976.

Wongdontri-Stuper, W., R. K. M. Jayanty, R. Simonaitis, and J. Heicklen, "The Cl_2-Photosensitized Decomposition of O_3: The Reactions of ClO and OClO with O_3," preprint, Lawrence Livermore Laboratory, Livermore, CA, 1978.

Wuebbles, D. J. and J. S. Chang, "A Theoretical Study of Stratospheric Trace Species Variations During a Solar Eclipse," *Geophys. Res. Lett.*, **6**, 179–182, 1979.

APPENDIX A
DESCRIPTION OF LLL ONE-DIMENSIONAL TRANSPORT-KINETICS MODEL (AS PRESENTED AT NASA HARPERS FERRY WORKSHOP 1979)

The local concentrations of trace species in an air parcel are determined by the chemical and photochemical processes and nonchemical sources and sinks occurring within the parcel, and by the transport and radiative fluxes into and out of the parcel. One-dimensional mathematical models of the chemical processes in the stratosphere are governed by the chemical species conservation equation

$$\partial c_i/\partial t + \frac{\partial}{\partial z} F_i(c_i,z,t) = P_i[c,J(z,t,c), k(z,t), \rho)] - L_i\{c,J(z,t,c)\, k[T(z,t), \rho]\}\, c_i + S_i(z,t) \qquad \text{(A-1)}$$

where $c_i = c_i(z,t)$ is the concentration of the i^{th} chemical constituent; c is the general representation of all constituents; P_i and $L_i c_i$ are the production and loss of c_i due to photochemical interactions; T is the ambient air temperature; ρ is the ambient air density; F_i is the vertical transport flux of c_i; S_i represents any other possible sinks or sources of c_i; J represents photodissociation coefficients; k represents chemical reaction rate coefficients; and all of these variables are defined at a given vertical position z at time t. The explicit display of the major interdependent relations of these variables in Eq. (A-1) illustrates the nonlinearity and general complexity of this mathematical system. Equation (A-1) is defined over a spatial domain D with appropriate boundary conditions. There is one conservation equation for each chemical species treated.

PHYSICAL DOMAIN

The LLL one-dimensional model extends from the ground to 56.25 km. The model currently calculates the vertical concentration distributions of 39 (2 of which are used only in sensitivity studies) atmospheric trace constituents. The model contains 134 (14 of which are used only in sensitivity studies) chemical or photochemical reactions. Table A-1 lists the species solved for in the model. Of these species, $O(^1D)$, H, and N are assumed to be in instantaneous equilibrium. The vertical grid structure is variable, but for the calculations reported here, we have a 0.5-km-thick layer at the surface, 1-km thick layers extending from 0.5 to 34.5 km, a 1.75-km thick layer between 34.5 and 36.25 km and 2.5-km thick layers extending to 56.25 km.

TRANSPORT REPRESENTATION

The net vertical transport flux, F_i, of any minor constituent c_i is represented through a diffusion approximation in which F_i is assumed to be proportional to the gradient of the mixing ratio of that trace species:

$$F_i = -K_z \rho \frac{\partial}{\partial z}(c_i/\rho) \qquad \text{(A-2)}$$

where K_z is the one-dimensional vertical diffusion coefficient. The LLL K_z profile (shown in Fig. A-1) used in the calculations for this report was originally based on an analysis of N_2O and CH_4 measurements (NAS, 1976) with considerations also given to measurements of radionuclide debris transport in the lower stratosphere.

The LLL one-dimensional model has been designed such that profiles of K_z utilized by other groups (or at previous times) can be easily incorporated. Such profiles have been utilized to test the sensitivity of the results to transport parameterization uncertainties.

TABLE A-1. Species calculated in LLL one-dimensional model.

$O(^3P)$	Cl	CH_4
O_3	ClO	HCO
NO	$ClONO_2$	CH_2O
NO_2	$ClNO_2$	CH_3
N_2O	HCl	CH_3OOH
HNO_3	OClO[a]	CH_3O
OH	HOCl	CH_3O_2
HO_2	CH_3Cl	CO
H_2O_2	CF_2Cl_2	H_2
NO_3	$CFCl_3$	$O(^1D)$
N_2O_5	CH_3CCl_3	N
H_2O	ClO_3[a]	H
HONO	CCl_4	
HNO_4		

[a]Used only in sensitivity studies.

CHEMISTRY

We have used two 1979 versions of model chemistry in this report (see Tables A-2 through A-4). 1979a chemistry was based primarily on the rate recommendations in JPL (1979). However, several reactions discussed in JPL (1979) are omitted in the model, and several reactions not discussed in JPL (1979) are included. This chemistry was used for many sensitivity calculations carried out in the spring of 1979. 1979b chemistry was based almost exclusively on the draft chapter on chemical reaction rates prepared at the NASA Harpers Ferry Workshop (June, 1979). It has a few comparatively minor differences from the final draft of that report, and it includes a few reactions not assessed at the NASA Workshop.

Two reactions treated in the 1979a chemistry are controversial and are of some importance to our sensitivity studies. These are

$$ClO + NO_2 \xrightarrow{M} ClONO_2 \tag{A3}$$

and

$$ClO + OH \rightarrow HCl + O_2 . \tag{A4}$$

In the 1979a chemistry, we used the slower of the two JPL-recommended rate constants for chlorine nitrate formation, and we adopted an expression for HCl formation from OH + ClO that is about half the upper limit for that reaction path. In the 1979b chemistry, we used the faster of the two recommendations for the chlorine nitrate formation rate coefficient. Three considerations inspired this choice: (1) the majority of the chemistry panel seemed to favor the faster expression, (2) even if the bulk of the reaction between ClO and NO_2 leads to other products (as suggested by those favoring the slower rate coefficient), the other products might easily have an effect on stratospheric chemistry similar to that of $ClONO_2$, and (3) it improved the comparison between calculation and observation for both ClO and $ClONO_2$.

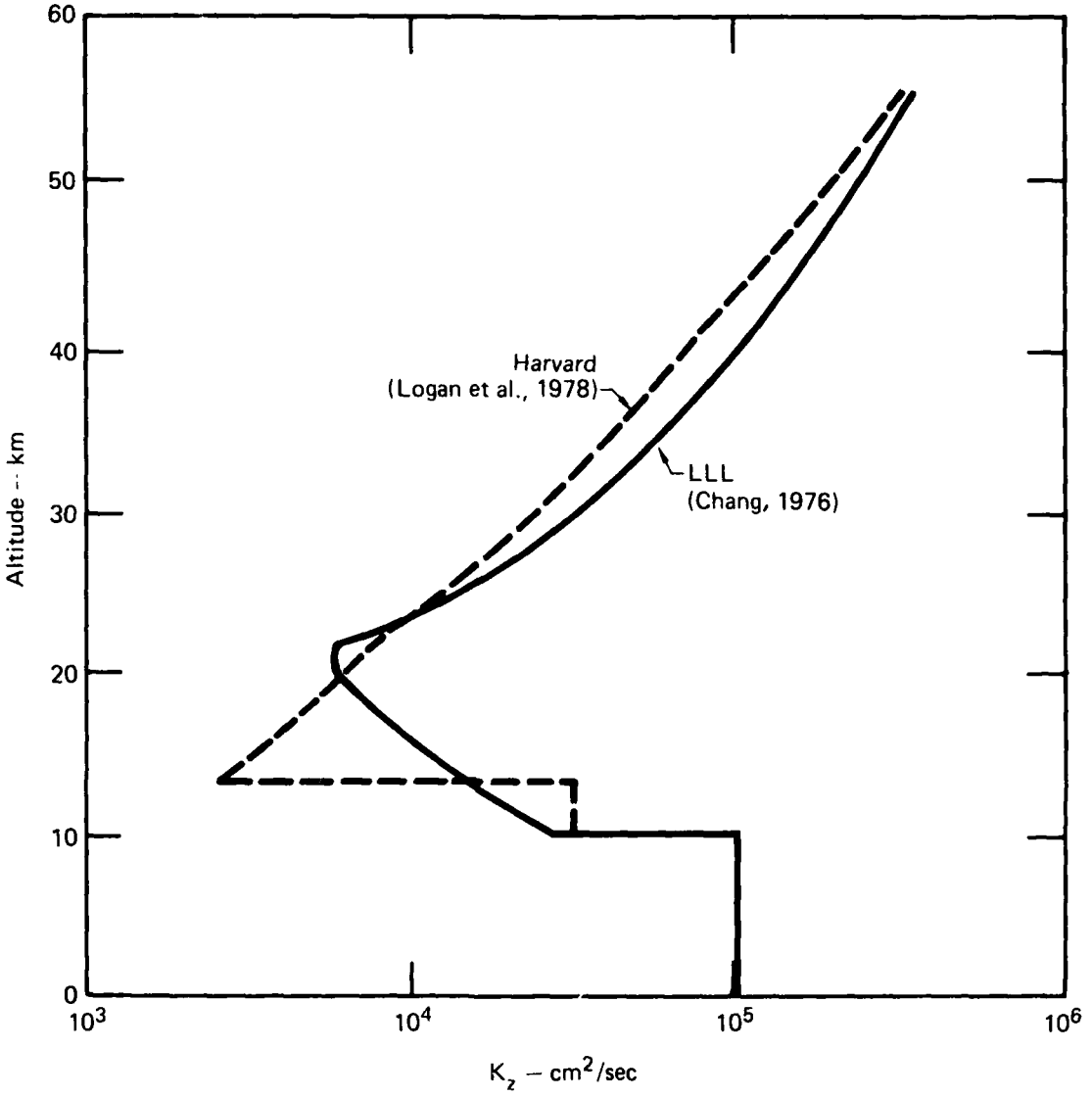

FIG. A-1. Vertical transport coefficients currently being used by two modeling groups.

In our 1979b chemistry we omitted the reaction forming HCl from OH + ClO. The decision to include this reaction in the 1979a chemistry was based on privately communicated preliminary results that seemed to suggest that the reaction probably occurred, but they have since been interpreted as providing only an upper limit. Both of these controversial choices of rate coefficient have a significant impact on model sensitivities (especially for ClX) but they oppose each other. As a result, 1979a and 1979b chemistries yield qualitatively similar perturbational sensitivities for both NO_x and ClX perturbations. The 1979b chemistry is less controversial than the 1979a chemistry and is to be preferred for purposes of comparison with other workers. All primary assessments have been repeated using 1979b chemistry. However, several sensitivity studies were not repeated, since it seemed unlikely that the qualitative results of those sensitivity studies would differ if they were repeated, and because the 1979a chemistry is well within the limits of reasonable uncertainty in our present knowledge of the atmosphere. The two chemistries are also useful in emphasizing the existence of processes for which no clear recommendation is available.

TABLE A-2. Chemical reactions and rate coefficients where $k = A\, e^{B/T}$ used in 1979 model chemistry.

	Reaction	A[a]	B	Note
1.	$O + O_2 \xrightarrow{M} O_3$	See Table A-3	-	3
2.	$O + O_3 \rightarrow 2O_2$	1.5×10^{-11}	-2218	1
3.	$O_3 + NO \rightarrow NO_2 + O_2$	2.3×10^{-12}	-1450	1
4.	$O + NO_2 \rightarrow NO + O_2$	9.3×10^{-12}	0	1
5.	$N_2O + O(^1D) \rightarrow N_2 + O_2$	4.8×10^{-11} 5.1×10^{-11}	0 0	1 2
6.	$N_2O + O(^1D) \rightarrow 2NO$	6.2×10^{-11} 5.9×10^{-11}	0 0	1 2
7.	$N + O_2 \rightarrow NO + O$	4.4×10^{-12}	-3220	1
8.	$N + NO \rightarrow N_2 + O$	3.4×10^{-11}	0	1
9.	$O(^1D) + H_2O \rightarrow 2OH$	2.3×10^{-10}	0	1
10.	$O_3 + OH \rightarrow HO_2 + O_2$	1.6×10^{-12}	-940	1
11.	$O + OH \rightarrow O_2 + H$	4.0×10^{-11}	0	1
12.	$O_3 + HO_2 \rightarrow OH + 2O_2$	1.1×10^{-14}	-580	1
13.	$O + HO_2 \rightarrow OH + O_2$	3.5×10^{-11}	0	1
14.	$H + O_2 \xrightarrow{M} HO_2$	See Table A-3	-	3
15.	$O_3 + H \rightarrow OH + O_2$	1.4×10^{-10}	-470	1
16.	$HO_2 + HO_2 \rightarrow H_2O_2 + O_2$	2.5×10^{-12}	0	1
17.	$HO_2 + OH \rightarrow H_2O + O_2$	4.0×10^{-11}	0	1
18.	$OH + NO_2 \xrightarrow{M} HNO_3$	See Table A-3	-	1
19.	$OH + HNO_3 \rightarrow H_2O + NO_3$	8.5×10^{-14}	0	1,10
20.	$H_2O_2 + OH \rightarrow H_2O + HO_2$	1.0×10^{-11}	-750	1
21.	$N_2 + O(^1D) \xrightarrow{M} N_2O$	See Table A-3	-	3
22.	$N + NO_2 \rightarrow N_2O + O$	2.1×10^{-11}	-800	1
23.	$NO + O \xrightarrow{M} NO_2$	See Table A-3	-	3
24.	$NO + HO_2 \rightarrow NO_2 + OH$	4.3×10^{-12} 3.4×10^{-12}	200 250	1 2
25.	$H_2 + O(^1D) \rightarrow OH + H$	9.9×10^{-11}	0	1
26.	$OH + OH \rightarrow H_2O + O$	1.0×10^{-11}	-500	1
27.	$N + O_3 \rightarrow NO + O_2$	2.0×10^{-11}	-3000	4
28.	$NO_2 + O_3 \rightarrow NO_3 + O_2$	1.2×10^{-13}	-2450	1
29.	$OH + OH \xrightarrow{M} H_2O_2$	See Table A-3	-	3
30.	$H_2O_2 + O \rightarrow OH + HO_2$	2.8×10^{-12}	-2125	1
31.	$CO + OH \xrightarrow{M} H + CO_2$	See Table A-3	-	3

[a]When two entries are given, the lower one corresponds to 1979a chemistry and the upper one corresponds to 1979b chemistry.

TABLE A-2. (Continued)

Reaction		A[a]	B	Note
32.	$O(^1D) + M \rightarrow O + M$	2.2×10^{-11}	99	5
33.	$Cl + O_3 \rightarrow ClO + O_2$	2.8×10^{-11}	-257	1
34.	$Cl + NO_2 \xrightarrow{M} ClNO_2$	See Table A-3	-	3
35.	$ClO + O \rightarrow Cl + O_2$	7.7×10^{-11}	-130	1
36.	$NO + ClO \rightarrow NO_2 + Cl$	7.8×10^{-12}	250	1
37.	$ClO + NO_2 \xrightarrow{M} ClONO_2$	See Table A-3	-	3
38.	$HCl + O(^1D) \rightarrow Cl + OH$	1.4×10^{-10}	0	1
39.	$OH + HCl \rightarrow H_2O + Cl$	2.8×10^{-12}	-425	1
40.	$O + HCl \rightarrow OH + Cl$	1.14×10^{-11}	-3370	1
41.	$Cl + HO_2 \rightarrow HCl + O_2$	4.5×10^{-11}	0	1
42.	$CFCl_3 + O(^1D) \rightarrow 3Cl$	2.2×10^{-10}	0	1,6
43.	$CF_2Cl_2 + O(^1D) \rightarrow 2Cl$	1.4×10^{-10}	0	1,6
44.	$Cl + H_2 \rightarrow HCl + H$	3.5×10^{-11}	-2290	1
45.	$Cl + H_2O_2 \rightarrow HCl + HO_2$	8.9×10^{-12} 1.7×10^{-12}	-925 -384	11 2
46.	$ClONO_2 + O \rightarrow ClO + NO_3$	3.0×10^{-12}	-808	1,10
47.	$CH_3Cl + OH \rightarrow Cl + H_2O + HO_2$	2.2×10^{-12}	-1142	1
48.	$NO + NO_3 \rightarrow 2NO_2$	2.0×10^{-11} 8.7×10^{-12}	0 0	1 3
49.	$NO_2 + O \xrightarrow{M} NO_3$	See Table A-3	-	3
50.	$NO_2 + NO_3 \xrightarrow{M} N_2O_5$	See Table A-3	-	3
51.	$N_2O_5 \xrightarrow{M} NO_2 + NO_3$	See Table A-3	-	3
52.	$N_2O_5 + H_2O \rightarrow 2HNO_3$	1.0×10^{-20}	0	7
53.	$O(^1D) + O_3 \rightarrow 2O_2$	1.2×10^{-10}	0	1
54.	$HO_2 + HO_2 + H_2O \rightarrow H_2O_2 + O_2 + H_2O$	See Table A-3	-	3
55.	$O + NO_3 \rightarrow O_2 + NO_2$	1.0×10^{-11}	0	1
56.	$HO_2 + NO_2 \xrightarrow{M} HNO_4$	See Table A-3	-	3
57.	$HNO_4 \xrightarrow{M} HO_2 + NO_2$	See Table A-3	-	3
58.	$OH + HNO_4 \rightarrow H_2O + NO_2 + O_2$	6.0×10^{-12}	-750	1,8
59.	$Cl + HNO_4 \rightarrow HCl + NO_2 + O_2$	3.0×10^{-12}	-300	8
60.	$HO_2 + ClO \rightarrow O_2 + HOCl$	7.0×10^{-13}	500	1
61.	$Cl + HOCl \rightarrow HCl + ClO$	3.0×10^{-12}	-300	8
62.	$OH + HOCl \rightarrow H_2O + ClO$	3.0×10^{-12}	-800	1

[a]When two entries are given, the lower one corresponds to 1979a chemistry and the upper one corresponds to 1979b chemistry.

TABLE A-2. (Continued)

Reaction		A[a]	B	Note
63.	$O + HOCl \rightarrow OH + ClO$	1.0×10^{-11}	-2200	1
64.	$OH + CH_4 \rightarrow CH_3 + H_2O$	2.4×10^{-12}	-1710	1
65.	$O + CH_4 \rightarrow CH_3 + OH$	3.5×10^{-11}	-4550	1
66.	$O(^1D) + CH_4 \rightarrow CH_2O + H_2$	1.0×10^{-11}	0	1
67.	$O(^1D) + CH_4 \rightarrow CH_3 + OH$	1.3×10^{-10}	0	1
68.	$CH_4 + Cl \rightarrow HCl + CH_3$	9.9×10^{-12}	-1359	1
69.	$Cl + CH_3Cl \rightarrow HO_2 + CO + 2HCl$	3.4×10^{-11}	-1256	1,6
70.	$CH_3O_2 + NO \rightarrow NO_2 + CH_3O$	7.0×10^{-12} 8.0×10^{-12}	0 0	1 2
71.	$Cl + CH_2O \rightarrow HCl + HCO$	9.2×10^{-11}	-68	1
72.	$CH_3O_2 + HO_2 \rightarrow CH_3OOH + O_2$	6.0×10^{-12} 1.0×10^{-12}	0 0	1 2
73.	$CH_3O + O_2 \rightarrow CH_2O + HO_2$	5.0×10^{-13}	-2000	1
74.	$OH + CH_2O \rightarrow H_2O + HCO$	1.0×10^{-11} 1.7×10^{-11}	0 -100	1 2
75.	$O + CH_2O \rightarrow HCO + OH$	3.2×10^{-11} 2.8×10^{-11}	-1550 -1540	1,10 2
76.	$HCO + O_2 \rightarrow CO + HO_2$	5.0×10^{-12}	0	1
77.	$OH + CH_3OOH \rightarrow CH_3O_2 + H_2O$	5.0×10^{-12} 6.2×10^{-12}	-750 -750	1,10 2
78.	$CH_3 + O \rightarrow CH_2O + H$	1.0×10^{-10}	0	1
79.	$CH_3O_2 + O_3 \rightarrow CH_3O + 2O_2$	1.0×10^{-14}	-600	9
80.	$CH_3O_2 + O \rightarrow CH_3O + O_2$	3.0×10^{-11}	0	9
81.	$ClO + OH \rightarrow HO_2 + Cl$	9.2×10^{-12} 2.0×10^{-11}	0 0	1 12
82.	$CH_3 + O_2 \xrightarrow{M} CH_3O_2$	See Table A-3	-	3
83.	$ClO + OH \rightarrow HCl + O_2$	Not used ($\sim 10^{-22}$) 2.0×10^{-12}	- -	 12
84.	$H_2 + OH \rightarrow H_2O + H$	1.2×10^{-11} Not used	-2200 -	1
85.	$H + HO_2 \rightarrow H_2 + O_2$	4.2×10^{-11} Not used	-350 -	1
86.	$OH + CH_3OOH \rightarrow CH_2O + H_2O + OH$	5.0×10^{-12} Not used	-750 -	1,10
87.	$O + HNO_4 \rightarrow OH + NO_2 + O_2$	1.0×10^{-12} Not used	-2200 -	1,10
88.	$OH + ClONO_2 \rightarrow HOCl + NO_3$	1.2×10^{-12} Not used	-333 -	1,10

[a]When two entries are given, the lower one corresponds to 1979a chemistry and the upper one corresponds to 1979b chemistry.

TABLE A-2. (Continued)

Reaction	A[a]	B	Note
89. $Cl + ClONO_2 \rightarrow 2Cl + NO_3$	1.7×10^{-12}	-607	1,10
	Not used	-	
90. $HONO + OH \rightarrow H_2O + NO_2$	6.6×10^{-12}	0	1
	Not used	-	
91. $OH + NO \xrightarrow{M} HONO$	See Table A-3	-	3
	Not used	-	
92-97. (not used; reactions used only in sensitivity studies)			
98. $O + OClO \rightarrow ClO + O_2$	2.5×10^{-11}	-1166	1
99. $NO + OClO \rightarrow NO_2 + ClO$	2.5×10^{-12}	-600	1

[a]When two entries are given, the lower one corresponds to 1979a chemistry and the upper one corresponds to 1979b chemistry.

Notes to Table A-2.

1. Draft report of NASA Harpers Ferry Workshop.
2. JPL (1979). Where only one entry is given for the rate coefficient, 1979a and 1979b are the same. Usually this means that the first two references at the end of this Appendix give the same recommendation.
3. The reaction is pressure-dependent. See Table A-3 for discussion.
4. Estimate designed to be compatible with upper limit given in the first reference at the end of this Appendix, and low enough to have no significant effect on model performance. Reaction is retained only to facilitate reintroduction if the evaluated upper limit should prove to be in error.
5. Weighted average of the rates of $O(^1D) + N_2$ and $O(^1D) + O_2$ from the first two references.
6. Product chemistry has been simplified.
7. Estimated reaction rate. This estimate is designed to include a possible heterogeneous contribution to the overall reaction. Important only in the lower troposphere.
8. Estimated reaction rate. This rate is estimated based on the assumption that HNO_4 and HOCl resemble H_2O_2 (as treated in JPL, 1979) in reactions with Cl and OH.
9. Estimated reaction rate. Rate is estimated based on the assumption that CH_3O_2 closely resembles HO_2 in reaction with O or O_3.
10. Products are not given in the first two references at the end of this Appendix. The assumed products are based on the products that seem most plausible based on chemical considerations.
11. Rate based on a draft of the first reference that trivially differs from the final draft.
12. 1979a chemistry treated the reactions of HO and ClO based on privately communicated qualitative preliminary results. The treatment is nearly an upper limit to the plausible rate coefficients based on the recent results of Leu and Lin (1979).

Our treatment of photolysis reactions has also been modified. There is evidence for a moderate temperature dependence for many photoabsorption cross sections. With the exception of ozone, NO, and O_2 photolysis, we have not treated this temperature dependence explicitly, but have used cross sections measured at roughly 230 K for all temperatures. As a result our calculated trace species photodissociation rates should be more accurate for the stratosphere than for the lower troposphere.

For ozone photolysis we use quantum yields based on the recommendations of NASA (1979). Our treatment of O_2 photolysis is based on Hudson and Mahle (1972) while our treatment of NO photolysis is based on Frederick and Hudson (1979).

TABLE A-3. Rate coefficients used for pressure-dependent reactions.

Expression 1

$$k = \frac{A_0[M](300/T)^{n0}}{1 + A_0[M](300/T)^{n0}/A_i(300/T)^{ni}} \; 0.06 \left\{ 1 + \left[\log_{10} \left(\frac{A_0[M](300/T)^{n0}}{A_i(300/T)^{n_i}} \right) \right]^2 \right\}^{-1}$$

Reaction	A_0[a]	n_0	A_i	n_i	Note
$HO_2 + NO_2 \xrightarrow{M} HNO_4$	2.1×10^{-31}	5.0	6.5×10^{-12}	5.0	1
$OH + NO_2 \xrightarrow{M} HNO_3$	2.6×10^{-30}	2.9	2.4×10^{-11}	1.3	1
$ClO + NO_2 \xrightarrow{M} ClONO_2$	1.6×10^{-31}	3.4	1.5×10^{-11}	1.9	1,2
	3.5×10^{-32}	3.8	1.5×10^{-11}	1.9	1,2
$O + O_2 \xrightarrow{M} O_3$	6.2×10^{-34}	2.1	-	0	1
$CH_3 + O_2 \xrightarrow{M} CH_3O_2$	2.2×10^{-31}	2.2	2.0×10^{-12}	1.7	1
$O(^1D) + N_2 \xrightarrow{M} N_2O$	3.5×10^{-37}	0.45	-	0	1
$Cl + NO_2 \xrightarrow{M} ClNO_2$	1.6×10^{-30}	1.9	3.0×10^{-11}	1.0	1
$H + O_2 \xrightarrow{M} HO_2$	5.5×10^{-32}	1.4	-	0	1
$OH + NO \xrightarrow{M} HNO_2$	6.7×10^{-31}	3.3	3.0×10^{-11}	1.0	1
$OH + OH \xrightarrow{M} H_2O_2$	2.5×10^{-31}	0.8	3.0×10^{-11}	1.0	1
$NO_2 + NO_3 \xrightarrow{M} N_2O_5$	1.4×10^{-30}	2.8	9.0×10^{-13}	-0.7	1
	$1.8 \times 10^{-32} e^{1316/T}$	0	$9.5 \times 10^{-13} e^{58/T}$	0	3
$O + NO \xrightarrow{M} NO_2$	1.2×10^{-31}	1.8	3.0×10^{-11}	-0.3	1
	$1.6 \times 10^{-32} e^{584/T}$	0	-		4
$O + NO_2 \xrightarrow{M} NO_3$	9.0×10^{-32}	2.0	2.2×10^{-11}	0	1
	1.0×10^{-31}	0	-	0	4
$N_2O_5 \xrightarrow{M} NO_2 + NO_3$	$1.18 \times 10^{-3} e^{-11180/T}$	2.8	$7.52 \times 10^{14} e^{-11180/T}$	-0.7	5
	$1.6 \times 10^{-5} e^{-9864/T}$	0	$7.94 \times 10^{14} e^{-11122}$	0	4
$HNO_4 \xrightarrow{M} HO_2 + NO_2$		$k = \frac{5.2 \times 10^{-6} e^{-10015/T}}{1 + 4.86 \times 10^{-12} M^{0.61}}$			7
$OH + CO \xrightarrow{M} H + CO_2$		$k = 1.35 \times 10^{-13} \left(1 + \frac{M}{2.46 \times 10^{19}} \right)$			1
$HO_2 + HO_2 + H_2O \rightarrow H_2O_2 + H_2O + O_2$		$k = \frac{1.1 \times 10^{-34} e^{3730/T}}{1 + M * 3.5 \times 10^{-16} e^{-2060/T}}$			6

[a]When two entries are given, the lower one corresponds to 1979a chemistry and the upper one corresponds to 1979b chemistry.

Notes to Table A-3

1. Expression given in NASA (1979). 1979a chemistry differed from 1979b chemistry in that the parameter 0.6 in expression (1) was set equal to 0.8 in the expression used for 1979a chemistry.
2. Both expressions are recommended with no clear preference. The lower value is used in the 1979a chemistry and the upper one is used in the 1979b chemistry.
3. Private communication, D. Golden, SRI International, Inc. (1979).
4. Based on data in NBS 513 (1978).
5. Based on data in the first reference and the equilibrium constant from NBS 513 (1978).
6. Based on Cox (1978).
7. Based on Graham *et al.* (1978).

TABLE A-4. Photolysis reactions. Alternative products of reaction are shown in parentheses, but they were not used in either the 1979a or 1979b chemistry.

Reaction	Note	Reaction	Note
1. $O_2 \rightarrow 2O$	1,2	16. $CF_2Cl_2 \rightarrow 2Cl$	4,8
2. $O_3 \rightarrow O + O_2$	1,3	17. $CFCl_3 \rightarrow 3Cl$	4,8
3. $O_3 \rightarrow O(^1D) + O_2$	1,3	18. $CCl_4 \rightarrow 4Cl$	4,8
4. $NO_2 \rightarrow NO + O$	1,4	19. $N_2O_5 \rightarrow NO_3 + NO_2$ ($2NO_2 + O$)	4,6
5. $N_2O \rightarrow N_2 + O(^1D)$	4	20. $NO_3 \rightarrow NO + O_2$	4
6. $NO \rightarrow N + O$	5	21. $NO_3 \rightarrow NO_2 + O$	4
7. $HNO_3 \rightarrow OH + NO_2$	4	22. $H_2O \rightarrow H + OH$	9
8. $H_2O_2 \rightarrow 2OH$	4	23. $HNO_4 \rightarrow HO + NO_3$ ($HO_2 + NO_2$)	10,6
9. $HO_2 \rightarrow OH + O$	4	24. $HOCl \rightarrow OH + Cl$	4
10. $ClONO_2 \rightarrow Cl + NO_3$($ClO + NO_2$)	4,6	25. $CH_3OOH \rightarrow CH_3O + OH$	4
11. $HCl \rightarrow H + Cl$	4	26. $CH_2O \rightarrow HCO + H$	11
12. $ClO \rightarrow Cl + O$	7	27. $CH_2O \rightarrow CO + H_2$	11
13. $ClO \rightarrow Cl + O(^1D)$	Not used	28. $CH_3Cl \rightarrow CH_3 + Cl$	4
14. $ClNO_2 \rightarrow Cl + NO_2$	4	29. $HONO \rightarrow OH + NO$	4
15. $OClO \rightarrow ClO + O$	7		

Notes to Table A-4.

1. Contributes to optical depth of model atmosphere.
2. Schumann-Runge bands are given special treatment based on Hudson and Mahle (1972).
3. Quantum yields of reactions (2) and (3) are given special treatment based on temperature-dependent treatment of JPL (1979).
4. Based on the data of JPL (1979). Where data for several temperatures is given, we have used the data at 230 K.
5. Nitric oxide photolysis is based on treatment of Frederick and Hudson (1979). We have used the photolysis rates averaged over the sunlit hemisphere for day time photolysis rates. 1979a chemistry used the treatment of Cieslik and Nicolet (1973).

6. The products used for XNO_3 (X = Cl, OH, NO_2) changed between our 1979a and 1979b chemistries. For 1979a they were based on the path of lowest endoergicity (except for N_2O_5 which was based on a recommendation of Johnston). For 1979b they are all based on analogy with $ClONO_2$ data of Chang *et al.* (1979). This treatment is highly uncertain.
7. Based on data in Watson (1974).
8. Product chemistry has been simplified.
9. Treatment based on Thompson *et al.* (1963).
10. Treatment based on Graham *et al.* (1978).
11. Treatment based on quantum yields of Moortgat and Warneck (1979) and cross sections of McQuigg and Calvert (1969).

BOUNDARY CONDITIONS

The model now allows for either fixed concentrations or a flux condition at the surface as a lower boundary condition. For most of the calculations in this study, six species were assumed to have fixed concentrations (See Table A-5), while a surface flux was assigned to the other species. Zero flux was assumed except for those species shown in Table A-5. When those species with fixed boundary conditions in Table A-5 were given flux boundaries, a flux was determined to give an ambient concentration the same as those in Table A-5.

Zero flux was assumed for all species except NO and NO_2 at the upper boundary. NO and NO_2 are assumed to have a very small flux from the mesosphere into the stratosphere.

Water vapor concentrations are fixed in the troposphere and calculated in the stratosphere. All runs are made with fixed boundary conditions unless otherwise noted.

SOURCES AND SINKS

In addition to sources and sinks from the chemistry and boundary conditions described above, there are additional sinks due to dry and/or wet removal for many species in the model. A source for nitric oxide from cosmic ray dissociation of N_2 is also included based on the results of Nicolet (1974).

Wet removal processes are parameterized by a first-order loss rate. The wet removal of the trace species HNO_3, H_2O_2, HCl, ClO, $ClONO_2$, $ClNO_2$, HNO_4, HOCl, CH_2O and CH_3OOH is assumed to vary with altitude as shown in Table A-6. NO_2 is assumed to have a loss rate half the above rate.

Dry deposition rates at the surface are also parameterized by a first-order loss rate as shown in Table A-7.

TABLE A-5. *Boundary conditions.*

Fixed concentrations (molecules cm^{-3})		Surface flux (molecules cm^{-2} s^{-1})	
N_2O	8.25×10^{12}	NO	3.41×10^{9}
CH_4	4.03×10^{13}	NO_2	6.59×10^{9}
H_2	1.42×10^{13}	HNO_3	1.67×10^{9}
CH_3Cl	1.56×10^{10}	HCl	3.67×10^{10}
H_2O	4.30×10^{17}	CCl_4	1.40×10^{6}
CO	3.04×10^{12}	CF_2CL_2, $CFCl_3$, CH_3CCl_3	function of time and scenario

TABLE A-6. Wet removal parameterization.

Altitude, km	Loss rate, sec^{-1}	Altitude, km	Loss rate, sec^{-1}
0	3.86×10^{-6}	6	1.93×10^{-6}
1	3.86×10^{-6}	7	1.93×10^{-7}
2	3.86×10^{-6}	8	9.58×10^{-7}
3	3.86×10^{-6}	9	4.78×10^{-7}
4	3.86×10^{-6}	10	0
5	3.86×10^{-6}		

TABLE A-7. Deposition rates in the lowest layer (z = 0).

Species	Loss rate, sec^{-1}	Species	Loss rate, sec^{-1}
$O(^3P)$	2.0×10^{-5}	NO_3	2.0×10^{-5}
O_3	1.0×10^{-5}	N_2O_5	2.0×10^{-5}
NO	1.0×10^{-6}	H_2O	0
NO_2	3.0×10^{-6}	HNO_4	2.0×10^{-5}
N_2O	0	HOCl	2.0×10^{-5}
HNO_3	2.0×10^{-5}	HCO	2.0×10^{-5}
OH	2.0×10^{-5}	CH_2O	1.0×10^{-5}
HO_2	2.0×10^{-5}	CH_3	2.0×10^{-5}
H_2O_2	2.0×10^{-5}	CH_3OOH	2.0×10^{-5}
Cl	2.0×10^{-5}	CH_3O	2.0×10^{-5}
$ClONO_2$	2.0×10^{-5}	CH_3O_2	2.0×10^{-5}
ClO	2.0×10^{-5}	CO	5.0×10^{-7}
CH_4	0	ClO_3	2.0×10^{-5}
H_2	1.0×10^{-7}	OClO	2.0×10^{-5}
CH_3Cl	0	HONO	2.0×10^{-5}
$ClNO_2$	2.0×10^{-5}	$CFCl_3$	0
HCl	2.0×10^{-5}	CF_2Cl_2	0
CCl_4	0	CH_3CCl_3	0

MULTIPLE SCATTERING

In order to accurately compute photodissociation rates, it is important to describe radiative processes, such as multiple scattering, in addition to attenuation by gases such as O_2, O_3 and NO_2. The importance of molecular scattering varies significantly with wavelength over the spectral range 200-750 nm. At shorter wavelengths gaseous absorption dominates and very little solar flux reaches the lower atmosphere. The region 290-330 nm is a transition region where molecular scattering is very important, especially at the longer wavelengths in this interval. Beyond 330 nm, surface reflection is very important since the atmosphere is nearly transparent in this spectral region.

Multiple scattering is included in the model using a simplified method that is computationally fast so that it can be used for diurnal calculations. The method is similar to that of Isaksen *et al.* (1977) in terms of the numerical method but quite different in terms of the physical assumptions. The atmosphere is divided into optically thin layers and each layer can absorb and scatter radiation. The layer is assumed to scatter radiation isotropically with half of the scattered flux going upward and the other half downward at an average zenith angle of $\pm\bar{\theta}$. The earth's surface is also assumed to scatter isotropically, and a surface albedo of 0.25 is used to approximate the effect of clouds on the upward scattered radiation. Using a high surface albedo and no clouds gives results that are nearly identical to those from dividing the atmosphere into clear and cloudy regimes and averaging the results (the exception being the region below the cloud layer, which is not important for the model applications considered here). For each atmospheric layer there is a contribution to the solar flux density from the direct flux and by the diffuse fluxes incident on the layer from above and from below. The flux density due to the various fluxes together can be much greater (depending on the wavelength and altitude) than the flux density computed considering only gaseous absorption (Luther and Gelinas, 1976; Luther and Wuebbles, 1976).

TEMPERATURE FEEDBACK

The temperature profile above 13 km is calculated using a stratospheric radiative transfer model, and the temperature profile is specified at lower altitudes. The model includes solar absorption and long-wave interaction by O_3, H_2O, and CO_2, along with solar absorption by NO_2. The techniques adopted for treating long-wave radiative transfer are the same as those described by Ramanathan (1974). This formulation was chosen because it is computationally efficient, and its accuracy has been demonstrated (Ramanathan, 1974, 1976) by comparison with much more complex models. The effects of and justification for the simplifying assumptions used in the model are discussed by Ramanathan (1976).

A band absorptance formulation is used to treat the 9.6-μm band of O_3 and the fundamental and several hot and isotopic bands of CO_2 in the 15-μm region. An emissivity formulation is used to treat long-wave radiative transfer by H_2O. Solar absorption by O_3 is treated by using the empirical formulation given by Lindzen and Will (1973). The band absorptance formulation by Houghton (1963) is adopted for solar absorption by H_2O, and the band absorptance formulation by Ramanathan and Cess (1974) is adopted for solar absorption by CO_2. The empirical formulation of Luther (1976) is used for solar absorption by NO_2. Solar absorption by O_3 and NO_2 are treated independently because absorption by these species is weak in the region where their absorption bands overlap. Solar radiation scattered from the troposphere is included by assuming an albedo of 0.3. Doppler broadening effects are included for CO_2 and O_3 as described in Appendix B of Ramanathan (1976). The temperature dependences of the band absorptance and band intensity are included in the longwave calculations of CO_2 and O_3.

A single cloud layer is included at 6.5 km with 42% cloud cover as was suggested by Cess (1974). The lapse rate within the troposphere is assumed to be -6.5 K/km, and the temperature at the earth's surface is specified to be 288 K.

NUMERICAL METHOD

Each of the 39 species in the model has its concentration calculated at each of 44 vertical levels extending from the surface to 55 km. The numerical technique used to solve the set of over 2000 differential equations (resulting from a continuity equation for each species at each grid level) is the method described by Chang *et al.* (1974). The main advantage of this method, which is a variable order, multistep, implicit method, is its ability to solve sets of mathematically stiff differential equations for almost any set of input parameters, initial and boundary conditions, in particular those resulting from the chemical kinetics system described in Table A-2.

DIURNAL AND DIURNAL-AVERAGED MODELS

We have developed a fully diurnal-averaged model that is consistent with our diurnal model. The diurnal model is used to generate species profiles for comparison with measurements and for perturbation studies involving short time integrations (e.g., solar eclipse effects). The diurnal-averaged model is used for perturbation and sensitivity studies involving longer time integrations.

The procedure that is used in developing the fully diurnal-averaged model is also applicable to two-dimensional models. If the continuity equation is averaged over a time period (24 hours in our case) that is very small compared to the time scale of the problem of interest, then one obtains averaged terms of the form $\overline{k_{ij} c_i c_j}$ and $\overline{J_i c_i}$ where c_i is the concentration of species i at time t and altitude z, k_{ij} is the two-body chemical rate coefficient, and J_i is the photodissociation rate coefficient for species i.

We define the diurnal weighting factors $\alpha_{ij}(z)$ and $\beta_i(z)$ by

$$\overline{k_{ij}\, c_i\, c_j} = \alpha_{ij}\, \overline{k_{ij}\, c_i\, c_j} \tag{A-5}$$

and

$$\overline{J_i\, c_i} = \beta_i\, \overline{J_i\, c_i} \quad . \tag{A-6}$$

Since k_{ij} is defined and is independent of time, we have

$$\alpha_{ij} = \overline{c_i\, c_j} \,/\, \overline{c_i}\;\overline{c_j} \tag{A-7}$$

and

$$\beta_i = \overline{J_i\, c_i} \,/\, \overline{J_i\, c_i} \tag{A-8}$$

The computation of photodissociation rates can be an expensive part of stratospheric model calculations, hence evaluation of J_i's in the diurnal-averaged model can be expensive. If we define β_i by

$$\beta_i = \overline{J_i\, c_i} \,/\, (J_i^{\text{noon}}\; \overline{c_i}) \;, \tag{A-9}$$

then the computation in the diurnal-averaged model is greatly simplified. The diurnal model is used to determine $\overline{c_i\, c_j}$, $\overline{J_i\, c_i}$, $\overline{c_i}$, $\overline{c_j}$, and J_i^{noon} so that α_{ij} and β_i can be obtained for every chemical and photochemical reaction in the model.

REFERENCES

Cess, R. D., "Radiative Transfer Due to Atmospheric Water Vapor: Global Considerations of the Earth's Energy Balance," *J. Quant. Spectrosc. Radiat. Transfer*, **14**, 861–871, 1974.

Chang, J. S., J. R. Barker, J. E. Davenport, and D. M. Golden, "Chlorine Nitrate Photolysis by a New Technique: Very Low Pressure Photolysis," *Chem. Phys. Lett.*, **60**, 385–390, 1979.

Chang, J. S., A. C. Hindmarsh, and N. K. Madsen, "Simulation of Chemical Kinetics Transport in the Stratosphere," in *Stiff Differential Systems*, R. A. Willoughby (ed.), Plenum Publishing Corp., New York, 1974, p. 51 ff.

Cieslik, S. and M. Nicolet, "The Aeronomic Dissociation of Nitric Oxide," *Planet. Space Sci.*, **21**, 925–938, 1973.

Cox, R. A., "Kinetics of HO_2 Radical Reactions of Atmospheric Interest," papers presented at WMO Symposium on the Geophysical Aspects and Consequences of Change in the Composition of the Stratosphere, Toronto, 26–30 June 1978, WMO No. 511, 1978.

Frederick, J. E. and R. D. Hudson, "Predissociation of Nitric Oxide in the Mesosphere and Stratosphere," *J. Atmos. Sci.*, **36**, 737–745, 1979.

Graham, R. A., A. M. Winer and J. N. Pitts, Jr., "Pressure and Temperature Dependance of the Unimolecular Decomposition of NO_2NO_2," *J. Chem. Phys.*, **68**, 4505–4510, 1978.

Houghton, J. T., "The Absorption of Solar Infrared Radiation by the Lower Stratosphere," *Quart. J. Roy. Meteorol. Soc.*, **89**, 319–331, 1963.

Hudson, R. D. and S. H. Mahle, "Photodissociation Rates of Molecular Oxygen in the Mesosphere and Lower Thermosphere," *J. Geophys. Res.*, **77**, 2902–2914, 1972.

Isaksen, I. S. A., K. M. Midtbo, J. Sunde, and P. J. Crutzen, "A Simplified Method to Include Molecular Multiple Scattering and Reflection in Calculations of Photon Fluxes and Photodissociation Rates," *Geophysica Norwegica*, **31**, 11–26, 1977.

JPL Publication 79-27, "Chemical Kinetic and Photochemical Data for Use in Stratospheric Modeling," NASA Panel for Data Evaluation, 1979.

Leu, M. T. and C. L. Lin, "Rate Constants for the Reactions of OH with ClO, Cl_2, and Cl_2O at 298 K," *Geophys. Res. Letters*, **6**, 425–428, 1979.

Lindzen, R. S. and D. I. Will, "An Analytical Formula for Heating Due to Ozone Absorption," *J. Atmos. Sci.*, **30**, 513–515, 1973.

Luther, F. M., "A Parameterization of Solar Absorption by Nitrogen Dioxide," *J. Appl. Meteorol.*, **15**, 479–481, 1976.

Luther, F. M. and R. J. Gelinas, "Effect of Molecular Multiple Scattering and Surface Albedo on Atmospheric Photodissociation Rates," *J. Geophys. Res.*, **81**, 1125–1132, 1976.

Luther, F. M. and D. J. Wuebbles, *Photodissociation Rate Calculations*, Lawrence Livermore Laboratory, Livermore, CA, UCRL-78911, 1976.

McQuigg, R. D. and J. G. Calvert, "The Photodecomposition of CH_2O, CD_2O, CHDO, and CH_2O–CD_2O Mixtures at Xenon Flash Lamp Intensities," *J. Am. Chem. Soc.*, **91**, 1590–1599, 1969.

Moortgat, G. K. and P. Warneck, "CO_2 and H_2 Quantum Yields in the Photodecomposition of Formaldehyde in Air," *J Chem. Phys.*, **70**, 3639–3651, 1979.

NAS, "Halocarbons: Effects on Stratospheric Ozone," U. S. National Academy of Sciences, Washington, D.C., 1976.

NASA Reference Publication (draft), "The Stratosphere: Present and Future," R. D. Hudson (ed.), prepared at the NASA Workshop, Harpers Ferry, Pennsylvania, June 1979.

NBS Special Publication 513, "Reaction Rate and Photochemical Data for Atmospheric Chemistry—1977," R. F. Hampson, Jr. and D. Garvin (eds.), National Bureau of Standards, Washington, D.C., 1978.

Nicolet, M., "On the Production of Nitric Oxide by Cosmic Rays in the Mesosphere and Stratosphere," *Aeronomica Acta-A*, No. 134, Institut D'Aeronomie Spatiale de Belgique, Brussels, 1974.

Ramanathan, V., "A Simplified Stratospheric Radiative Transfer Model: Theoretical Estimates of the Thermal Structure of the Basic and Perturbed Stratosphere," paper presented at the *Second International Conference on the Environmental Impact of Aerospace Operations in the High Atmosphere*, American Meteorological Society/American Institute of Aeronautics and Astronautics, San Diego, Calif., July 8–10, 1974.

Ramanathan, V., "Radiative Transfer Within the Earth's Troposphere and Stratosphere: A Simplified Radiative-Convective Model," *J. Atmos. Sci.*, **33**, 1330–1346, 1976.

Ramanathan, V. and R. D. Cess, "Radiative Transfer Within the Mesospheres of Venus and Mars," *Astrophys. J.*, **188**, 407–416, 1974.

Thompson, B. A., P. Harteck and R. R. Reeves, Jr., "Ultraviolet Absorption Coefficients of CO_2, CO, O_2, H_2O, N_2O, NH_3, NO, SO_2, and CH_4 between 1850 and 4000 $\AA$," *J. Geophys. Res.*, **68**, 6431–6436, 1963.

Watson, R. T., *Chemical Kinetics Data Survey VIII. Rate Constants of ClO_x of Atmospheric Interest*, NBSIR 74-516, National Bureau of Standards, 1974.

APPENDIX B
BIBLIOGRAPHY OF PUBLICATIONS PRODUCED IN LLL'S WORK ON HIGH ALTITUDE POLLUTION PROGRAM (1975–1979)

Burt, J. E. and F. M. Luther, "Effect of Receiver Orientation on Erythema Dose," *Photochem. and Photobio.*, **29**, 85–91, 1979.

Chang, J. S. (Ed.), *General Circulation Models of the Atmosphere*, Vol. 17 of *Methods in Computational Physics*, Series eds., B. Alder, S. Fernbach, and M. Rotenberg (Academic Press, N.Y., 1977).

Chang, J. S., "Some Fundamental Concepts and Problems in Stratospheric Modeling," preprint, Lawrence Livermore Laboratory, Livermore, CA. To appear in the *Proceedings of the NATO Advanced Study Institute on Atmospheric Ozone*, Aldeia das Acoteias, Albufeira, Algarve, Portugal, October 1–13, 1979.

Chang, J. S., coauthor of *Halocarbons: Effects on Stratospheric Ozone*, National Research Council, National Academy of Sciences, Washington, D.C., 1976.

Chang, J. S., coauthor of *Stratospheric Ozone Depletion by Halocarbons: Chemistry and Transport*, National Research Council, National Academy of Sciences, Washington, D.C., 1979.

Chang, J. S. and W. H. Duewer, "Modeling Chemical Process in the Stratosphere," *Annual Review of Physical Chemistry*, **30**, 443–469, 1979.

Chang, J. S., W. H. Duewer, and D. J. Wuebbles, "The Atmospheric Nuclear Tests of the 1950's and 1960's: A Possible Test of Ozone Depletion Theories," *J. Geophys. Res.*, **84**, 1755–1765, 1979.

Chang, J. S. and J. E. Penner, "Analysis of Global Budgets of Halocarbons," *Atmos. Environ.*, **12**, 1867–1873, 1978.

Chang, J. S. and D. J. Wuebbles, "A Theoretical Model of Global Tropospheric OH Distribution," in *Proceedings of the Joint AGU/AMS Symposium on the Non-Urban Tropospheric Composition*, Hollywood, FL, November 10–12, 1976. Lawrence Livermore Laboratory, Livermore, CA, UCRL-78392, 1976.

Chang, J. S. and D. J. Wuebbles, "One-Dimensional Coupled Transport and Chemical Kinetics Models of the Stratosphere," Lawrence Livermore Laboratory, Livermore, CA, UCRL-83790, 1979. Also in *Proceedings of the NATO Advanced Study Institute on Stratospheric Ozone*, Aldeia das Acoteias, Albufeira, Algarue, Portugal, October 1–13, 1979.

Chang, J. S., D. J. Wuebbles, and D. D. Davis, "A Theoretical Model of Global Tropospheric OH Distribution," revision to paper presented at the Joint AGU/AMS Symposium on the Non-Urban Tropospheric Composition, Hollywood, FL, November 10–12, 1976. Lawrence Livermore Laboratory, Livermore, CA, UCRL-78392, Rev. 1, 1977.

Chang, J. S., D. J. Wuebbles, and W. H. Duewer, "Sensitivity to Parameter Uncertainties for Ozone Reduction from Chlorofluoromethanes,' paper presented at 12th International Symposium on Free Radicals, Laguna Beach, CA, January 4–9, 1976 (sponsored by University of California, Irvine). Lawrence Livermore Laboratory, Livermore, CA, UCRL-77432, 1976.

Duewer, W. H., "Recombination-Dissociation Theory for NO_2 and NOCl," appeared as a comment in *J. Phys. Chem.*, **83**, 18, 1979.

Duewer, W. H. and D. J. Wuebbles, *Predictions of the Effects on the Stratosphere of Changes in the Oxides of Nitrogen*, Lawrence Livermore Laboratory, Livermore, CA, UCRL-82553, incorporated in NASA report in progress, 1979.

Duewer, W. H. and D. J. Wuebbles, "Tropospheric Methane: Response to Stratospheric Ozone Trends," Lawrence Livermore Laboratory, Livermore, CA, UCRL-82968, 1979.

Duewer, W. H., D. J. Wuebbles, and J. S. Chang, "Effect of NO Photolysis on NO_y Mixing Ratios," *Nature*, **265**, 523–525, 1977.

Duewer, W. H., D. J. Wuebbles, and J. S. Chang, *The Effects of a Massive Pulse Injection of NO_x Into the Stratosphere*, Lawrence Livermore Laboratory, Livermore, CA, UCRL-80397, also in papers presented at *WMO Symposium on the Geophysical Aspects and Consequences of Changes in the Composition of the Stratosphere*, WMO-No. 511, Toronto, June 26–30, 1978.

Duewer, W. H., D. J. Wuebbles, H. W. Ellsaesser, and J. S. Chang, "NO_x Catalytic Ozone Destruction: Sensitivity to Uncertainties in Rate Coefficients," *J. Geophys. Res.*, **82**, 935–942, 1977.

Duewer, W. H., D. J. Wuebbles, H. W. Ellsaesser, and J. S. Chang, "Authors Reply to Comment by Johnston and Nelson," *J. Geophys. Res.*, **82**, 2599–2605, 1977.

Ehhalt, D. H., J. S. Chang, and D. M. Butler, "The Probability Distribution of Ozone Changes Predicted from Anthropogenic Activities," *J. Geophys. Res.*, **84**, 7889–7894, 1979.

Ellsaesser, H. W., *"Ozone Drop and Depletion Theories,"* Lawrence Livermore Laboratory, Livermore, CA, UCRL-77854, 1976.

Ellsaesser, H. W., *"Has the Solar Constant Kept Pace with Solar Luminosity?"*, Lawrence Livermore Laboratory, Livermore, CA, UCRL-77854, 1976.

Ellsaesser, H. W., "A Reassessment of Stratospheric Ozone: Credibility of the Threat," invited paper presented at the *Environmental Health Sciences Symposium on SST Pollution and Skin Cancer*, Hollywood, FL, October 25–29, 1976. Lawrence Livermore Laboratory, Livermore, CA, UCRL-78285, 1976.

Ellsaesser, H. W., "Comments on 'Estimate of the Global Change in Temperature, Surface to 100 mb, Between 1958 and 1975'," *Mon. Wea. Rev.*, **105**, 1200–1201, 1977.

Ellsaesser, H. W., "Comments on 'The Distribution of Water Vapor in the Stratosphere'," *Rev. Geophys. Space Phys.*, **15**, 501, 1977.

Ellsaesser, H. W., "Has Man Increased Stratospheric Ozone?" *Nature*, **270**, 592–593, 1977.

Ellsaesser, H. W., "Stratospheric H_2O," position paper presented at the *NASA Stratospheric Workshop, Harpers Ferry, WV, June 4–8, 1979*; Lawrence Livermore Laboratory, Livermore, CA, UCRL-82542, 1979.

Ellsaesser, H. W., "Man's Effect on Stratospheric Ozone," paper presented at the 4th International Symposium on Environmental Biogeochemistry, Canberra, Australia, August 26–31, 1979; Lawrence Livermore Laboratory, Livermore, CA, UCRL-82556, 1979.

Ellsaesser, H. W., J. E. Harries and D. Kley, *Stratospheric H_2O*, Lawrence Livermore Laboratory, Livermore, CA, UCRL-82512, Rev. 1, 1979, to be included in NASA Reference Publication 1049, "The Stratosphere: Present and Future," R. Hudson, Ed., NASA Goddard Space Flight Center, 1979.

Ellsaesser, H. W., J. E. Harries, D. Kley, and R. Penndorf, *Stratospheric H_2O*, Lawrence Livermore Laboratory, Livermore, CA, UCRL-82542, Rev. 2, 1979.

Ellsaesser, H. W., M. C. MacCracken, G. L. Potter, and F. M. Luther, "An Additional Model Test of Positive Feedback from High Desert Albedo," *Quart. J. Roy. Meteoro. Soc.*, **102**, 543–554, 1976.

Lovill, J. E., T. J. Sullivan, and J. A. Korver, "Measurement of Atmospheric Ozone by Satellite," in *Proceedings of the Seventh Conference on Aerospace and Aeronautical Meteorology and Symposium on Remote Sensing from Satellites*, Melbourne, FL, November 16–19, 1976. (Lawrence Livermore Laboratory, Livermore, CA, UCRL-78094)

Lovill, J. E., J. S. Ellis, and P. P. Weidhaas, *The Global Observation of Atmospheric Ozone by Satellite*, Lawrence Livermore Laboratory, Livermore, CA, UCRL-82028, presented at the WMO Technical Conference on Regional and Global Observation of Atmospheric Pollution Relative to Climate, University of Colorado, Boulder, CO, August 20–24, 1979.

Lovill, J. E., T. Sullivan, J. B. Knox, J. A. Korver, "Satellite Ozone Analysis Center (SOAC)," p. 67, in *Proceedings of the Joint Symposium on Atmospheric Ozone; Volume 1*, K. H. Grasnick, Ed., (Berlin, G.D.R., 1977). (Lawrence Livermore Laboratory, Livermore, CA, UCRL-78092)

Lovill, J. E. and T. Sullivan, "An Extremely High Resolution Ozone Sensor for Spacelab," p. 201, in *Proceedings of the Joint Symposium on Atmospheric O_3; Volume 1*, H. Grasnick, Ed., (Berlin, G.D.R., 1977). (Also Lawrence Livermore Laboratory, Livermore, CA, UCRL-77910)

Lovill, J. E., "Facts about Ozone," in *Energy and Technology Review*, monthly Journal of the Lawrence Livermore Laboratory, Nov. 1976, (Lawrence Livermore Laboratory, Livermore, CA, UCRL-52000-76-11), p. 110.

Lovill, J. E., T. Sullivan, R. Weichel, J. S. Ellis, J. G. Huebel, J. A. Korver, P. P. Weidhaas, F. A. Phelps, *Total Ozone Retrieval from Satellite Multichannel Filter Radiometer Measurements*, Lawrence Livermore Laboratory, Livermore, CA, UCRL-52473, 1978.

Luther, F. M., "Relative Influence of Stratospheric Aerosols on Solar and Longwave Radiative Fluxes for a Tropical Atmosphere," *J. Appl. Meteor.*, **15**, 951–955, 1976.

Luther, F. M., "One-Wavelength Solar Radiation Calculations: Rayleigh Scattering and Gaseous Absorption," paper presented at *2nd Conference on Atmospheric Radiation, Arlington, VA, October 29–31, 1975*; Lawrence Livermore Laboratory, Livermore, CA, UCRL-76680, 1976.

Luther, F. M., "Solar Absorption in a Stratosphere Perturbed by NO_x Injection," *Science*, **192**, 49–51, 1976.

Luther, F. M., "A Parameterization of Solar Absorption by Nitrogen Dioxide," *J. Appl. Meteoro.*, **15**, 479–481, 1976.

Luther, F. M., *Effects of Stratospheric Perturbations on the Solar Radiation Budget*, Lawrence Livermore Laboratory, Livermore, CA, UCRL-80429; also in papers presented at the *WMO Symposium on the Geophysical Aspects and Consequences of Changes in the Composition of the Stratosphere*, WMO-No. 511, Toronto, June 26–30, 1978.

Luther, F. M., "The Ozone Layer: Assessing Man-Made Perturbations," in *Energy and Technology Review*, monthly Journal of the Lawrence Livermore Laboratory, January 1978, 17–25.

Luther, F. M. (principal investigator), *Annual Report of Lawrence Livermore Laboratory to the High Altitude Pollution Program—1976*, Lawrence Livermore Laboratory, Livermore, CA, UCRL-50042-76, 1976.

Luther, F.M. (principal investigator), *Annual Report of Lawrence Livermore Laboratory to the High Altitude Pollution Program—1977*, Lawrence Livermore Laboratory, Livermore, CA, UCRL-50042-77, 1977.

Luther, F. M. (principal investigator), *Annual Report of Lawrence Livermore Laboratory to the FAA on the High Altitude Pollution Program—1978*, Lawrence Livermore Laboratory, Livermore, CA, UCRL-50042-78, 1978.

Luther, F. M. and W. H. Duewer, "Effect of Changes in Stratospheric Water Vapor on Ozone Reduction Estimates," *J. Geophys. Res.*, **83**, 2395–2402, 1978.

Luther, F. M., and R. J. Gelinas, "Effect of Molecular Multiple Scattering and Surface Albedo on Atmospheric Photodissociation Rates," *J. Geophys. Res.*, **81**, 1125–1132, 1976.

Luther, F. M. and D. J. Wuebbles, "Photodissociation Rate Calculations," paper presented at the NASA Workshop on CFM Assessment, Warrenton, VA, January 10–14, 1977; Lawrence Livermore Laboratory, Livermore, CA, UCRL-78911, 1977.

Luther, F. M., D. J. Wuebbles, and J. S. Chang, "Temperature Feedback in a Stratospheric Model," *J. Geophys. Res.*, **82**, 4935–4942, 1977.

Luther, F. M., D. J. Wuebbles, W. H. Duewer, and J. S. Chang, "Effect of Multiple Scattering on Species Concentrations and Model Sensitivity," *J. Geophys. Res.*, **83**, 3563–3570, 1978.

Penner, J. E., "Trends in Other Species," position paper prepared for the *NASA Stratospheric Workshop, Harpers Ferry, WV, June 4–8*, 1979, Lawrence Livermore Laboratory, Livermore, CA, UCRL-82576, 1979.

Penner, J. E. and J. S. Chang, "Possible Variations in Atmospheric Ozone Related to the 11 Year Solar Cycle," in papers presented at the *WMO Symposium on the Geophysical Aspects and Consequences of Changes in the Composition of the Stratosphere*, WMO-No. 511, Toronto, June 26–30, 1978, also *Geophys. Res. Lett.*, **5**, 817-820, 1978.

Penner, J. E. and J. S. Chang, "The Relation Between Atmospheric Trace Species Variabilities and Solar UV Variability," Lawrence Livermore Laboratory, Livermore, CA, UCRL-83029 Rev. 1, 1979. Submitted to *J. Geophys. Res.*

Potter, G. L., M. C. MacCracken, H. W. Ellsaesser, and F. M. Luther, "Possible Climatic Impact of Tropical Deforestation," *Nature*, **258** (5537), 697–698, 1975.

Wuebbles, D. J., *A Reexamination of Potential Space Shuttle Effects on the Stratosphere*, Lawrence Livermore Laboratory UCID-17689, 1977.

Wuebbles, D. J. and J. S. Chang, "A Theoretical Study of Solar Eclipse Effects on the Stratosphere," *Geophys. Res. Letters*, **6**, 179–182, 1979.

☆ U.S. GOVERNMENT PRINTING OFFICE: 1981 - 341-428/535


DATE
ILME